

Dissipative spin dynamics in hot quantum paramagnets

Dmytro Tarasevych and Peter Kopietz
*Institut für Theoretische Physik, Universität Frankfurt,
 Max-von-Laue Strasse 1, 60438 Frankfurt, Germany*
 (Dated: July 16, 2021)

We use the functional renormalization approach for quantum spin systems developed by Krieg and Kopietz [Phys. Rev. B **99**, 060403(R) (2019)] to calculate the spin-spin correlation function $G(\mathbf{k}, \omega)$ of quantum Heisenberg magnets at infinite temperature. For small wavevectors \mathbf{k} and frequencies ω we find that $G(\mathbf{k}, \omega)$ assumes in dimensions $d > 2$ the diffusive form predicted by hydrodynamics. In three dimensions our result for the spin-diffusion coefficient \mathcal{D} is somewhat smaller than previous theoretical predictions based on the extrapolation of the short-time expansion, but is still about 30% larger than the measured high-temperature value of \mathcal{D} in the Heisenberg ferromagnet $\text{Rb}_2\text{CuBr}_4 \cdot 2\text{H}_2\text{O}$. In reduced dimensions $d \leq 2$ we find superdiffusion characterized by a frequency-dependent complex spin-diffusion coefficient $\mathcal{D}(\omega)$ which diverges logarithmically in $d = 2$, and as a power-law $\mathcal{D}(\omega) \propto \omega^{-1/3}$ in $d = 1$. Our result in one dimension implies scaling with dynamical exponent $z = 3/2$, in agreement with recent calculations for integrable spin chains. Our approach is not restricted to the hydrodynamic regime and allows us to calculate the dynamic structure factor $S(\mathbf{k}, \omega)$ for all wavevectors. We show how the short-wavelength behavior of $S(\mathbf{k}, \omega)$ at high temperatures reflects the relative sign and strength of competing exchange interactions.

CONTENTS

I. Introduction	1	C. Three dimensions	22
II. SFRG with classical-quantum decomposition	3	D. Common features in all dimensions	22
A. Subtracted exchange interaction and irreducible dynamic susceptibility	3	VI. Summary and conclusions	23
B. Hybrid functional and generalized Wetterich equation	4	Acknowledgments	25
C. Vertex expansion	6	APPENDIX A: High-temperature spin diffusion on a bcc lattice	25
D. Exact flow equations for the two-point vertices	8	APPENDIX B: High-temperature spin diffusion on hypercubic lattices	26
III. Truncated flow equations and integral equation for the irreducible dynamic susceptibility	8	1. One dimension	26
A. Truncation with bare interaction vertices	8	2. Square lattice	26
B. Vertex corrections	12	3. Simple cubic lattice	27
1. Equations of motion	12	References	28
2. Fixing four-point vertices via Ward identity and continuity condition	12		
3. Renormalized three-point vertex	13		
C. Integral equation for the irreducible dynamic susceptibility	14		
IV. Dissipative spin dynamics at infinite temperature	16		
A. General strategy	16		
B. Spin-diffusion coefficient in $d \geq 2$	17		
C. Spin diffusion on a body-centered cubic lattice including next-nearest-neighbor exchange	17		
D. Anomalous spin diffusion in reduced dimensions	18		
V. Dissipation energy and dynamic structure factor for all wavevectors	20		
A. One dimension	20		
B. Two dimensions	21		

I. INTRODUCTION

Calculating the dynamic spin-spin correlation function of quantum Heisenberg models in the paramagnetic regime is a challenging problem which requires advanced many-body techniques or large-scale numerical simulations. Even in the limit of infinite temperature the spin dynamics remains non-trivial. Hydrodynamic arguments suggest that for sufficiently small wavevectors \mathbf{k} and frequencies ω the Fourier transform $G(\mathbf{k}, \omega)$ of the retarded spin-spin correlation function of spin-rotationally invariant Heisenberg magnets has the diffusive form [1, 2]

$$G(\mathbf{k}, \omega) = G(\mathbf{k}) \frac{\mathcal{D}k^2}{\mathcal{D}k^2 - i\omega}, \quad (1.1)$$

where $G(\mathbf{k}) \equiv G(\mathbf{k}, 0)$ is the static (i.e., zero-frequency) limit of the spin-spin correlation function, and \mathcal{D} is the spin-diffusion coefficient. In the regime where the temperature T is large compared with the exchange energy,

the static correlation function $G(\mathbf{k})$ can be approximated by the susceptibility of an isolated spin S ,

$$G(\mathbf{k}) \approx \frac{S(S+1)}{3T}, \quad (1.2)$$

where the spin operator is normalized such that $S^2 = S(S+1)$. On the other hand, the calculation of the spin-diffusion coefficient \mathcal{D} remains highly non-trivial even in the limit $T \rightarrow \infty$. For three-dimensional Heisenberg magnets with nearest-neighbor exchange J the spin-diffusion coefficient is expected to approach a constant of order $|J|$ at high temperatures. Note that at infinite temperature \mathcal{D} is independent of the sign of J , indicating that a simple expansion in powers of J is not possible. In the 1960s and 1970s several approximate calculations of the numerical value of \mathcal{D} at high temperatures have been published [3–11]. Thereafter the interest in this problem has waned (see, however, Ref. [12 and 13]), although a convergence of the results for \mathcal{D} has not been achieved. Surprisingly, an experiment [14] measuring \mathcal{D} in the three-dimensional Heisenberg ferromagnet $\text{Rb}_2\text{CuBr}_4 \cdot 2\text{H}_2\text{O}$ at high temperatures produced a result which was consistently smaller (by a factor ranging between 0.5 and 0.7) than theoretical predictions [4–6, 8]. As far as we know, this discrepancy between theory and experiment has never been resolved. The authors of Ref. [14] speculated that methods based on the extrapolation of the short-time expansion of the spin-spin correlation function to long times [3–5, 7, 10–13] tend to overestimate the magnitude of the spin-diffusion coefficient. A numerical simulation [15] for classical Heisenberg models at infinite temperatures revealed long-time tails in dimensions $d = 1, 2, 3$ which are incompatible with a frequency-independent spin-diffusion coefficient assumed by hydrodynamics. It is not clear, however, whether in $d = 3$ the simulated systems are large enough to eliminate finite-size effects.

In $d = 1$ the problem of infinite-temperature spin-transport has recently been studied by several authors [16–24] using insights from the Bethe ansatz for integrable chains and state-of-the-art numerical methods. Most authors found that for $T = \infty$ the spin transport in isotropic spin chains is superdiffusive and can be described by a frequency-dependent diffusion coefficient $\mathcal{D}(\omega) \propto \omega^{-1/3}$. However, contrary to that, recent numerical simulations [22] based on tensor network methods predict at $T = \infty$ normal diffusion for non-integrable spin chains with $S > 1/2$. At this point the conditions for the persistence of superdiffusive spin dynamics in non-integrable spin chains are not completely understood [23, 24].

In this work we use recent advances in the application of functional renormalization group (FRG) methods to quantum spin systems [25–28] to calculate the dynamic spin-spin correlation function of Heisenberg magnets in the high-temperature limit. By integrating the truncated FRG flow equation for the suitably defined irreducible part of the spin-spin correlation function $G(\mathbf{k}, \omega)$

we derive an integral equation in momentum space which determines $G(\mathbf{k}, \omega)$ in the entire paramagnetic phase of a Heisenberg magnet on a d -dimensional Bravais lattice with arbitrary exchange interaction. We explicitly solve this equation in the limit of infinite temperature in dimensions $d = 1, 2, 3$. In three dimensions we find normal diffusion and explicitly calculate the numerical value of the spin-diffusion coefficient \mathcal{D} for Heisenberg magnets with nearest- and next-nearest-neighbor coupling on a simple cubic lattice. We also calculate \mathcal{D} for a body-centered cubic lattice describing the material $\text{Rb}_2\text{CuBr}_4 \cdot 2\text{H}_2\text{O}$ where experimental high-temperature data for \mathcal{D} are available [14]. It turns out that our result for \mathcal{D} is somewhat closer to the experimental value than previous theoretical predictions based on the extrapolation of the short-time expansion, although the measured value of \mathcal{D} is still smaller than predicted by theory. In two dimensions we find anomalous diffusion in the sense that the hydrodynamic form (1.1) should be generalized by replacing \mathcal{D} with a frequency-dependent function $\mathcal{D}(\omega)$ which diverges logarithmically for $\omega \rightarrow 0$. In $d = 1$ we find that the singularity is even stronger, $\mathcal{D}(\omega) \propto \omega^{-1/3}$; the usual dynamic scaling $\mathcal{D}(\omega)k^2 \propto \omega \propto k^z$ then implies the dynamical exponent $z = 3/2$, in agreement with the established result for integrable spin chains [16–24].

The spin functional renormalization group (SFRG) approach developed in this work also allows us to calculate $G(\mathbf{k}, \omega)$ for all wavevectors \mathbf{k} , including the short-wavelength regime which cannot be described by hydrodynamics. Therefore we parametrize the retarded spin-spin correlation function in the form

$$G(\mathbf{k}, \omega) = G(\mathbf{k}) \frac{\Delta(\mathbf{k}, \omega)}{\Delta(\mathbf{k}, \omega) - i\omega}, \quad (1.3)$$

and explicitly calculate the dissipation energy $\Delta(\mathbf{k}, \omega)$ at infinite temperature for all wavevectors \mathbf{k} in the first Brillouin zone. For a three-dimensional nearest-neighbor Heisenberg model on a cubic lattice we find that $\Delta(\mathbf{k}, 0)$ assumes a global maximum at the corners of the Brillouin zone. For Heisenberg magnets with interactions beyond nearest neighbors the momentum dependence of $\Delta(\mathbf{k}, \omega)$ in the first Brillouin zone leads to characteristic features in the dynamic structure factor which put constraints on the relative sign and strength of competing exchange interactions.

The rest of this article is organized as follows: In Sec. II we present a specific variant of the SFRG approach [25] which enables us to calculate the dynamic spin-spin correlation function in the paramagnetic regime of quantum Heisenberg models. We also write down exact flow equations for the suitably defined irreducible static self-energy $\Sigma(\mathbf{k})$ and the irreducible dynamic susceptibility $\tilde{\Pi}(\mathbf{k}, \omega)$ which is inversely proportional to the dissipation energy $\Delta(\mathbf{k}, \omega)$ defined via Eq. (1.3). In Sec. III we use constraints on the irreducible three-point and four-point vertices imposed by Ward identities and a continuity condition due to ergodicity to derive a truncated flow equation for $\tilde{\Pi}(\mathbf{k}, \omega)$. We then integrate this flow

equation to obtain an integral equation for the dissipation energy $\Delta(\mathbf{k}, \omega)$ which depends on the static spin-spin correlation function $G(\mathbf{k})$. Using the fact that in the high-temperature limit $G(\mathbf{k})$ can be obtained from a controlled expansion in powers of $1/T$, in Sec. IV we explicitly solve the integral equation for $\Delta(\mathbf{k}, \omega)$ in the limit of infinite temperature and calculate the resulting dynamic spin-spin correlation function $G(\mathbf{k}, \omega)$ in different dimensions. In Sec. V we discuss the behavior of the dissipation energy $\Delta(\mathbf{k}, \omega)$ defined via Eq. (1.3) and the corresponding dynamic structure factor as a function of \mathbf{k} in the first Brillouin zone. In the concluding Sec. VI we summarize our results and give an outlook on future applications of our method. Finally, in two appendices we present technical details of the solution of the integral equation for $\Delta(\mathbf{k}, \omega)$ on different lattices.

II. SFRG WITH CLASSICAL-QUANTUM DECOMPOSITION

In this section we shall develop a variant of the SFRG approach proposed in Ref. [25] which is specially tailored to the problem of calculating the dynamic spin-spin correlation function in the paramagnetic phase of spin-rotationally invariant quantum Heisenberg models with Hamiltonian

$$\mathcal{H} = \frac{1}{2} \sum_{ij} J_{ij} \mathbf{S}_i \cdot \mathbf{S}_j. \quad (2.1)$$

Here \mathbf{S}_i are spin- S operators localized at the sites \mathbf{R}_i of a d -dimensional Bravais lattice with lattice spacing a , where the index $i = 1, \dots, N$ labels the lattice sites. The exchange couplings J_{ij} are assumed to depend only on the difference $\mathbf{R}_i - \mathbf{R}_j$ so that they can be expanded in a Fourier series,

$$J_{ij} = \frac{1}{N} \sum_{\mathbf{k}} e^{i\mathbf{k} \cdot (\mathbf{R}_i - \mathbf{R}_j)} J(\mathbf{k}), \quad (2.2)$$

where the \mathbf{k} -sum is over the first Brillouin zone.

A. Subtracted exchange interaction and irreducible dynamic susceptibility

The basic idea of Ref. [25] is to replace the exchange couplings J_{ij} in the original Heisenberg model (2.1) by some continuous deformation J_{ij}^Λ and to derive a formally exact flow equation describing the evolution of the imaginary-time ordered connected spin correlation functions under changes of the deformation parameter Λ . For classical spin models this strategy has been implemented previously by Machado and Dupuis [29]. A related strategy has also been adopted for bosonic quantum lattice models [30–34]. Starting point is the deformed generating functional of the imaginary-time ordered connected

spin correlation functions of our deformed quantum spin model,

$$\mathcal{G}_\Lambda[\mathbf{h}] = \ln \text{Tr} \left[\mathcal{T} e^{\int_0^\beta d\tau [\sum_i \mathbf{h}_i(\tau) \cdot \mathbf{S}_i(\tau) - \frac{1}{2} \sum_{ij} J_{ij}^\Lambda \mathbf{S}_i(\tau) \cdot \mathbf{S}_j(\tau)]} \right], \quad (2.3)$$

where $\beta = 1/T$ denotes the inverse temperature, $\mathbf{h}_i(\tau)$ is fluctuating source magnetic field, \mathcal{T} denotes time-ordering in imaginary time, and the imaginary-time label τ of the spin operators $\mathbf{S}_i(\tau)$ keeps track of the time-ordering. By simply differentiating both sides of Eq. (2.3) with respect to the deformation parameter Λ we obtain the exact flow equation [25],

$$\partial_\Lambda \mathcal{G}_\Lambda[\mathbf{h}] = -\frac{1}{2} \int_0^\beta d\tau \sum_{ij, \alpha} (\partial_\Lambda J_{ij}^\Lambda) \left[\frac{\delta^2 \mathcal{G}_\Lambda[\mathbf{h}]}{\delta h_i^\alpha(\tau) \delta h_j^\alpha(\tau)} + \frac{\delta \mathcal{G}_\Lambda[\mathbf{h}]}{\delta h_i^\alpha(\tau)} \frac{\delta \mathcal{G}_\Lambda[\mathbf{h}]}{\delta h_j^\alpha(\tau)} \right], \quad (2.4)$$

where $\alpha = x, y, z$ labels the three Cartesian components of $\mathbf{h}_i(\tau)$. In principle, we can now introduce the (subtracted) Legendre transform of $\mathcal{G}_\Lambda[\mathbf{h}]$ in the usual way [35–39] and derive the corresponding Wetterich equation [40]. The problem with this procedure is that in a deformation scheme where at the initial value $\Lambda = 0$ of the deformation parameter the deformed exchange interaction vanishes the Legendre transform of $\mathcal{G}_{\Lambda=0}[\mathbf{h}]$ does not exist [27, 34] because for vanishing exchange couplings the spins do not have any dynamics. As already noticed in Refs. [25, 27, and 28], this problem can be avoided by introducing a hybrid functional which generates amputated correlation functions where the external interaction lines are removed. In this work we further develop this idea by noting that in the classical approximation where the time-dependence of all operators is simply neglected the Legendre transform of $\mathcal{G}_\Lambda[\mathbf{h}]$ does exist. It is therefore useful to decompose the source field $\mathbf{h}_i(\tau)$ into classical and quantum components. Technically, this can be achieved by expanding $\mathbf{h}_i(\tau)$ in frequency space and identifying the zero-frequency component with the classical source \mathbf{h}_i^c ,

$$\mathbf{h}_i(\tau) = T \sum_{\omega} e^{-i\omega\tau} \mathbf{h}_{i,\omega} = \mathbf{h}_i^c + \mathbf{h}_i^q(\tau), \quad (2.5)$$

where

$$\mathbf{h}_i^c = T \mathbf{h}_{i,\omega=0}, \quad (2.6a)$$

$$\mathbf{h}_i^q(\tau) = T \sum_{\omega \neq 0} e^{-i\omega\tau} \mathbf{h}_{i,\omega}. \quad (2.6b)$$

In frequency space this decomposition is equivalent with

$$\mathbf{h}_{i,\omega} = \beta \delta_{\omega,0} \mathbf{h}_i^c + (1 - \delta_{\omega,0}) \mathbf{h}_{i,\omega}^q. \quad (2.7)$$

Since in the classical sector the Legendre transform of $\mathcal{G}_\Lambda[\mathbf{h}^c]$ is well defined even for vanishing exchange coupling, it is convenient to introduce a hybrid functional

$\Gamma_\Lambda[\mathbf{m}^c, \boldsymbol{\eta}^q]$ which for vanishing quantum source $\boldsymbol{\eta}^q = 0$ reduces to the Legendre transform of the generating functional $\mathcal{G}_\Lambda[\mathbf{h}^c]$ with classical sources. To construct such a functional, recall that in the paramagnetic phase the imaginary-frequency spin-spin correlation function can be written as

$$G(\mathbf{k}, i\omega) = \frac{\Pi(\mathbf{k}, i\omega)}{1 + J(\mathbf{k})\Pi(\mathbf{k}, i\omega)}, \quad (2.8)$$

where $\Pi(\mathbf{k}, i\omega)$ is the interaction-irreducible part of $G(\mathbf{k}, i\omega)$. We shall refer to $\Pi(\mathbf{k}, i\omega)$ as the irreducible dynamic susceptibility. In the spin-diagram technique developed by Vaks, Larkin, and Pikin [41, 42] (see also the textbook by Izyumov and Skryabin [43]) the function $\Pi(\mathbf{k}, i\omega)$ is the sum of all diagrams contributing to $G(\mathbf{k}, i\omega)$ which cannot be separated into two parts by cutting a single interaction line representing $J(\mathbf{k})$. For our purpose, it is more convenient to parametrize the spin-spin correlation function in a slightly different way,

$$G(\mathbf{k}, i\omega) = \frac{\tilde{\Pi}(\mathbf{k}, i\omega)}{1 + \tilde{J}(\mathbf{k})\tilde{\Pi}(\mathbf{k}, i\omega)}, \quad (2.9)$$

where the subtracted exchange interaction is defined by

$$\tilde{J}(\mathbf{k}) \equiv J(\mathbf{k}) + \Pi^{-1}(\mathbf{k}, 0). \quad (2.10)$$

Combining this with the definition of $G(\mathbf{k}, 0) \equiv G(\mathbf{k})$ in Eq. (2.8) we find

$$\frac{1}{\tilde{J}(\mathbf{k})} = \frac{1}{J(\mathbf{k}) + \Pi^{-1}(\mathbf{k}, 0)} = \frac{\Pi(\mathbf{k}, 0)}{1 + J(\mathbf{k})\Pi(\mathbf{k}, 0)} = G(\mathbf{k}), \quad (2.11)$$

i.e., our subtracted exchange interaction $\tilde{J}(\mathbf{k})$ is the inverse of the static spin-spin correlation function $G(\mathbf{k})$. Using the definitions (2.8)–(2.10), we conclude that for finite frequency the irreducible susceptibility $\Pi(\mathbf{k}, i\omega)$ and its subtracted counterpart are related as follows

$$\tilde{\Pi}^{-1}(\mathbf{k}, i\omega) \equiv \Pi^{-1}(\mathbf{k}, i\omega) - \Pi^{-1}(\mathbf{k}, 0). \quad (2.12)$$

For vanishing exchange interaction the imaginary frequency spin-spin correlation function has a non-analytic frequency dependence,

$$G_0(\mathbf{k}, i\omega) = \Pi_0(\mathbf{k}, i\omega) = \delta_{\omega,0} \frac{b'_0}{T}, \quad (2.13)$$

where

$$b'_0 = \frac{S(S+1)}{3} \quad (2.14)$$

is the first order coefficient in the Taylor expansion of the spin- S Brillouin function

$$\begin{aligned} b(y) &= \left(S + \frac{1}{2}\right) \coth \left[\left(S + \frac{1}{2}\right) y \right] - \frac{1}{2} \coth \left[\frac{y}{2} \right] \\ &= b'_0 y + \mathcal{O}(y^3). \end{aligned} \quad (2.15)$$

Whether or not such a non-analytic contribution proportional to $\delta_{\omega,0}$ survives for finite exchange coupling is closely related to the ergodicity of the system and the distinction between the isolated (Kubo) susceptibility and the isothermal susceptibility [45–49]. Note that for $\mathbf{k} = 0$ the zero-frequency limit of the finite-frequency thermal spin-spin correlation function $G(\mathbf{k} = 0, i\omega)$ gives the isolated (Kubo) susceptibility, which in general does not agree with the isothermal susceptibility defined via the derivative of the magnetization with respect to an external magnetic field at constant temperature [45–49]. However, as recently shown by Chiba *et al.* [49], under conditions similar to the eigenstate thermalization hypothesis [50], at finite momentum $\mathbf{k} \neq 0$ all static susceptibilities agree. This rules out a non-analytic contribution to the thermal spin-spin correlation function $G(\mathbf{k}, i\omega)$ similar to Eq. (2.13) for finite exchange coupling and finite \mathbf{k} . Consequently, in this case the irreducible susceptibility $\Pi(\mathbf{k}, i\omega)$ is expected to be a continuous function of ω , so that for finite exchange coupling and finite momentum we conclude from Eq. (2.12) that in the zero-frequency limit the inverse of the irreducible subtracted susceptibility defined via Eqs. (2.9) and (2.10) vanishes,

$$\tilde{\Pi}^{-1}(\mathbf{k} \neq 0, 0) \equiv \lim_{\omega \rightarrow 0} \tilde{\Pi}^{-1}(\mathbf{k} \neq 0, i\omega) = 0. \quad (2.16)$$

We shall refer to Eq. (2.16) as the *continuity condition*.

B. Hybrid functional and generalized Wetterich equation

Let us write the deformed exchange interaction in momentum space in the form

$$J_\Lambda(\mathbf{k}) = J(\mathbf{k}) + R_\Lambda(\mathbf{k}), \quad (2.17)$$

where $R_\Lambda(\mathbf{k})$ is some momentum dependent regulator which vanishes at $\Lambda = 1$ where we recover our original model. The deformed spin-spin correlation function can then be written in two equivalent ways,

$$G_\Lambda(\mathbf{k}, i\omega) = \frac{\Pi_\Lambda(\mathbf{k}, i\omega)}{1 + J_\Lambda(\mathbf{k})\Pi_\Lambda(\mathbf{k}, i\omega)} \quad (2.18a)$$

$$= \frac{\tilde{\Pi}_\Lambda(\mathbf{k}, i\omega)}{1 + \tilde{J}_\Lambda(\mathbf{k})\tilde{\Pi}_\Lambda(\mathbf{k}, i\omega)}, \quad (2.18b)$$

where the deformed subtracted exchange interaction is defined analogously to $\tilde{J}(\mathbf{k})$ in Eq. (2.10),

$$\tilde{J}_\Lambda(\mathbf{k}) = J_\Lambda(\mathbf{k}) + \Pi_\Lambda^{-1}(\mathbf{k}, 0) = G_\Lambda^{-1}(\mathbf{k}, 0) \equiv G_\Lambda^{-1}(\mathbf{k}). \quad (2.19)$$

The subtracted irreducible susceptibility therefore satisfies by construction the continuity condition

$$\tilde{\Pi}_\Lambda^{-1}(\mathbf{k} \neq 0, 0) = 0, \quad (2.20)$$

which generalizes the condition (2.16) for all values of the deformation parameter Λ .

Our aim is to derive exact FRG flow equations for the static self-energy

$$\Sigma_\Lambda(\mathbf{k}) \equiv \Pi_\Lambda^{-1}(\mathbf{k}, 0) \quad (2.21)$$

and for the subtracted irreducible dynamic susceptibility $\tilde{\Pi}_\Lambda(\mathbf{k}, i\omega)$ defined via Eq. (2.18b). To construct the corresponding generating functional, we first introduce the auxiliary functional

$$\mathcal{F}_\Lambda[\mathbf{h}^c, \mathbf{s}^q] = \mathcal{G}_\Lambda[\mathbf{h}^c - \tilde{\mathbf{J}}_\Lambda \mathbf{s}^q] - \frac{1}{2}(\mathbf{s}^q, \tilde{\mathbf{J}}_\Lambda \mathbf{s}^q), \quad (2.22)$$

which depends on the classical component \mathbf{h}_i^c of the source field $\mathbf{h}_i(\tau)$ defined in Eq. (2.6a) and on a quantum field $\mathbf{s}_i^q(\tau)$ which is introduced via the following substitution of the quantum component $\mathbf{h}_i^q(\tau)$ of the source field defined in Eq. (2.6b),

$$\mathbf{h}_i^q(\tau) = -[\tilde{\mathbf{J}}_\Lambda \mathbf{s}^q]_{i\tau} = -\sum_j \tilde{J}_{ij}^\Lambda \mathbf{s}_j^q(\tau). \quad (2.23)$$

In Eq. (2.22) the symbol $\tilde{\mathbf{J}}_\Lambda$ represents an infinite matrix in the site label i and imaginary time τ ,

$$[\tilde{\mathbf{J}}_\Lambda]_{i\tau, j\tau'} = \delta(\tau - \tau') \tilde{J}_{ij}^\Lambda, \quad (2.24)$$

and the last term in Eq. (2.22) is a short notation for

$$(\mathbf{s}^q, \tilde{\mathbf{J}}_\Lambda \mathbf{s}^q) = \int_0^\beta d\tau \sum_{ij} \tilde{J}_{ij}^\Lambda \mathbf{s}_i^q(\tau) \cdot \mathbf{s}_j^q(\tau). \quad (2.25)$$

Differentiation of the auxiliary functional $\mathcal{F}_\Lambda[\mathbf{h}^c, \mathbf{s}^q]$ defined in Eq. (2.22) with respect to the source fields generates connected correlation functions which are partially amputated in the quantum sector. The corresponding two-point function at finite frequencies can then be interpreted as an effective, subtracted exchange interaction, while higher order correlation functions can be obtained from their connected counterparts by multiplying

the quantum legs by factors of $-\tilde{\mathbf{J}}_\Lambda$. A related auxiliary functional has been introduced in Ref. [27]. Our hybrid functional with the desired properties is now given by the subtracted Legendre transform of the above auxiliary functional $\mathcal{F}_\Lambda[\mathbf{h}^c, \mathbf{s}^q]$,

$$\Gamma_\Lambda[\mathbf{m}^c, \boldsymbol{\eta}^q] = (\mathbf{m}^c, \mathbf{h}^c) + (\boldsymbol{\eta}^q, \mathbf{s}^q) - \mathcal{F}_\Lambda[\mathbf{h}^c, \mathbf{s}^q] - \frac{1}{2}(\mathbf{m}^c, \mathbf{R}_\Lambda^c \mathbf{m}^c) - \frac{1}{2}(\boldsymbol{\eta}^q, \mathbf{R}_\Lambda^q \boldsymbol{\eta}^q), \quad (2.26)$$

where on the right-hand side we should substitute $\mathbf{h}^c = \mathbf{h}^c[\mathbf{m}^c, \boldsymbol{\eta}^q]$ and $\mathbf{s}^q = \mathbf{s}^q[\mathbf{m}^c, \boldsymbol{\eta}^q]$ as functionals of \mathbf{m}^c and $\boldsymbol{\eta}^q$ by inverting the relations

$$\mathbf{m}^c = \frac{\delta \mathcal{F}_\Lambda[\mathbf{h}^c, \mathbf{s}^q]}{\delta \mathbf{h}^c}, \quad (2.27)$$

$$\boldsymbol{\eta}^q = \frac{\delta \mathcal{F}_\Lambda[\mathbf{h}^c, \mathbf{s}^q]}{\delta \mathbf{s}^q}. \quad (2.28)$$

The regulator matrices in Eq. (2.26) are in the momentum-time domain given by

$$[\mathbf{R}_\Lambda^\alpha]_{\mathbf{k}\tau, \mathbf{k}'\tau'} = \delta(\tau - \tau') \delta(\mathbf{k} + \mathbf{k}') R_\Lambda^\alpha(\mathbf{k}), \quad \alpha = c, q, \quad (2.29)$$

with

$$R_\Lambda^c(\mathbf{k}) = J_\Lambda(\mathbf{k}) - J(\mathbf{k}) = R_\Lambda(\mathbf{k}), \quad (2.30a)$$

$$R_\Lambda^q(\mathbf{k}) = -\frac{1}{\tilde{J}_\Lambda(\mathbf{k})} + \frac{1}{\tilde{J}(\mathbf{k})}. \quad (2.30b)$$

Here the δ -symbol in wavevector space is defined by $\delta(\mathbf{k}) = N\delta_{\mathbf{k},0}$.

After some standard manipulations similar to those outlined in Ref. [27] we find that the hybrid functional $\Gamma_\Lambda[\mathbf{m}^c, \boldsymbol{\eta}^q]$ defined in Eq. (2.26) satisfies the generalized Wetterich equation

$$\begin{aligned} \partial_\Lambda \Gamma_\Lambda[\mathbf{m}^c, \boldsymbol{\eta}^q] &= \frac{1}{2} \text{Tr} \left\{ \left[(\boldsymbol{\Gamma}_\Lambda''[\mathbf{m}^c, \boldsymbol{\eta}^q] + \mathbf{R}_\Lambda)^{-1} + \mathbf{J}_\Lambda^q \right] \dot{\mathbf{R}}_\Lambda \right\} \\ &\quad - \frac{1}{2} \sum_{ij} (\partial_\Lambda \Sigma_{ij}^\Lambda) \int_0^\beta d\tau d\tau' \delta^q(\tau - \tau') \left(\frac{\delta \Gamma_\Lambda}{\delta \boldsymbol{\eta}_i^q(\tau)} + [\tilde{\mathbf{J}}^{-1} \boldsymbol{\eta}^q]_{i\tau} \right) \cdot \left(\frac{\delta \Gamma_\Lambda}{\delta \boldsymbol{\eta}_j^q(\tau')} + [\tilde{\mathbf{J}}^{-1} \boldsymbol{\eta}^q]_{j\tau'} \right), \end{aligned} \quad (2.31)$$

where

$$\Sigma_{ij}^\Lambda = \frac{1}{N} \sum_{\mathbf{k}} e^{i\mathbf{k} \cdot (\mathbf{R}_i - \mathbf{R}_j)} \Sigma_\Lambda(\mathbf{k}) \quad (2.32)$$

is the real-space Fourier transform of the flowing static self-energy, the finite-frequency part of the periodic imaginary-time δ -function $\delta(\tau) = T \sum_\omega e^{i\omega\tau}$ is denoted

by

$$\delta^q(\tau) = T \sum_{\omega \neq 0} e^{i\omega\tau} = \delta(\tau) - T, \quad (2.33)$$

and the matrix $\boldsymbol{\Gamma}_\Lambda''[\mathbf{m}^c, \boldsymbol{\eta}^q]$ of second functional derivatives of $\Gamma_\Lambda[\mathbf{m}^c, \boldsymbol{\eta}^q]$ is explicitly given by

$$(\boldsymbol{\Gamma}_\Lambda''[\mathbf{m}^c, \boldsymbol{\eta}^q])_{i\tau\alpha, j\tau'\alpha'} = \frac{\delta^2 \Gamma_\Lambda[\mathbf{m}^c, \boldsymbol{\eta}^q]}{\delta \Phi_i^\alpha(\tau) \delta \Phi_j^{\alpha'}(\tau')}. \quad (2.34)$$

Here we have combined the components of \mathbf{m}_i^c and $\boldsymbol{\eta}_i^q(\tau)$ into a six-component field

$$\begin{pmatrix} \Phi_i^{m_x}(\tau) \\ \Phi_i^{m_y}(\tau) \\ \Phi_i^{m_z}(\tau) \\ \Phi_i^{\eta_x}(\tau) \\ \Phi_i^{\eta_y}(\tau) \\ \Phi_i^{\eta_z}(\tau) \end{pmatrix} = \begin{pmatrix} m_{x,i}^c \\ m_{y,i}^c \\ m_{z,i}^c \\ \eta_{x,i}^q(\tau) \\ \eta_{y,i}^q(\tau) \\ \eta_{z,i}^q(\tau) \end{pmatrix} = \begin{pmatrix} \mathbf{m}_i^c \\ \boldsymbol{\eta}_i^q(\tau) \end{pmatrix}. \quad (2.35)$$

The regulator matrix \mathbf{R}_Λ and the matrix \mathbf{J}_Λ^q in the generalized Wetterich equation (2.31) have the following block structure in the space of field components,

$$\mathbf{R}_\Lambda = \begin{pmatrix} \mathbf{R}_\Lambda^c & 0 \\ 0 & \mathbf{R}_\Lambda^q \end{pmatrix}, \quad \mathbf{J}_\Lambda^q = \begin{pmatrix} 0 & 0 \\ 0 & \tilde{\mathbf{J}}_\Lambda \end{pmatrix}, \quad (2.36)$$

and the matrix $\dot{\mathbf{R}}_\Lambda$ is defined by

$$\dot{\mathbf{R}}_\Lambda \equiv \begin{pmatrix} \partial_\Lambda \mathbf{J}_\Lambda & 0 \\ 0 & \tilde{\mathbf{J}}_\Lambda^{-1} [\partial_\Lambda \mathbf{J}_\Lambda] \tilde{\mathbf{J}}_\Lambda^{-1} \end{pmatrix}, \quad (2.37)$$

where the deformed exchange interaction matrix

$$[\mathbf{J}_\Lambda]_{i\tau, j\tau'} = \delta(\tau - \tau') J_{ij}^\Lambda \quad (2.38)$$

is defined analogously to its subtracted counterpart in Eq. (2.24). Note that $\dot{\mathbf{R}}_\Lambda \neq \partial_\Lambda \mathbf{R}_\Lambda$, because by taking the Λ -derivative of $\Gamma_\Lambda[\mathbf{m}^c, \boldsymbol{\eta}^q]$ in Eq. (2.26) we generate only terms involving derivatives $\partial_\Lambda \mathbf{J}_\Lambda$ of the deformed bare coupling; due to the Λ -dependent subtraction $\Pi_\Lambda^{-1}(\mathbf{k}, 0)$ in the definition (2.19) of $\tilde{J}_\Lambda(\mathbf{k})$, the quan-

tum sector of the matrix $\dot{\mathbf{R}}_\Lambda$ is therefore in general different from $\partial_\Lambda \mathbf{R}_\Lambda^q$. Diagrammatically, the vertices generated by $\Gamma_\Lambda[\mathbf{m}^c, \boldsymbol{\eta}^q]$ are classical propagator irreducible, i.e. the diagrams contributing to the vertices cannot be separated into two parts by cutting a single classical propagator line representing $G_\Lambda(\mathbf{k}, 0)$. Moreover, for finite frequencies the vertices generated by $\Gamma_\Lambda[\mathbf{m}^c, \boldsymbol{\eta}^q]$ are also interaction-irreducible, which means that diagrammatically the vertices generated by expanding $\Gamma_\Lambda[\mathbf{m}^c, \boldsymbol{\eta}^q]$ in powers of $\boldsymbol{\eta}^q$ cannot be separated into two parts by cutting a single effective interaction line representing $\tilde{J}_\Lambda(\mathbf{k})$. Note that the last term on the right-hand side of Eq. (2.31), which is absent in the usual Wetterich equation,[40] is generated by the scale-dependent subtraction $\Pi_\Lambda^{-1}(\mathbf{k}, 0) = \Sigma_\Lambda(\mathbf{k})$ in the definition (2.19) of $\tilde{J}_\Lambda(\mathbf{k})$. This term gives rise to local tree contributions to the flow equations for the vertex functions which do not contribute to the flow of $\Sigma_\Lambda(\mathbf{k})$ or any other static irreducible vertices, due to the subtraction of the time-independent contribution in the second line of Eq. (2.31).

C. Vertex expansion

The generalized Wetterich equation (2.31) implies an infinite hierarchy of exact FRG flow equations for the irreducible vertices which can be obtained by expanding the functional $\Gamma_\Lambda[\mathbf{m}^c, \boldsymbol{\eta}^q]$ in powers of the fields. Let us first consider the vertex expansion in the classical sector, which is obtained by setting $\boldsymbol{\eta}^q = 0$. To simplify our notation, let us rename $\mathbf{m}^c \rightarrow \mathbf{m}$. In the paramagnetic regime the classical magnetization field \mathbf{m} vanishes for vanishing external magnetic fields, so that the first few terms of the vertex expansion in the classical sector are

$$\begin{aligned} \Gamma_\Lambda[\mathbf{m}, 0] &= \Gamma_\Lambda[0, 0] + \frac{\beta}{2!} \int_{\mathbf{k}} [J(\mathbf{k}) + \Sigma_\Lambda(\mathbf{k})] \mathbf{m}_{-\mathbf{k}} \cdot \mathbf{m}_{\mathbf{k}} \\ &+ \beta \int_{\mathbf{k}_1} \int_{\mathbf{k}_2} \int_{\mathbf{k}_3} \int_{\mathbf{k}_4} \delta(\mathbf{k}_1 + \mathbf{k}_2 + \mathbf{k}_3 + \mathbf{k}_4) \left\{ \frac{1}{(2!)^2} \Gamma_\Lambda^{-++}(k_1, k_2, k_3, k_4) m_{\mathbf{k}_1}^- m_{\mathbf{k}_2}^- m_{\mathbf{k}_3}^+ m_{\mathbf{k}_4}^+ \right. \\ &+ \frac{1}{2!} \Gamma_\Lambda^{-zz}(k_1, k_2, k_3, k_4) m_{\mathbf{k}_1}^- m_{\mathbf{k}_2}^+ m_{\mathbf{k}_3}^z m_{\mathbf{k}_4}^z + \frac{1}{4!} \Gamma_\Lambda^{zzzz}(k_1, k_2, k_3, k_4) m_{\mathbf{k}_1}^z m_{\mathbf{k}_2}^z m_{\mathbf{k}_3}^z m_{\mathbf{k}_4}^z \left. \right\} + \dots, \quad (2.39) \end{aligned}$$

where $\int_{\mathbf{k}} = \frac{1}{N} \sum_{\mathbf{k}}$, the interaction vertices are given in the spherical basis with $m_{\mathbf{k}}^\pm = (m_{\mathbf{k}}^x \pm i m_{\mathbf{k}}^y)/\sqrt{2}$, and we have omitted vertices with five and more external legs. Note that by adding to the coefficient of the quadratic term in Eq. (2.39) the regulator $R_\Lambda(\mathbf{k})$ we obtain

$$\begin{aligned} J(\mathbf{k}) + \Sigma_\Lambda(\mathbf{k}) + R_\Lambda(\mathbf{k}) &= J_\Lambda(\mathbf{k}) + \Sigma_\Lambda(\mathbf{k}) \\ &= J_\Lambda(\mathbf{k}) + \Pi_\Lambda^{-1}(\mathbf{k}, 0) = G_\Lambda^{-1}(\mathbf{k}, 0) \equiv G_\Lambda^{-1}(\mathbf{k}), \quad (2.40) \end{aligned}$$

which can be identified with the inverse of the deformed static spin-spin correlation function defined via Eq. (2.18a). In a cutoff scheme where for $\Lambda = 0$ the

deformed exchange coupling vanishes, $J_{\Lambda=0}(\mathbf{k}) = 0$, we see from Eq. (2.13) that the classical self-energy $\Sigma_\Lambda(\mathbf{k})$ satisfies the initial condition

$$\Sigma_0(\mathbf{k}) = T/b'_0, \quad (2.41)$$

with $b'_0 = S(S+1)/3$, see Eq. (2.14). To determine the initial values for the classical four-point vertices in Eq. (2.39) in a cutoff scheme with initially vanishing exchange interaction, we use the tree expansion [37] to relate these vertices to the corresponding four-spin corre-

lation functions [28, 37],

$$G_{\Lambda}^{++--}(\mathbf{k}_1, \mathbf{k}_2, \mathbf{k}_3, \mathbf{k}_4) = -G_{\Lambda}(\mathbf{k}_1)G_{\Lambda}(\mathbf{k}_2)G_{\Lambda}(\mathbf{k}_3)G_{\Lambda}(\mathbf{k}_4) \\ \times \Gamma_{\Lambda}^{-++-}(-\mathbf{k}_1, -\mathbf{k}_2, -\mathbf{k}_3, -\mathbf{k}_4), \quad (2.42a)$$

$$G_{\Lambda}^{+-zz}(\mathbf{k}_1, \mathbf{k}_2, \mathbf{k}_3, \mathbf{k}_4) = -G_{\Lambda}(\mathbf{k}_1)G_{\Lambda}(\mathbf{k}_2)G_{\Lambda}(\mathbf{k}_3)G_{\Lambda}(\mathbf{k}_4) \\ \times \Gamma_{\Lambda}^{-+zz}(-\mathbf{k}_1, -\mathbf{k}_2, -\mathbf{k}_3, -\mathbf{k}_4), \quad (2.42b)$$

$$G_{\Lambda}^{zzzz}(\mathbf{k}_1, \mathbf{k}_2, \mathbf{k}_3, \mathbf{k}_4) = -G_{\Lambda}(\mathbf{k}_1)G_{\Lambda}(\mathbf{k}_2)G_{\Lambda}(\mathbf{k}_3)G_{\Lambda}(\mathbf{k}_4) \\ \times \Gamma_{\Lambda}^{zzzz}(-\mathbf{k}_1, -\mathbf{k}_2, -\mathbf{k}_3, -\mathbf{k}_4). \quad (2.42c)$$

For vanishing exchange coupling $G_0(\mathbf{k}) = \beta b'_0$ and

$$G_0^{++--}(\mathbf{k}_1, \mathbf{k}_2, \mathbf{k}_3, \mathbf{k}_4) = \frac{2}{3}\beta^3 b_0''', \quad (2.43a)$$

$$G_0^{+-zz}(\mathbf{k}_1, \mathbf{k}_2, \mathbf{k}_3, \mathbf{k}_4) = \frac{1}{3}\beta^3 b_0''', \quad (2.43b)$$

$$G_0^{zzzz}(\mathbf{k}_1, \mathbf{k}_2, \mathbf{k}_3, \mathbf{k}_4) = \beta^3 b_0''', \quad (2.43c)$$

where b_0''' is the third order coefficient in the Taylor expansion of the spin- S Brillouin function $b(y)$ given in Eq. (2.15),

$$b(y) = b'_0 y + \frac{1}{3!} b_0''' y^3 + \mathcal{O}(y^5). \quad (2.44)$$

Explicitly,

$$b'_0 = \frac{(2S+1)^2 - 1}{12} = \frac{S(S+1)}{3}, \quad (2.45a)$$

$$b_0''' = -\frac{(2S+1)^4 - 1}{120} = -\frac{6}{5}b'_0 \left(b'_0 + \frac{1}{6}\right). \quad (2.45b)$$

The initial values of the classical four-point vertices in Eq. (2.39) in a cutoff scheme where for $\Lambda = 0$ the exchange interaction is completely switched off are therefore

$$\Gamma_0^{-++-}(\mathbf{k}_1, \mathbf{k}_2, \mathbf{k}_3, \mathbf{k}_4) = -\frac{2T}{3} \frac{b_0'''}{(b'_0)^4}, \quad (2.46a)$$

$$\Gamma_0^{-+zz}(\mathbf{k}_1, \mathbf{k}_2, \mathbf{k}_3, \mathbf{k}_4) = -\frac{T}{3} \frac{b_0'''}{(b'_0)^4}, \quad (2.46b)$$

$$\Gamma_0^{zzzz}(\mathbf{k}_1, \mathbf{k}_2, \mathbf{k}_3, \mathbf{k}_4) = -T \frac{b_0'''}{(b'_0)^4}. \quad (2.46c)$$

In order to calculate correlation functions at finite frequencies, we have to include also the quantum vertices in the expansion of our generating functional $\Gamma_{\Lambda}[\mathbf{m}, \boldsymbol{\eta}]$, where for notational simplicity we have renamed the quantum field $\boldsymbol{\eta}^a \rightarrow \boldsymbol{\eta}$. Apart from pure quantum vertices involving only the $\boldsymbol{\eta}$ -field, the vertex expansion contains also various types of mixed vertices,

$$\Gamma_{\Lambda}[\mathbf{m}, \boldsymbol{\eta}] = \Gamma_{\Lambda}[\mathbf{m}, 0] - \frac{1}{2} \int_K \left[\tilde{J}^{-1}(\mathbf{k}) + \tilde{\Pi}_{\Lambda}(K) \right] \boldsymbol{\eta}_{-K} \cdot \boldsymbol{\eta}_K \\ + [\text{green}] \eta^- \eta^+ \eta^z + \frac{1}{3!} [\text{green}] \eta^z \eta^z \eta^z + \frac{1}{(2!)^2} [\text{red}] \eta^- \eta^- \eta^+ \eta^+ + \frac{1}{2!} [\text{red}] \eta^- \eta^+ \eta^z \eta^z + \frac{1}{4!} [\text{red}] \eta^z \eta^z \eta^z \eta^z \\ + [\text{green}] m^- \eta^+ \eta^z + [\text{green}] m^+ \eta^z \eta^- + [\text{green}] m^z \eta^- \eta^+ + \frac{1}{2!} [m^z \eta^z \eta^z] \\ + [\text{blue}] m^- m^+ \eta^- \eta^+ + \frac{1}{(2!)^2} [m^+ m^+ \eta^- \eta^-] + \frac{1}{(2!)^2} [m^- m^- \eta^+ \eta^+] + \frac{1}{(2!)^2} [m^z m^z \eta^z \eta^z] \\ + \frac{1}{2!} [\text{blue}] m^- m^+ \eta^z \eta^z + \frac{1}{2!} [\text{pink}] m^z m^z \eta^- \eta^+ + [m^- m^z \eta^+ \eta^z] + [m^+ m^z \eta^- \eta^z] \\ + [m\eta\eta\eta]\text{-vertices} + \text{terms with } n > 4 \text{ fields}. \quad (2.47)$$

Here $\int_K = \frac{1}{\beta N} \sum_{\mathbf{k}, \omega}$ and $K = (\mathbf{k}, i\omega)$ is a collective label for wavevector and Matsubara frequency. For later reference we have marked the vertices by various colors which match the colors in Fig. 1 and in the exact flow equations (2.50) and (2.51) given below. We have also introduced the short notation

$$[\text{green}] \eta^- \eta^+ \eta^z = \int_{K_1} \int_{K_2} \int_{K_3} \delta(K_1 + K_2 + K_3) \Gamma_{\Lambda}^{\eta^- \eta^+ \eta^z}(K_1, K_2, K_3) \eta_{K_1}^- \eta_{K_2}^+ \eta_{K_3}^z, \quad (2.48)$$

$$[\text{red}] \eta^- \eta^- \eta^+ \eta^+ = \int_{K_1} \int_{K_2} \int_{K_3} \int_{K_4} \delta(K_1 + K_2 + K_3 + K_4) \Gamma_{\Lambda}^{\eta^- \eta^- \eta^+ \eta^+}(K_1, K_2, K_3, K_4) \eta_{K_1}^- \eta_{K_2}^- \eta_{K_3}^+ \eta_{K_4}^+, \quad (2.49)$$

where $\delta(K) = \beta N \delta_{\mathbf{k}, 0} \delta_{\omega, 0}$. The other terms are defined similarly with the convention that in all expressions involving classical fluctuations we should set $\mathbf{m}_K = \beta \delta_{\omega, 0} \mathbf{m}_{\mathbf{k}}$, so that the frequencies associated with the classical magnetization field \mathbf{m}_K vanish. Note that there are no vertices of the type $[mm\eta]$ and $[mmm\eta]$ because the m -field does not transfer any frequency. The initial value of the vertices in Eq. (2.47) in a cutoff scheme where the exchange interaction is initially switched off are rather complicated and will be discussed in Sec. III A.

D. Exact flow equations for the two-point vertices

Substituting the vertex expansions (2.39) and (2.47) into the generalized Wetterich equation (2.31) we obtain FRG flow equations for the vertices. In particular, the classical self-energy $\Sigma_\Lambda(\mathbf{k})$ appearing in the quadratic part of Eq. (2.39) satisfies the exact flow equation

$$\begin{aligned} \partial_\Lambda \Sigma_\Lambda(\mathbf{k}) = & T \int_{\mathbf{q}} \dot{G}_\Lambda(\mathbf{q}) \left[\Gamma_\Lambda^{-++}(-\mathbf{k}, -\mathbf{q}, \mathbf{q}, \mathbf{k}) + \frac{1}{2!} \Gamma_\Lambda^{-+zz}(-\mathbf{k}, \mathbf{k}, -\mathbf{q}, \mathbf{q}) \right] \\ & + T \sum_{\omega' \neq 0} \int_{\mathbf{q}} \dot{G}_\Lambda^\eta(Q) \left[\Gamma_\Lambda^{m^- m^+ \eta^- \eta^+}(-\mathbf{k}, \mathbf{k}, -Q, Q) + \frac{1}{2!} \Gamma_\Lambda^{m^- m^+ \eta^z \eta^z}(-\mathbf{k}, \mathbf{k}, -Q, Q) \right] \\ & - T \sum_{\omega' \neq 0} \int_{\mathbf{q}} [G_\Lambda^\eta(Q) G_\Lambda^\eta(Q + \mathbf{k})]^\bullet \Gamma_\Lambda^{m^- \eta^+ \eta^z}(-\mathbf{k}, -Q, Q + \mathbf{k}) \Gamma_\Lambda^{m^+ \eta^- \eta^z}(\mathbf{k}, Q, -Q - \mathbf{k}), \end{aligned} \quad (2.50)$$

while the interaction-irreducible subtracted dynamic susceptibility $\tilde{\Pi}_\Lambda(K)$ in the quadratic part of Eq. (2.47) satisfies

$$\begin{aligned} -\partial_\Lambda \tilde{\Pi}_\Lambda(K) = & T \sum_{\omega' \neq 0} \int_{\mathbf{q}} \dot{G}_\Lambda^\eta(Q) \left[\Gamma_\Lambda^{\eta^- \eta^- \eta^+ \eta^+}(-K, -Q, Q, K) + \frac{1}{2!} \Gamma_\Lambda^{\eta^- \eta^+ \eta^z \eta^z}(-K, K, -Q, Q) \right] \\ & + T \int_{\mathbf{q}} \dot{G}_\Lambda(\mathbf{q}) \left[\Gamma_\Lambda^{m^- m^+ \eta^- \eta^+}(-\mathbf{q}, \mathbf{q}, -K, K) + \frac{1}{2!} \Gamma_\Lambda^{m^z m^z \eta^- \eta^+}(-\mathbf{q}, \mathbf{q}, -K, K) \right] \\ & - T \int_{\mathbf{q}} \left\{ [G_\Lambda(\mathbf{q}) G_\Lambda^\eta(\mathbf{q} + K)]^\bullet \Gamma_\Lambda^{m^z \eta^- \eta^+}(-\mathbf{q}, -K, \mathbf{q} + K) \Gamma_\Lambda^{m^z \eta^- \eta^+}(\mathbf{q}, -\mathbf{q} - K, K) + (K \rightarrow -K) \right\} \\ & - T \sum_{\omega' \neq 0} \int_{\mathbf{q}} [G_\Lambda^\eta(Q) G_\Lambda^\eta(Q + K)]^\bullet \Gamma_\Lambda^{\eta^- \eta^+ \eta^z}(-K, K + Q, -Q) \Gamma_\Lambda^{\eta^- \eta^+ \eta^z}(-K - Q, K, Q) \\ & - \tilde{\Pi}_\Lambda^2(K) \partial_\Lambda \Sigma_\Lambda(\mathbf{k}). \end{aligned} \quad (2.51)$$

Here the external momentum-frequency label is denoted by $K = (\mathbf{k}, i\omega)$, the loop momentum-frequency is $Q = (\mathbf{q}, i\omega')$, and the symbol $\mathbf{q} + K$ represents $(\mathbf{q} + \mathbf{k}, i\omega)$ where the frequency ω belongs to K . The deformed classical propagator

$$G_\Lambda(\mathbf{k}) = \frac{1}{J_\Lambda(\mathbf{k}) + \Sigma_\Lambda(\mathbf{k})} \quad (2.52)$$

has already been defined in Eq. (2.40), and the corresponding single-scale propagator is

$$\dot{G}_\Lambda(\mathbf{k}) \equiv -G_\Lambda^2(\mathbf{k}) \partial_\Lambda J_\Lambda(\mathbf{k}) = -G_\Lambda^2(\mathbf{k}) \partial_\Lambda R_\Lambda(\mathbf{k}). \quad (2.53)$$

The quantum propagator and its single-scale counterpart are

$$G_\Lambda^\eta(K) = -F_\Lambda(K) \equiv -\frac{\tilde{J}_\Lambda(\mathbf{k})}{1 + \tilde{J}_\Lambda(\mathbf{k}) \tilde{\Pi}_\Lambda(K)}, \quad (2.54a)$$

$$\dot{G}_\Lambda^\eta(K) = -\dot{F}_\Lambda(K) \equiv -\frac{\partial_\Lambda J_\Lambda(\mathbf{k})}{[1 + \tilde{J}_\Lambda(\mathbf{k}) \tilde{\Pi}_\Lambda(K)]^2}. \quad (2.54b)$$

Graphical representations of the flow equations (2.50) and (2.51) are shown in Fig. 1.

III. TRUNCATED FLOW EQUATIONS AND INTEGRAL EQUATION FOR THE IRREDUCIBLE DYNAMIC SUSCEPTIBILITY

We now specify our cutoff scheme. For our purpose, it is sufficient to work with an interaction cutoff [25] where the exchange interaction is initially switched off at $\Lambda = 0$ and assumes the physical value $J(\mathbf{k})$ at the final value $\Lambda = 1$ of the deformation parameter. Formally, this scheme can be implemented via the regulator

$$R_\Lambda(\mathbf{k}) = (\Lambda - 1)J(\mathbf{k}), \quad \Lambda \in [0, 1], \quad (3.1)$$

so that the deformed exchange interaction is

$$J_\Lambda(\mathbf{k}) = \Lambda J(\mathbf{k}), \quad \Lambda \in [0, 1]. \quad (3.2)$$

A. Truncation with bare interaction vertices

In the simplest truncation, we neglect the flow of the three-point and four-point vertices in Eqs. (2.50) and (2.51). This amounts to neglecting the effect of the exchange interaction on the higher-order spin correlations, which are then determined by the on-site SU(2)-algebra of a single non-interacting spin. Although this truncation is too simple to give physically correct results for the low-energy spin dynamics, it is instructive to work out

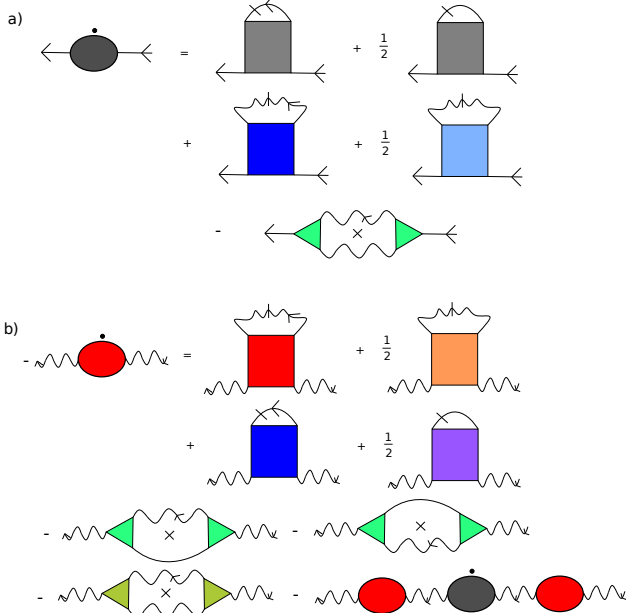


FIG. 1. The upper diagram (a) represents the exact flow equation (2.50) for the classical self-energy $\Sigma_\Lambda(\mathbf{k})$, while (b) represents the exact flow equation (2.51) for the subtracted irreducible dynamic susceptibility $\tilde{\Pi}_\Lambda(\mathbf{k}, i\omega)$. We use the same color coding for the vertices as in the flow equations (2.50) and (2.51). Here the dotted bubbles represent the scale derivatives $\partial_\Lambda \Sigma_\Lambda(\mathbf{k})$ and $\partial_\Lambda \tilde{\Pi}_\Lambda(\mathbf{k}, i\omega)$, the solid arrows and lines represent the transverse and longitudinal classical propagator $G_\Lambda^{+-}(\mathbf{k})$ and $G_\Lambda^{zz}(\mathbf{k})$, while wavy arrows and lines represent the corresponding quantum propagators $G_\Lambda^{\eta,+-}(\mathbf{k}, i\omega)$ and $G_\Lambda^{\eta,zz}(\mathbf{k}, i\omega)$. Slashed lines represent the corresponding single-scale propagators, and crosses inside loops mean that each of the propagators forming the loop should successively be replaced by the relevant single-scale propagator. Note that spin-rotational invariance implies $G_\Lambda^{+-}(\mathbf{k}) = G_\Lambda^{zz}(\mathbf{k}) = G_\Lambda(\mathbf{k})$ and $G_\Lambda^{\eta,+-}(\mathbf{k}, i\omega) = G_\Lambda^{\eta,zz}(\mathbf{k}, i\omega) = G_\Lambda^\eta(\mathbf{k}, i\omega)$. The above diagrams describe also the FRG flow in the presence of an external magnetic field where transverse and longitudinal correlation functions should be distinguished.

the explicit form the three-point and four-point vertices because it gives us a hint for more accurate truncations.

Using the initial values of the classical four-point vertices given in Eq. (2.46) we obtain for the relevant combination in Eq. (2.50) at $\Lambda = 0$,

$$\begin{aligned} & \Gamma_0^{--++}(-\mathbf{k}, -\mathbf{q}, \mathbf{q}, \mathbf{k}) + \frac{1}{2!} \Gamma_0^{-++z}(-\mathbf{k}, \mathbf{k}, -\mathbf{q}, \mathbf{q}) \\ &= \frac{T}{(b'_0)^3} \left(b'_0 + \frac{1}{6} \right). \end{aligned} \quad (3.3)$$

Next, consider the initial conditions for the three-point vertices for vanishing exchange couplings. In this limit the pure quantum vertices in the last line of Eq. (2.51) vanish, while the mixed three-legged vertices with one

classical leg are related to the corresponding Fourier transform of the imaginary-time ordered three-spin correlation function via the tree expansion [27, 37]

$$\begin{aligned} & \tilde{J}_\Lambda(\mathbf{k}_2) \tilde{J}_\Lambda(\mathbf{k}_3) G_\Lambda^{+-z}(-\mathbf{k}_1, -K_2, -K_3) = \\ & -G_\Lambda(\mathbf{k}_1) G_\Lambda^\eta(K_2) G_\Lambda^\eta(K_3) \Gamma_\Lambda^{m^-\eta^+\eta^z}(\mathbf{k}_1, K_2, K_3), \end{aligned} \quad (3.4a)$$

$$\begin{aligned} & \tilde{J}_\Lambda(\mathbf{k}_2) \tilde{J}_\Lambda(\mathbf{k}_3) G_\Lambda^{+-z}(-K_2, -\mathbf{k}_1, -K_3) = \\ & -G_\Lambda(\mathbf{k}_1) G_\Lambda^\eta(K_2) G_\Lambda^\eta(K_3) \Gamma_\Lambda^{m^+\eta^-\eta^z}(\mathbf{k}_1, K_2, K_3), \end{aligned} \quad (3.4b)$$

$$\begin{aligned} & \tilde{J}_\Lambda(\mathbf{k}_2) \tilde{J}_\Lambda(\mathbf{k}_3) G_\Lambda^{+-z}(-K_2, -K_3, -\mathbf{k}_1) = \\ & -G_\Lambda(\mathbf{k}_1) G_\Lambda^\eta(K_2) G_\Lambda^\eta(K_3) \Gamma_\Lambda^{m^z\eta^-\eta^+}(\mathbf{k}_1, K_2, K_3). \end{aligned} \quad (3.4c)$$

In the limit $\Lambda \rightarrow 0$ where $G_\Lambda^\eta(K) \rightarrow 0$ and $G_\Lambda(\mathbf{k}) \rightarrow \beta b'_0$ these equations imply the initial conditions

$$\Gamma_0^{m^-\eta^+\eta^z}(\mathbf{k}_1, K_2, K_3) = -\frac{1}{\beta b'_0} G_0^{+-z}(0, -\omega_2, \omega_2), \quad (3.5a)$$

$$\Gamma_0^{m^+\eta^-\eta^z}(\mathbf{k}_1, K_2, K_3) = -\frac{1}{\beta b'_0} G_0^{+-z}(-\omega_2, 0, \omega_2), \quad (3.5b)$$

$$\Gamma_0^{m^z\eta^-\eta^+}(\mathbf{k}_1, K_2, K_3) = -\frac{1}{\beta b'_0} G_0^{+-z}(-\omega_2, \omega_2, 0). \quad (3.5c)$$

Explicit expressions for the imaginary-time ordered connected spin correlation functions in frequency space have first been derived by VLP [41, 42], see also Refs. [26, 27, and 43]. In the zero-field limit of the mixed three-spin correlation function is [26]

$$\begin{aligned} G_0^{+-z}(\omega_1, \omega_2, \omega_3) &= \beta b'_0 (1 - \delta_{\omega_1,0} \delta_{\omega_2,0} \delta_{\omega_3,0}) \\ &\times \left[\frac{\delta_{\omega_1,0}}{i\omega_2} + \frac{\delta_{\omega_2,0}}{i\omega_3} + \frac{\delta_{\omega_3,0}}{i\omega_1} \right]. \end{aligned} \quad (3.6)$$

We conclude that

$$\begin{aligned} & \Gamma_0^{m^-\eta^+\eta^z}(\mathbf{k}_1, K_2, K_3) = -\Gamma_0^{m^+\eta^-\eta^z}(\mathbf{k}_1, K_2, K_3) \\ &= \Gamma_0^{m^z\eta^-\eta^+}(\mathbf{k}_1, K_2, K_3) = \frac{1}{i\omega_2}, \end{aligned} \quad (3.7)$$

so that for the relevant momentum-frequency labels in the flow equation (2.50) we obtain

$$\begin{aligned} & \Gamma_0^{m^-\eta^+\eta^z}(-\mathbf{k}, -Q, Q + \mathbf{k}) \\ &= \Gamma_0^{m^+\eta^-\eta^z}(\mathbf{k}, Q, -Q - \mathbf{k}) = \frac{1}{-i\omega'}, \end{aligned} \quad (3.8)$$

and in the flow equation (2.51) for the irreducible dynamic susceptibility the relevant initial vertices are

$$\begin{aligned} & \Gamma_0^{m^z\eta^-\eta^+}(-\mathbf{q}, -K, \mathbf{q} + K) \\ &= \Gamma_0^{m^z\eta^-\eta^+}(\mathbf{q}, -\mathbf{q} - K, K) = \frac{1}{-i\omega}. \end{aligned} \quad (3.9)$$

Let us now consider the quantum four-point vertices in the first line of Eq. (2.51) which are irreducible with respect to cutting a single interaction line. These vertices are related to the connected four-spin correlation function via the tree expansions [27],

$$\begin{aligned}
& \left[\prod_{i=1}^4 \tilde{J}_\Lambda(\mathbf{k}_i) \right] G_\Lambda^{++++}(-K_1, -K_2, -K_3, -K_4) = - \left[\prod_{i=1}^4 G_\Lambda^\eta(K_i) \right] \left\{ \Gamma_\Lambda^{\eta^- \eta^+ \eta^+ \eta^+}(K_1, K_2, K_3, K_4) \right. \\
& - \left[\Gamma_\Lambda^{m^z \eta^- \eta^+}(-\mathbf{k}_1 - \mathbf{k}_3, K_1, K_3) \delta_{\omega_1 + \omega_3, 0} G_\Lambda(-\mathbf{k}_1 - \mathbf{k}_3) \Gamma_\Lambda^{m^z \eta^- \eta^+}(-\mathbf{k}_2 - \mathbf{k}_4, K_2, K_4) + (K_3 \leftrightarrow K_4) \right] \\
& \left. - \left[\Gamma_\Lambda^{\eta^- \eta^+ \eta^z}(K_1, K_3, -K_1 - K_3) G_\Lambda^\eta(-K_1 - K_3) \Gamma_\Lambda^{\eta^- \eta^+ \eta^z}(K_2, K_4, -K_2 - K_4) + (K_3 \leftrightarrow K_4) \right] \right\}, \quad (3.10)
\end{aligned}$$

and

$$\begin{aligned}
& \left[\prod_{i=1}^4 \tilde{J}_\Lambda(\mathbf{k}_i) \right] G_\Lambda^{+-zz}(-K_1, -K_2, -K_3, -K_4) = - \left[\prod_{i=1}^4 G_\Lambda^\eta(K_i) \right] \left\{ \Gamma_\Lambda^{\eta^- \eta^+ \eta^z \eta^z}(K_1, K_2, K_3, K_4) \right. \\
& - \left[\Gamma_\Lambda^{m^- \eta^+ \eta^z}(-\mathbf{k}_1 - \mathbf{k}_3, K_1, K_3) \delta_{\omega_1 + \omega_3, 0} G_\Lambda(-\mathbf{k}_1 - \mathbf{k}_3) \Gamma_\Lambda^{m^+ \eta^- \eta^z}(-\mathbf{k}_2 - \mathbf{k}_4, K_2, K_4) + (K_3 \leftrightarrow K_4) \right] \\
& - \left[\Gamma_\Lambda^{\eta^- \eta^+ \eta^z}(K_1, -K_1 - K_3, K_3) G_\Lambda^\eta(-K_1 - K_3) \Gamma_\Lambda^{\eta^- \eta^+ \eta^z}(-K_2 - K_4, K_2, K_4) + (K_3 \leftrightarrow K_4) \right] \\
& \left. - \Gamma_\Lambda^{\eta^z \eta^z \eta^z}(K_3, K_4, -K_3 - K_4) G_\Lambda^\eta(-K_3 - K_4) \Gamma_\Lambda^{\eta^- \eta^+ \eta^z}(K_1, K_2, -K_1 - K_2) \right\}. \quad (3.11)
\end{aligned}$$

Taking the limit $\Lambda \rightarrow$ in Eqs. (3.10) and (3.11) we obtain the initial conditions

$$\begin{aligned}
& \Gamma_0^{\eta^- \eta^+ \eta^+ \eta^+}(K_1, K_2, K_3, K_4) = -G_0^{++++}(-\omega_1, -\omega_2, -\omega_3, -\omega_4) \\
& + \left[\Gamma_0^{m^z \eta^- \eta^+}(-\mathbf{k}_1 - \mathbf{k}_3, K_1, K_3) \delta_{\omega_1 + \omega_3, 0} \beta b'_0 \Gamma_0^{m^z \eta^- \eta^+}(-\mathbf{k}_2 - \mathbf{k}_4, K_2, K_4) + (K_3 \leftrightarrow K_4) \right] \\
& = -G_0^{++++}(-\omega_1, -\omega_2, -\omega_3, -\omega_4) + \frac{1}{\beta b'_0} (\delta_{\omega_1 + \omega_3, 0} + \delta_{\omega_1 + \omega_4, 0}) G_0^{+-z}(-\omega_1, \omega_1, 0) G_0^{+-z}(-\omega_2, \omega_2, 0) \\
& = -G_0^{++++}(-\omega_1, -\omega_2, -\omega_3, -\omega_4) - \frac{\beta b'_0}{\omega_1 \omega_2} (\delta_{\omega_1 + \omega_3, 0} + \delta_{\omega_1 + \omega_4, 0}), \quad (3.12)
\end{aligned}$$

and

$$\begin{aligned}
& \Gamma_0^{\eta^- \eta^+ \eta^z \eta^z}(K_1, K_2, K_3, K_4) = -G_0^{+-zz}(-\omega_1, -\omega_2, -\omega_3, -\omega_4) \\
& + \left[\Gamma_0^{m^- \eta^+ \eta^z}(-\mathbf{k}_1 - \mathbf{k}_3, K_1, K_3) \delta_{\omega_1 + \omega_3, 0} \beta b'_0 \Gamma_0^{m^+ \eta^- \eta^z}(-\mathbf{k}_2 - \mathbf{k}_4, K_2, K_4) + (K_3 \leftrightarrow K_4) \right] \\
& = -G_0^{+-zz}(-\omega_1, -\omega_2, -\omega_3, -\omega_4) + \frac{1}{\beta b'_0} (\delta_{\omega_1 + \omega_3, 0} + \delta_{\omega_1 + \omega_4, 0}) G_0^{+-z}(0, -\omega_1, \omega_1) G_0^{+-z}(-\omega_2, 0, \omega_2) \\
& = -G_0^{+-zz}(-\omega_1, -\omega_2, -\omega_3, -\omega_4) + \frac{\beta b'_0}{\omega_1 \omega_2} (\delta_{\omega_1 + \omega_3, 0} + \delta_{\omega_1 + \omega_4, 0}). \quad (3.13)
\end{aligned}$$

For the frequency combinations needed in the first line of Eq. (2.51) we obtain

$$\begin{aligned}
& G_0^{++++}(\omega, \omega', -\omega', -\omega) \\
& = \frac{2}{3} \beta^3 b_0''' \quad \text{if } \omega = \omega' = 0, \quad (3.14a)
\end{aligned}$$

$$= \frac{\beta b'_0}{(\omega')^2} \quad \text{if } \omega = 0 \text{ and } \omega' \neq 0, \quad (3.14b)$$

$$= \frac{\beta b'_0}{\omega^2} \quad \text{if } \omega \neq 0 \text{ and } \omega' = 0, \quad (3.14c)$$

$$= -2 \frac{\beta b'_0}{\omega^2} \quad \text{if } \omega = \omega' \neq 0, \quad (3.14d)$$

$$= \frac{\beta b'_0}{\omega^2} \quad \text{if } \omega = -\omega' \neq 0, \quad (3.14e)$$

$$= 0 \quad \text{else,} \quad (3.14f)$$

$$\begin{aligned}
& G_0^{+-zz}(\omega, -\omega, \omega', -\omega') \\
& = \frac{1}{3} \beta^3 b_0''' \quad \text{if } \omega = \omega' = 0, \quad (3.15a)
\end{aligned}$$

$$= 2 \frac{\beta b'_0}{(\omega')^2} \quad \text{if } \omega = 0 \text{ and } \omega' \neq 0, \quad (3.15b)$$

$$= 2 \frac{\beta b'_0}{\omega^2} \quad \text{if } \omega \neq 0 \text{ and } \omega' = 0, \quad (3.15c)$$

$$= -\frac{\beta b'_0}{\omega^2} \quad \text{if } |\omega| = |\omega'| \neq 0, \quad (3.15d)$$

$$= 0 \quad \text{else.} \quad (3.15e)$$

Keeping in mind that both Matsubara frequencies in the first line of Eq. (2.51) are non-zero, the initial condition

of the relevant linear combination is

$$\begin{aligned}
& \Gamma_0^{\eta^- \eta^- \eta^+ \eta^+}(-K, -Q, Q, K) + \frac{1}{2!} \Gamma_0^{\eta^- \eta^+ \eta^z \eta^z}(-K, K, -Q, Q) \\
&= \frac{\beta b'_0}{\omega^2} \left[\frac{5}{2} \delta_{\omega, \omega'} - \frac{1}{2!} \delta_{\omega, -\omega'} \right] \\
&\quad - \frac{\beta b'_0}{\omega \omega'} (\delta_{\omega, \omega'} + 1) - \frac{\beta b'_0}{\omega^2} \frac{1}{2!} (\delta_{\omega, \omega'} + \delta_{\omega, -\omega'}) \\
&= \frac{\beta b'_0}{\omega^2} (\delta_{\omega, \omega'} - \delta_{\omega, -\omega'}) - \frac{\beta b'_0}{\omega \omega'} \\
&= \frac{\beta b'_0}{\omega \omega'} (\delta_{\omega, \omega'} + \delta_{\omega, -\omega'} - 1). \tag{3.16}
\end{aligned}$$

Noting that this is an odd function of ω' while in the paramagnetic phase the single-scale propagator $\hat{G}_\Lambda^\eta(\mathbf{q}, i\omega')$ in the first line of the flow equation (2.51) as an even function of ω' , we conclude that the contribution from the quantum vertices in the first line of Eq. (2.51) vanishes if we approximate the vertices by their initial values.

Next, consider the four-point vertices with two classical and two quantum fields in Eqs. (2.50) and (2.51). The relevant tree expansions are

$$\begin{aligned}
& \tilde{J}_\Lambda(\mathbf{k}_3) \tilde{J}_\Lambda(\mathbf{k}_4) G_\Lambda^{+-+--}(-\mathbf{k}_1, -K_3, -\mathbf{k}_2, -K_4) = -G_\Lambda(\mathbf{k}_1) G_\Lambda(\mathbf{k}_2) G_\Lambda^\eta(K_3) G_\Lambda^\eta(K_4) \left\{ \Gamma_\Lambda^{m^- m^+ \eta^- \eta^+}(\mathbf{k}_1, \mathbf{k}_2, K_3, K_4) \right. \\
& \quad \left. - \Gamma_\Lambda^{m^- \eta^+ \eta^z}(\mathbf{k}_1, K_4, -\mathbf{k}_1 - K_4) G_\Lambda^\eta(-\mathbf{k}_1 - K_4) \Gamma_\Lambda^{m^+ \eta^- \eta^z}(\mathbf{k}_2, K_3, -\mathbf{k}_2 - K_3) \right\}, \tag{3.17a}
\end{aligned}$$

$$\begin{aligned}
& \tilde{J}_\Lambda(\mathbf{k}_3) \tilde{J}_\Lambda(\mathbf{k}_4) G_\Lambda^{+-zz}(-\mathbf{k}_1, -\mathbf{k}_2, -K_3, -K_4) = -G_\Lambda(\mathbf{k}_1) G_\Lambda(\mathbf{k}_2) G_\Lambda^\eta(K_3) G_\Lambda^\eta(K_4) \left\{ \Gamma_\Lambda^{m^- m^+ \eta^z \eta^z}(\mathbf{k}_1, \mathbf{k}_2, K_3, K_4) \right. \\
& \quad \left. - \left[\Gamma_\Lambda^{m^- \eta^+ \eta^z}(\mathbf{k}_1, -\mathbf{k}_1 - K_3, K_3) G_\Lambda^\eta(-\mathbf{k}_1 - K_3) \Gamma_\Lambda^{m^+ \eta^- \eta^z}(\mathbf{k}_2, -\mathbf{k}_2 - K_4, K_4) + (K_3 \leftrightarrow K_4) \right] \right\}, \tag{3.17b}
\end{aligned}$$

$$\begin{aligned}
& \tilde{J}_\Lambda(\mathbf{k}_3) \tilde{J}_\Lambda(\mathbf{k}_4) G_\Lambda^{+-zz}(-K_3, -K_4, -\mathbf{k}_1, -\mathbf{k}_2) = -G_\Lambda(\mathbf{k}_1) G_\Lambda(\mathbf{k}_2) G_\Lambda^\eta(K_3) G_\Lambda^\eta(K_4) \left\{ \Gamma_\Lambda^{m^z m^z \eta^- \eta^+}(\mathbf{k}_1, \mathbf{k}_2, K_3, K_4) \right. \\
& \quad \left. - \left[\Gamma_\Lambda^{m^z \eta^- \eta^+}(\mathbf{k}_1, K_3, -\mathbf{k}_1 - K_3) G_\Lambda^\eta(-\mathbf{k}_1 - K_3) \Gamma_\Lambda^{m^z \eta^- \eta^+}(\mathbf{k}_2, -\mathbf{k}_2 - K_4, K_4) + (\mathbf{k}_1 \leftrightarrow \mathbf{k}_2) \right] \right\}. \tag{3.17c}
\end{aligned}$$

Using the initial conditions (3.7) for the three-point vertices and the fact that for vanishing exchange coupling $G_0^\eta(K) = -\tilde{J}_0(\mathbf{k}) = -1/(\beta b'_0)$ we obtain from Eq. (3.17) for $\Lambda \rightarrow 0$,

$$\begin{aligned}
& \Gamma_0^{m^- m^+ \eta^- \eta^+}(\mathbf{k}_1, \mathbf{k}_2, K_3, K_4) \\
&= -\frac{1}{(\beta b'_0)^2} G_0^{+-+--}(0, -\omega_3, 0, \omega_3) - \frac{1}{\beta b'_0} \Gamma_0^{m^- \eta^+ \eta^z}(\mathbf{k}_1, K_4, -\mathbf{k}_1 - K_4) \Gamma_0^{m^+ \eta^- \eta^z}(\mathbf{k}_2, K_3, -\mathbf{k}_2 - K_3) \\
&= -\frac{1}{\beta b'_0 \omega_3^2} + \frac{1}{\beta b'_0 \omega_3^2} = 0, \tag{3.18a}
\end{aligned}$$

$$\begin{aligned}
& \Gamma_0^{m^- m^+ \eta^z \eta^z}(\mathbf{k}_1, \mathbf{k}_2, K_3, K_4) \\
&= -\frac{1}{(\beta b'_0)^2} G_0^{+-zz}(0, 0, -\omega_3, \omega_3) - \frac{1}{\beta b'_0} \left[\Gamma_0^{m^- \eta^+ \eta^z}(\mathbf{k}_1, -\mathbf{k}_1 - K_3, K_3) \Gamma_0^{m^+ \eta^- \eta^z}(\mathbf{k}_2, -\mathbf{k}_2 - K_4, K_4) + (K_3 \leftrightarrow K_4) \right] \\
&= -\frac{2}{\beta b'_0 \omega_3^2} + \frac{2}{\beta b'_0 \omega_3^2} = 0, \tag{3.18b}
\end{aligned}$$

$$\begin{aligned}
& \Gamma_0^{m^z m^z \eta^- \eta^+}(\mathbf{k}_1, \mathbf{k}_2, K_3, K_4) \\
&= -\frac{1}{(\beta b'_0)^2} G_0^{+-zz}(-\omega_3, \omega_3, 0, 0) - \frac{1}{\beta b'_0} \left[\Gamma_0^{m^z \eta^- \eta^+}(\mathbf{k}_1, K_3, -\mathbf{k}_1 - K_3) \Gamma_0^{m^z \eta^- \eta^+}(\mathbf{k}_2, -\mathbf{k}_2 - K_4, K_4) + (\mathbf{k}_1 \leftrightarrow \mathbf{k}_2) \right] \\
&= -\frac{2}{\beta b'_0 \omega_3^2} + \frac{2}{\beta b'_0 \omega_3^2} = 0. \tag{3.18c}
\end{aligned}$$

In summary, if we approximate the three-point and

four-point vertices in the exact flow equations (2.50) and

(2.51) by their initial values for vanishing exchange cou-

plings, we obtain the following truncated system of flow equations,

$$\partial_\Lambda \Sigma_\Lambda(\mathbf{k}) = \frac{T^2}{(b'_0)^3} \left(b'_0 + \frac{1}{6} \right) \int_{\mathbf{q}} \dot{G}_\Lambda(\mathbf{q}) + T \sum_{\omega \neq 0} \frac{1}{\omega^2} \int_{\mathbf{q}} [F_\Lambda(\mathbf{q}, i\omega) F_\Lambda(\mathbf{q} + \mathbf{k}, i\omega)]^\bullet, \quad (3.19)$$

$$\partial_\Lambda \tilde{\Pi}_\Lambda(\mathbf{k}, i\omega) = \frac{T}{\omega^2} \int_{\mathbf{q}} \left\{ [F_\Lambda(\mathbf{q}, i\omega) G_\Lambda(\mathbf{q} + \mathbf{k})]^\bullet + (\mathbf{k} \rightarrow -\mathbf{k}) \right\} + \tilde{\Pi}_\Lambda^2(\mathbf{k}, i\omega) \partial_\Lambda \Sigma_\Lambda(\mathbf{k}), \quad (3.20)$$

where the effective dynamical interaction $F(\mathbf{q}, i\omega) = -G^\eta(\mathbf{q}, i\omega)$ is the negative of the η -propagator defined in Eq. (2.54a), and we have introduced the notation

$$[F_\Lambda(\mathbf{q}, i\omega) G_\Lambda(\mathbf{q} + \mathbf{k})]^\bullet = \dot{F}_\Lambda(\mathbf{q}, i\omega) G_\Lambda(\mathbf{q} + \mathbf{k}) + F_\Lambda(\mathbf{q}, i\omega) \dot{G}_\Lambda(\mathbf{q} + \mathbf{k}). \quad (3.21)$$

Unfortunately, the truncated flow equation (3.20) violates the Ward identity $\tilde{\Pi}_\Lambda(\mathbf{k} = 0, i\omega \neq 0) = 0$ due to the conservation of the total spin, see Eq. (3.24) below. Moreover, the last term $\tilde{\Pi}_\Lambda^2(\mathbf{k}, i\omega) \partial_\Lambda \Sigma_\Lambda(\mathbf{k})$ leads to a violation of the continuity condition (2.20), which is obvious by writing the corresponding contribution to the flow equation as $\partial_\Lambda \tilde{\Pi}_\Lambda^{-1}(\mathbf{k}, i\omega) = -\partial_\Lambda \Sigma_\Lambda(\mathbf{k}) + \dots$. Given the fact that the constraints imposed by Ward identities are expected to be essential for a correct description of the spin dynamics, we conclude that the truncation in this subsection with bare three-point and four-point vertices is not sufficient to obtain reliable results for the spin dynamics.

B. Vertex corrections

In principle, we could now write down flow equations for the three-point and four-point vertices in Eqs. (2.50) and (2.51) which depend in turn on various types of higher-order vertices. We thus obtain an infinite hierarchy of the flow equations for the vertices generated by $\Gamma_\Lambda[\mathbf{m}^c, \mathbf{h}^q]$. The construction of sensible approximation schemes for this infinite hierarchy is one of the main technical challenges of our SFRG approach. A powerful strategy to construct truncation strategies for FRG flow equations is based on the use of Ward identities providing exact relations between vertices of different order. This strategy has been adopted previously in different contexts in Refs. [37, 51, and 52] and we will use it again in this work to express the four-point vertices in the FRG flow equations for the irreducible spin susceptibility in terms of two-point vertices.

1. Equations of motion

Ward identities for imaginary-time ordered spin correlation functions of different order can be derived using

the Heisenberg equations of motion of the spin operators and the resulting equations of motion for the correlation functions, as described in Ref. [27]. After transforming the equations of motion to momentum-frequency space, we find that the two-spin correlation function $G(K) = G(\mathbf{k}, i\omega)$ is related to the mixed three-spin correlation function $G^{+-z}(Q + K, -Q, -K)$ via the integral equation

$$i\omega G(K) = \int_Q [J(\mathbf{q}) - J(\mathbf{q} + \mathbf{k})] G^{+-z}(Q + K, -Q, -K), \quad (3.22)$$

where we assume that the spin-rotational invariance is not spontaneously broken. Setting $\mathbf{k} = 0$ for finite frequency $\omega \neq 0$ we obtain

$$G(\mathbf{k} = 0, i\omega \neq 0) = \frac{\tilde{\Pi}(0, i\omega)}{1 + \tilde{J}(0)\tilde{\Pi}(0, i\omega)} = 0, \quad (3.23)$$

and hence

$$\tilde{\Pi}(\mathbf{k} = 0, i\omega \neq 0) = 0. \quad (3.24)$$

Similarly, we can derive the following equation of motion for the mixed three-spin correlation function,

$$\begin{aligned} i\omega G^{+-z}(Q + K, -Q, -K) &= G(Q) - G(Q + K) \\ &+ [J(\mathbf{q}) - J(\mathbf{q} + \mathbf{k})] G(Q) G(Q + K) \\ &- \int_{Q'} [J(\mathbf{q}') - J(\mathbf{q}' + \mathbf{k})] \\ &\times G^{++--}(Q + K, -Q' - K, Q', -Q), \end{aligned} \quad (3.25)$$

which depends on the connected four-spin correlation function $G^{++--}(Q + K, -Q' - K, Q', -Q)$.

2. Fixing four-point vertices via Ward identity and continuity condition

By approximating the three-point and four-point vertices in Eq. (2.51) by their non-interacting limits we have neglected the contribution from the finite-frequency (quantum) four-point vertex

$$\begin{aligned} \Gamma_\Lambda^{\eta\eta\eta\eta}(-K, K, -Q, Q) &= \Gamma_\Lambda^{\eta^- \eta^- \eta^+ \eta^+}(-K, -Q, Q, K) \\ &+ \frac{1}{2!} \Gamma_\Lambda^{\eta^- \eta^+ \eta^z \eta^z}(-K, K, -Q, Q), \end{aligned} \quad (3.26)$$

as well as the contribution from the mixed classical-quantum four-point vertex

$$\Gamma_{\Lambda}^{mm\eta\eta}(-\mathbf{q}, \mathbf{q}, -K, K) = \Gamma_{\Lambda}^{m^-m^+\eta^-\eta^+}(-\mathbf{q}, \mathbf{q}, -K, K) + \frac{1}{2!} \Gamma_{\Lambda}^{m^z m^z \eta^-\eta^+}(-\mathbf{q}, \mathbf{q}, -K, K). \quad (3.27)$$

Although for $\Lambda = 0$ these vertices do not contribute to the flow of the irreducible susceptibility, for finite Λ this is not true any more, which is the reason for the violation of the Ward identity (3.24) within a truncation where all higher-order vertices are approximated by their initial values. To restore the Ward identity, we should therefore take the flow of at least one of the above vertices into account. For simplicity let us still approximate the quantum four-point vertex $\Gamma_{\Lambda}^{\eta\eta\eta\eta}(-K, K, -Q, Q)$ by its initial value given in Eq. (3.16),

$$\Gamma_{\Lambda}^{\eta\eta\eta\eta}(-K, K, -Q, Q) \approx \Gamma_0^{\eta\eta\eta\eta}(-K, K, -Q, Q) = \frac{\beta b'_0}{\omega\omega'} (\delta_{\omega, \omega'} + \delta_{\omega, -\omega'} - 1), \quad (3.28)$$

so that this vertex does not contribute to the flow of $\tilde{\Pi}_{\Lambda}(K)$. This leaves us with the mixed classical-quantum vertex $\Gamma_{\Lambda}^{mm\eta\eta}(-\mathbf{q}, \mathbf{q}, -K, K)$ to restore the Ward identity (3.24). To simplify the algebra, let us also neglect the dependence of this vertex on the momentum \mathbf{q} of the classical field,

$$\Gamma_{\Lambda}^{mm\eta\eta}(-\mathbf{q}, \mathbf{q}, -K, K) \approx \Gamma_{\Lambda}^{mm\eta\eta}(0, 0, -K, K). \quad (3.29)$$

With these approximations, the exact flow equation (2.51) for the subtracted irreducible susceptibility reduces to

$$\begin{aligned} \partial_{\Lambda} \tilde{\Pi}_{\Lambda}(\mathbf{k}, i\omega) &= \tilde{\Pi}_{\Lambda}^2(\mathbf{k}, i\omega) \partial_{\Lambda} \Sigma_{\Lambda}(\mathbf{k}) \\ &- T \int_{\mathbf{q}} \dot{G}_{\Lambda}(\mathbf{q}) \Gamma_{\Lambda}^{mm\eta\eta}(0, 0, -K, K) \\ &+ \frac{T}{\omega^2} \int_{\mathbf{q}} \left\{ [F_{\Lambda}(\mathbf{q}, i\omega) G_{\Lambda}(\mathbf{q} + \mathbf{k})]^{\bullet} + (\mathbf{k} \rightarrow -\mathbf{k}) \right\}, \end{aligned} \quad (3.30)$$

which replaces Eq. (3.20). Instead of writing down an additional flow equation for $\Gamma_{\Lambda}^{mm\eta\eta}(0, 0, -K, K)$, we now fix this vertex by demanding that the solution of the flow equation (3.30) satisfies the Ward identity (3.24) as well as the continuity condition (2.20) for all values of the deformation parameter Λ , i.e.,

$$\tilde{\Pi}_{\Lambda}(0, i\omega \neq 0) = 0, \quad (3.31)$$

$$\tilde{\Pi}_{\Lambda}^{-1}(\mathbf{k} \neq 0, 0) = 0. \quad (3.32)$$

The simplest way to satisfy these constraints which is compatible with the initial conditions at $\Lambda = 0$ is to choose the scale-dependent mixed four-point vertex as follows,

$$\Gamma_{\Lambda}^{mm\eta\eta}(0, 0, -K, K) = \frac{1}{\omega^2} [W_{\Lambda}(i\omega) + C_{\Lambda}(\mathbf{k}, i\omega)], \quad (3.33)$$

where the Ward identity (3.31) is enforced by the contribution

$$W_{\Lambda}(i\omega) \equiv \frac{2 \int_{\mathbf{q}} [F_{\Lambda}(\mathbf{q}, i\omega) G_{\Lambda}(\mathbf{q})]^{\bullet}}{\int_{\mathbf{q}} \dot{G}_{\Lambda}(\mathbf{q})}, \quad (3.34)$$

while the continuity condition (3.32) is enforced by

$$C_{\Lambda}(\mathbf{k}, i\omega) \equiv \frac{\omega^2 \tilde{\Pi}_{\Lambda}^2(\mathbf{k}, i\omega) \partial_{\Lambda} \Sigma_{\Lambda}(\mathbf{k})}{T \int_{\mathbf{q}} \dot{G}_{\Lambda}(\mathbf{q})}. \quad (3.35)$$

Note that $C_{\Lambda}(\mathbf{k}, i\omega)$ cancels the term $\tilde{\Pi}_{\Lambda}^2(\mathbf{k}, i\omega) \partial_{\Lambda} \Sigma_{\Lambda}(\mathbf{k})$ on the right-hand side of Eq. (3.30) which would otherwise violate the continuity condition (3.32). It is important to note that our choice (3.33) of the mixed four-point vertex is consistent with the initial condition (3.18) at $\Lambda = 0$ where the deformed exchange coupling $J_{\Lambda=0}(\mathbf{k})$ and hence also the vertex $\Gamma_{\Lambda=0}^{mm\eta\eta}(0, 0, -K, K)$ vanish. This follows from the fact that for small J_{Λ} the expressions in the numerator of Eqs. (3.34) and (3.35) vanish as J_{Λ}^2 while the integral $\int_{\mathbf{q}} \dot{G}_{\Lambda}(\mathbf{q})$ in the denominator vanishes as J_{Λ} , implying $W_{\Lambda=0}(i\omega) = C_{\Lambda=0}(\mathbf{k}, i\omega) = 0$. Substituting Eqs. (3.33), (3.34), and (3.35) into the flow equation (3.30) we obtain the following flow equation for the dynamic irreducible susceptibility,

$$\begin{aligned} \partial_{\Lambda} \tilde{\Pi}_{\Lambda}(\mathbf{k}, i\omega) &= \frac{T}{\omega^2} \int_{\mathbf{q}} \left[F_{\Lambda}(\mathbf{q}, i\omega) [G_{\Lambda}(\mathbf{q} + \mathbf{k}) \right. \\ &\quad \left. + G_{\Lambda}(\mathbf{q} - \mathbf{k}) - 2G_{\Lambda}(\mathbf{q}) \right]^{\bullet}. \end{aligned} \quad (3.36)$$

The vanishing of the integrand on the right-hand side for $\mathbf{k} = 0$ guarantees that the solution of Eq. (3.36) satisfies the Ward identity (3.31). The fact that the solution of Eq. (3.36) satisfies also the continuity condition (3.32) is guaranteed by the prefactor of $1/\omega^2$ which implies that the inverse of $\tilde{\Pi}_{\Lambda}(\mathbf{k} \neq 0, i\omega)$ vanishes for $\omega \rightarrow 0$.

3. Renormalized three-point vertex

It turns out that the flow equation (3.36) still does not include all vertex corrections which are necessary to calculate the dynamic spin susceptibility for finite momentum \mathbf{k} . To see this, consider the equation of motion (3.25) for the mixed three-spin correlation function. The approximations (3.28) and (3.29) are consistent with neglecting the momentum dependence of the four-spin correlation function $G^{++--}(Q + K, -Q' - K, Q', Q)$ in the last line of Eq. (3.25). By shifting the loop momentum $\mathbf{q}' \rightarrow \mathbf{q}' + \mathbf{k}$ it is then easy to see that this term does not contribute to the equation of motion, which therefore reduces to

$$\begin{aligned} i\omega G^{+-z}(Q + K, -Q, -K) &= G(Q) - G(Q + K) \\ &\quad + [J(\mathbf{q}) - J(\mathbf{q} + \mathbf{k})] G(Q) G(Q + K) \\ &= G(Q) \left[1 + \frac{J(\mathbf{q}) - J(\mathbf{q} + \mathbf{k})}{2} G(Q + K) \right] \\ &\quad - G(Q + K) \left[1 + \frac{J(\mathbf{q} + \mathbf{k}) - J(\mathbf{q})}{2} G(Q) \right]. \end{aligned} \quad (3.37)$$

Taking the limit $J \rightarrow 0$ and assuming $\omega \neq 0$ this reduces to

$$G_0^{+-z}(Q+K, -Q, -K) = \frac{\beta b'_0}{i\omega} [\delta_{\omega',0} - \delta_{\omega'+\omega,0}], \quad (3.38)$$

where again $K = (\mathbf{k}, i\omega)$ and $Q = (\mathbf{q}, i\omega')$. Eq. (3.38) is equivalent with the zeroth-order approximation (3.7) for the mixed three-point vertices which we have used to derive Eqs. (3.20) and (3.36). To construct an approximation consistent with the equation of motion (3.37) for finite J , we retain the terms in the square braces in the last two lines of Eq. (3.37) neglecting the frequency dependence of the propagators. Then Eq. (3.38) should be

replaced by

$$G_\Lambda^{+-z}(Q+K, -Q, -K) = \frac{\beta b'_0}{i\omega} \left[\delta_{\omega',0} Y_\Lambda(\mathbf{q}, \mathbf{q} + \mathbf{k}) - \delta_{\omega'+\omega,0} Y_\Lambda(\mathbf{q} + \mathbf{k}, \mathbf{q}) \right], \quad (3.39)$$

with scale-dependent vertex correction factor

$$Y_\Lambda(\mathbf{q} + \mathbf{k}, \mathbf{q}) \equiv 1 + \frac{J_\Lambda(\mathbf{q} + \mathbf{k}) - J_\Lambda(\mathbf{q})}{2} G_\Lambda(\mathbf{q}). \quad (3.40)$$

Using the tree expansion (3.17c) to calculate the corresponding irreducible three-point vertices and defining

$$Z_\Lambda(\mathbf{q}, \mathbf{k}) \equiv Y_\Lambda^2(\mathbf{q} + \mathbf{k}, \mathbf{q}), \quad (3.41)$$

we obtain instead of Eq. (3.36) for the flow of the irreducible dynamic susceptibility,

$$\partial_\Lambda \tilde{\Pi}_\Lambda(\mathbf{k}, i\omega) = \frac{T}{\omega^2} \int_{\mathbf{q}} \left\{ [F_\Lambda(\mathbf{q}, i\omega) G_\Lambda(\mathbf{q} + \mathbf{k})]^\bullet Z_\Lambda(\mathbf{q}, \mathbf{k}) + [F_\Lambda(\mathbf{q}, i\omega) G_\Lambda(\mathbf{q} - \mathbf{k})]^\bullet Z_\Lambda(\mathbf{q}, -\mathbf{k}) - 2[F_\Lambda(\mathbf{q}, i\omega) G_\Lambda(\mathbf{q})]^\bullet \right\}. \quad (3.42)$$

Moreover, taking into account the flow of the purely classical four-point vertex

$$\Gamma_\Lambda^{(4)}(-\mathbf{k}, \mathbf{k}, -\mathbf{q}, \mathbf{q}) = \Gamma_\Lambda^{-++}(-\mathbf{k}, -\mathbf{q}, \mathbf{q}, \mathbf{k}) + \frac{1}{2!} \Gamma_\Lambda^{-+zz}(-\mathbf{k}, \mathbf{k}, -\mathbf{q}, \mathbf{q}), \quad (3.43)$$

as well as all vertex corrections discussed above we obtain instead of Eq. (3.19) for the flow equation of the static self-energy,

$$\begin{aligned} \partial_\Lambda \Sigma_\Lambda(\mathbf{k}) = T \int_{\mathbf{q}} \dot{G}_\Lambda(\mathbf{q}) \Gamma_\Lambda^{(4)}(-\mathbf{k}, \mathbf{k}, -\mathbf{q}, \mathbf{q}) + T \sum_{\omega \neq 0} \int_{\mathbf{q}} \frac{\dot{F}_\Lambda(\mathbf{q}, i\omega)}{\omega^2} \left[-W_\Lambda(i\omega) - C_\Lambda(\mathbf{q}, i\omega) \right. \\ \left. + F_\Lambda(\mathbf{q} + \mathbf{k}, i\omega) Z_\Lambda(\mathbf{k}, \mathbf{q}) + F_\Lambda(\mathbf{q} - \mathbf{k}, i\omega) Z_\Lambda(-\mathbf{k}, \mathbf{q}) \right]. \end{aligned} \quad (3.44)$$

Here the energies $W_\Lambda(i\omega)$ and $C_\Lambda(\mathbf{q}, i\omega)$ are defined in Eqs. (3.34) and (3.35); these terms are due to the mixed classical-quantum four-point vertices in the second line of the exact flow equation (2.50) which we approximate again by Eq. (3.33).

We conclude this subsection with three remarks:

1. To obtain a closed system of flow equation, we should add a flow equation for the classical four-point vertex $\Gamma_\Lambda^{(4)}(-\mathbf{k}, \mathbf{k}, -\mathbf{q}, \mathbf{q})$ which contributes to the flow of the static self-energy in Eq. (3.44). In the simplest approximation we can replace this vertex by its initial value given in Eq. (3.3).
2. Keeping in mind that $Z_\Lambda(\mathbf{q}, 0) = 1$, we note that the solution of the flow equation (3.42) satisfies the Ward identity $\tilde{\Pi}_\Lambda(0, i\omega \neq 0) = 0$ for all values of the deformation parameter Λ .
3. Within our truncation the flow equation (3.42) for

the irreducible dynamic susceptibility does not involve any frequency summations. The Matsubara frequency $i\omega$ therefore plays the role of an external parameter so that the analytic continuation to real frequencies can be trivially performed. Obviously, within our truncation only elastic scattering processes are taken into account for the calculation of $\tilde{\Pi}(\mathbf{k}, i\omega)$. On the other hand, our flow equation (3.44) for the static self-energy $\Sigma(\mathbf{k})$ involves a frequency summation, so that it takes also inelastic scattering processes into account.

C. Integral equation for the irreducible dynamic susceptibility

Although Eqs. (3.42) and (3.44) can be used to calculate the static self-energy $\Sigma(\mathbf{k})$ and thus detect possible magnetic instabilities, in this work we will focus

on the finite-frequency spin dynamics in the paramagnetic phase at high temperatures. To this end, it is sufficient to simplify the above system of flow equations by ignoring the flow equation (3.44) for the static self-energy, assuming that the static two-spin correlation function $G(\mathbf{k}) = G_{\Lambda=1}(\mathbf{k})$ can be determined by some other method. In fact, at high temperatures, we can simply calculate $G(\mathbf{k})$ via an expansion in powers of J/T , as will be discussed in Sec. IV. The vertex correction factor

$$Z(\mathbf{q}, \mathbf{k}) = Y^2(\mathbf{q} + \mathbf{k}, \mathbf{q}) = \left[1 + \frac{J(\mathbf{q} + \mathbf{k}) - J(\mathbf{q})}{2} G(\mathbf{q}) \right]^2 \quad (3.45)$$

is then independent of the deformation parameter Λ so that our flow equation (3.42) for the dynamic susceptibility reduces to

$$\partial_\Lambda \tilde{\Pi}_\Lambda(\mathbf{k}, i\omega) = \frac{T}{\omega^2} \int_{\mathbf{q}} \dot{F}_\Lambda(\mathbf{q}, i\omega) [G(\mathbf{q} + \mathbf{k})Z(\mathbf{q}, \mathbf{k}) + G(\mathbf{q} - \mathbf{k})Z(\mathbf{q}, -\mathbf{k}) - 2G(\mathbf{q})]. \quad (3.46)$$

To convert this integro-differential equation into an integral equation we use the Katanin substitution [53], which amounts to replacing the single-scale propagator $\dot{F}_\Lambda(\mathbf{q}, i\omega)$ by a total scale-derivative $\partial_\Lambda F_\Lambda(\mathbf{q}, i\omega)$. The right-hand side of Eq. (3.46) is then a total Λ -derivative so that by integrating both sides over Λ we obtain an integral equation for the irreducible dynamic susceptibility $\tilde{\Pi}(\mathbf{k}, i\omega) = \tilde{\Pi}_{\Lambda=1}(\mathbf{k}, i\omega)$. The lower limit $\Lambda = 0$ does not contribute because for finite ω the function $\tilde{\Pi}_{\Lambda=0}(\mathbf{k}, i\omega)$ vanishes. Then Eq. (3.46) reduces to the following integral equation for the subtracted irreducible dynamic susceptibility,

$$\tilde{\Pi}(\mathbf{k}, i\omega) = \frac{1}{\omega^2} \int_{\mathbf{q}} \frac{\tilde{V}(\mathbf{k}, \mathbf{q})}{G(\mathbf{q}) + \tilde{\Pi}(\mathbf{q}, i\omega)}, \quad (3.47)$$

where the dimensionless kernel $\tilde{V}(\mathbf{k}, \mathbf{q})$ is defined by

$$\tilde{V}(\mathbf{k}, \mathbf{q}) \equiv T [G(\mathbf{q} + \mathbf{k})Z(\mathbf{q}, \mathbf{k}) + G(\mathbf{q} - \mathbf{k})Z(\mathbf{q}, -\mathbf{k}) - 2G(\mathbf{q})]. \quad (3.48)$$

It is convenient to parametrize the subtracted irreducible dynamic susceptibility in terms of an energy $\Delta(\mathbf{k}, i\omega)$ as follows

$$\tilde{\Pi}(\mathbf{k}, i\omega) = G(\mathbf{k}) \frac{\Delta(\mathbf{k}, i\omega)}{|\omega|}. \quad (3.49)$$

Substituting this definition into Eq. (2.9) relating $\tilde{\Pi}(\mathbf{k}, i\omega)$ to the dynamic spin-spin correlation function $G(\mathbf{k}, i\omega)$ and using the fact that by construction $\tilde{J}(\mathbf{k}) = G^{-1}(\mathbf{k})$, we obtain

$$G(\mathbf{k}, i\omega) = G(\mathbf{k}) \frac{\Delta(\mathbf{k}, i\omega)}{\Delta(\mathbf{k}, i\omega) + |\omega|}. \quad (3.50)$$

After analytic continuation to real frequencies $i\omega \rightarrow \omega + i0^+$ this reduces to Eq. (1.3). We call $\Delta(\mathbf{k}, \omega)$ the

dissipation energy, because a purely real value of this energy implies a pole of the retarded spin-spin correlation function $G(\mathbf{k}, \omega)$ on the imaginary axis in the complex frequency plane. The energy $\Delta(\mathbf{k}, \omega)$ can then be identified with the energy scale associated with the dissipative decay of spin fluctuations with wavevector \mathbf{k} . Substituting the definition (3.49) into the integral equation (3.47) we find that within our truncation of the FRG flow equations the dissipation energy $\Delta(\mathbf{k}, i\omega)$ satisfies the integral equation

$$\Delta(\mathbf{k}, i\omega) = \int_{\mathbf{q}} \frac{V(\mathbf{k}, \mathbf{q})}{\Delta(\mathbf{q}, i\omega) + |\omega|}, \quad (3.51)$$

where the kernel

$$V(\mathbf{k}, \mathbf{q}) = G^{-1}(\mathbf{k})G^{-1}(\mathbf{q})\tilde{V}(\mathbf{k}, \mathbf{q}) = TG^{-1}(\mathbf{k})G^{-1}(\mathbf{q}) \times [G(\mathbf{q} + \mathbf{k})Z(\mathbf{q}, \mathbf{k}) + G(\mathbf{q} - \mathbf{k})Z(\mathbf{q}, -\mathbf{k}) - 2G(\mathbf{q})] \quad (3.52)$$

has units of energy squared. Here the vertex renormalization factor $Z(\mathbf{q}, \mathbf{k})$ is defined in Eq. (3.45). Assuming that for small wavevectors the dissipation energy $\Delta(\mathbf{k}, i\omega)$ can be expanded as

$$\Delta(\mathbf{k}, i\omega) = \mathcal{D}(i\omega)k^2 + \mathcal{O}(k^4), \quad (3.53)$$

we conclude that if the dynamics is indeed diffusive, then the spin-diffusion coefficient is given by

$$\mathcal{D} = \mathcal{D}(0) = \lim_{k \rightarrow 0} \frac{\Delta(\mathbf{k}, 0)}{k^2}. \quad (3.54)$$

The non-linear integral equation (3.51) can be solved for the dissipation energy $\Delta(\mathbf{k}, i\omega)$ if the static spin-spin correlation function $G(\mathbf{k})$ has been determined by some other method. We could now go back to the system of flow equations (3.42) and (3.44) to determine both the dynamic susceptibility $\tilde{\Pi}_\Lambda(\mathbf{k}, i\omega)$ and the static self-energy $\Sigma_\Lambda(\mathbf{k})$. However, the explicit solution of this system of equations requires extensive numerical calculations which are beyond the scope of this work. In the rest of this work we will focus on the dissipative dynamics at high temperatures where the static spin-spin correlations can be obtained by means of an expansion in powers of J/T which can then be used to determine the kernel $V(\mathbf{k}, \mathbf{q})$ in the integral equation (3.51).

To conclude this section, let us point out that within the framework of the so-called mode-coupling theory [54] (see Refs. [55 and 56] for reviews) a similar parametrization of the retarded spin-spin correlation function is used. Typically, in mode-coupling theory one starts from a generalized Langevin equation for the Kubo relaxation function [57], where the memory kernel, involving higher order correlations, is closely related to the dissipation energy $\Delta(\mathbf{k}, \omega)$ used by us. After applying several approximations to the kernel, one arrives at a closed integro-differential equation for the relaxation function, which has been extensively studied in the literature [9, 54–56, 58]. However, in contrast to our integral equation

(3.51), the integro-differential equation for the relaxation function obtained in mode-coupling theory is non-local in frequency-space.

IV. DISSIPATIVE SPIN DYNAMICS AT INFINITE TEMPERATURE

The problem of spin diffusion in quantum Heisenberg magnets at infinite temperature has been discussed by many authors. Older works focused on three-dimensional systems [3–12], while recently the high-temperature spin dynamics in one-dimensional Heisenberg magnets has attracted considerable attention [16–22, 24]. Even at $T = \infty$ the problem of calculating the dynamic spin-spin correlation function of Heisenberg magnets is non-trivial and requires non-perturbative resummation and extrapolation schemes. In fact, up until now, a resummation scheme based on the diagrammatic approach to quantum spin systems developed by Vaks, Larkin and Pikin [41–43] which generates a diffusive pole in the spin-spin correlation function has not been found. We now show that by solving the integral equation (3.51) we obtain such a non-perturbative resummation. Although in this work we focus on the limit of infinite temperature, we have preliminary evidence [44] that our approach gives sensible results in the entire paramagnetic regime, including the temperature range in the vicinity of the critical point.

Once we have calculated the dissipation energy $\Delta(\mathbf{k}, i\omega)$ by solving the integral equation (3.51), we can obtain the retarded spin-spin correlation function by analytic continuation to real frequencies, $i\omega \rightarrow \omega + i0$, which amounts to the replacement $|\omega| \rightarrow -i\omega$. From Eq. (3.50) we then obtain the retarded spin-spin correlation function in the form (1.3), where the retarded dissipation energy $\Delta(\mathbf{k}, \omega)$ is in general a complex function which we decompose into real and imaginary part,

$$\Delta(\mathbf{k}, \omega) = \Delta_R(\mathbf{k}, \omega) + i\Delta_I(\mathbf{k}, \omega). \quad (4.1)$$

The dynamic structure factor can then be obtained with the help of the fluctuation-dissipation theorem,

$$\begin{aligned} S(\mathbf{k}, \omega) &= \left[1 + \frac{1}{e^{\beta\omega} - 1} \right] \frac{1}{\pi} \text{Im} G(\mathbf{k}, \omega) \\ &= \frac{\omega G(\mathbf{k})}{1 - e^{-\beta\omega}} \frac{1}{\pi} \frac{\Delta_R(\mathbf{k}, \omega)}{\Delta_R^2(\mathbf{k}, \omega) + [\omega - \Delta_I(\mathbf{k}, \omega)]^2}. \end{aligned} \quad (4.2)$$

In the limit of infinite temperature this reduces to

$$S(\mathbf{k}, \omega) = \frac{b'_0}{\pi} \frac{\Delta_R(\mathbf{k}, \omega)}{\Delta_R^2(\mathbf{k}, \omega) + [\omega - \Delta_I(\mathbf{k}, \omega)]^2}. \quad (4.3)$$

A. General strategy

At temperatures $T \gg J$ it is sufficient to approximate the static self-energy by its truncated expansion in pow-

ers of $1/T$ up to order J^2/T ,

$$\Sigma(\mathbf{k}) = \frac{T}{b'_0} + \frac{\Sigma_2(\mathbf{k})}{T} + \mathcal{O}\left(\frac{J^3}{T^2}\right), \quad (4.4)$$

where

$$\Sigma_2(\mathbf{k}) = \frac{1}{12} \int_{\mathbf{q}} J(\mathbf{q}) J(\mathbf{q} + \mathbf{k}) + \left(b'_0 + \frac{1}{6}\right) \int_{\mathbf{q}} J^2(\mathbf{q}). \quad (4.5)$$

The kernel $V(\mathbf{k}, \mathbf{q})$ defined in Eq. (3.52) then reduces to

$$\begin{aligned} V(\mathbf{k}, \mathbf{q}) &= \frac{b'_0}{4} \left[[J(\mathbf{q}) - J(\mathbf{q} + \mathbf{k})]^2 + [J(\mathbf{q}) - J(\mathbf{q} - \mathbf{k})]^2 \right] \\ &\quad + 2\Sigma_2(\mathbf{q}) - \Sigma_2(\mathbf{q} + \mathbf{k}) - \Sigma_2(\mathbf{q} - \mathbf{k}) + \mathcal{O}\left(\frac{J^3}{T}\right). \end{aligned} \quad (4.6)$$

Note that at high temperatures $V(\mathbf{k}, \mathbf{q})$ is a non-trivial function of order J^2 satisfying $V(0, \mathbf{q}) = 0$. To explicitly solve the integral equation (3.51) for the dissipation energy $\Delta(\mathbf{k}, i\omega)$, we note that for exchange couplings J_{ij} with finite range the kernel $V(\mathbf{k}, \mathbf{q})$ can be expanded as

$$V(\mathbf{k}, \mathbf{q}) = \sum_{\alpha=1}^n e^{i\mathbf{k} \cdot \mathbf{R}_\alpha} V_\alpha(\mathbf{q}), \quad (4.7)$$

where $\mathbf{R}_1, \mathbf{R}_2, \dots, \mathbf{R}_n$ is a finite set of vectors of the underlying Bravais lattice which depends on the precise form of $J(\mathbf{k})$ and on the geometry and dimensionality of the lattice. The solution of Eq. (3.51) is then of the form

$$\Delta(\mathbf{k}, i\omega) = \sum_{\alpha=1}^n e^{i\mathbf{k} \cdot \mathbf{R}_\alpha} \Delta_\alpha(i\omega), \quad (4.8)$$

where the n coefficients $\Delta_1(i\omega), \dots, \Delta_n(i\omega)$ satisfy the following system of non-linear equations,

$$\Delta_\alpha(i\omega) = \int_{\mathbf{q}} \frac{V_\alpha(\mathbf{q})}{|\omega| + \sum_{\alpha'=1}^n e^{i\mathbf{q} \cdot \mathbf{R}_{\alpha'}} \Delta_{\alpha'}(i\omega)}, \quad \alpha = 1, \dots, n. \quad (4.9)$$

To obtain an explicit solution of these equations, let us assume here for simplicity that the spins are located on a d -dimensional hypercubic lattice with spacing a and that the exchange couplings J_{ij} connect only pairs of nearest neighbors. In Sec. IV C and in Appendix B we will discuss more general models including next-nearest-neighbor exchange. Denoting by J the strength of the nearest-neighbor coupling, the Fourier transform of the exchange couplings on a d -dimensional hypercubic lattice is

$$J(\mathbf{k}) = J \sum_{\boldsymbol{\delta}} e^{i\mathbf{k} \cdot \boldsymbol{\delta}} = 2dJ\gamma_{\mathbf{k}}, \quad (4.10)$$

where the sum is over the $2d$ vectors $\boldsymbol{\delta}$ with length $|\boldsymbol{\delta}| = a$ connecting a given site to its nearest neighbors. For later convenience we have introduced the normalized nearest-neighbor hypercubic form factor

$$\gamma_{\mathbf{k}} = \frac{1}{2d} \sum_{\boldsymbol{\delta}} e^{i\mathbf{k} \cdot \boldsymbol{\delta}} = \frac{1}{d} \sum_{\mu=1}^d \cos(k_\mu a). \quad (4.11)$$

Using

$$\int_{\mathbf{q}} \gamma_{\mathbf{q}} \gamma_{\mathbf{q}+\mathbf{k}} = \frac{\gamma_{\mathbf{k}}}{2d}, \quad (4.12)$$

the integral $\Sigma_2(\mathbf{k})$ defined in Eq. (4.5) is easily evaluated,

$$\Sigma_2(\mathbf{k}) = 2dJ^2 \left[\frac{\gamma_{\mathbf{k}}}{12} + b'_0 + \frac{1}{6} \right]. \quad (4.13)$$

We conclude that for nearest-neighbor exchange on a hypercubic lattice

$$\begin{aligned} & 2\Sigma_2(\mathbf{q}) - \Sigma_2(\mathbf{q} + \mathbf{k}) - \Sigma_2(\mathbf{q} - \mathbf{k}) \\ &= \frac{dJ^2}{6} [2\gamma_{\mathbf{q}} - \gamma_{\mathbf{q}+\mathbf{k}} - \gamma_{\mathbf{q}-\mathbf{k}}]. \end{aligned} \quad (4.14)$$

At this point it is convenient to measure all energies in units of $|J|\sqrt{b'_0}$, defining the dimensionless quantities

$$\tilde{\Delta}(\mathbf{k}, i\omega) \equiv \frac{\Delta(\mathbf{k}, i\omega)}{|J|\sqrt{b'_0}}, \quad \tilde{\omega} \equiv \frac{\omega}{|J|\sqrt{b'_0}}. \quad (4.15)$$

B. Spin-diffusion coefficient in $d \geq 2$

The cubic symmetry and the condition $\Delta(\mathbf{k} = 0, i\omega) = 0$ imply that for nearest-neighbor coupling the expansion (4.8) can be expressed in terms of only three independent form factors. In dimensionless form the expansion is therefore

$$\begin{aligned} \tilde{\Delta}(\mathbf{k}, i\omega) &= (1 - \gamma_{\mathbf{k}}) \tilde{\Delta}_1(i\omega) + (1 - \gamma_{2\mathbf{k}}) \tilde{\Delta}_2^{\parallel}(i\omega) \\ &\quad + (1 - \gamma_{\mathbf{k}}^{\perp}) \tilde{\Delta}_2^{\perp}(i\omega), \end{aligned} \quad (4.16)$$

where we have introduced the off-diagonal next-nearest-neighbor form factor

$$\gamma_{\mathbf{k}}^{\perp} = \frac{2}{d(d-1)} \sum_{1 \leq \mu < \mu' \leq d} \cos(k_{\mu}a) \cos(k_{\mu'}a). \quad (4.17)$$

In d dimensions we find from Eq. (4.9) that the three amplitudes in Eq. (4.16) satisfy the following system of equations,

$$\begin{aligned} \tilde{\Delta}_1(i\omega) &= 2d \int_{\mathbf{q}} \frac{1}{|\tilde{\omega}| + \tilde{\Delta}(\mathbf{q}, i\omega)} + \frac{d}{3b'_0} \int_{\mathbf{q}} \frac{\gamma_{\mathbf{q}}}{|\tilde{\omega}| + \tilde{\Delta}(\mathbf{q}, i\omega)} \\ &\quad - 2\tilde{\Delta}_2^{\parallel}(i\omega) - 2\tilde{\Delta}_2^{\perp}(i\omega), \end{aligned} \quad (4.18a)$$

$$\tilde{\Delta}_2^{\parallel}(i\omega) = -d \int_{\mathbf{q}} \frac{\gamma_{2\mathbf{q}}}{|\tilde{\omega}| + \tilde{\Delta}(\mathbf{q}, i\omega)}, \quad (4.18b)$$

$$\tilde{\Delta}_2^{\perp}(i\omega) = -2d(d-1) \int_{\mathbf{q}} \frac{\gamma_{\mathbf{q}}^{\perp}}{|\tilde{\omega}| + \tilde{\Delta}(\mathbf{q}, i\omega)}. \quad (4.18c)$$

It turns out that for $d > 2$ the self-consistent solution of these equations have a finite limit for $\omega \rightarrow 0$, implying that the static dissipation energy $\Delta(\mathbf{k}, i\omega = 0)$ is finite. [59] According to Eq. (3.54) the spin-diffusion coefficient \mathcal{D} can then be obtained from the quadratic term in the

S	$\frac{1}{2}$	1	$\frac{3}{2}$	2	∞
$\frac{\mathcal{D}}{ J a^2\sqrt{4b'_0}}$	0.217	0.189	0.179	0.175	0.167

TABLE I. Spin-diffusion coefficient \mathcal{D} of the nearest-neighbor spin- S Heisenberg model on a cubic lattice with lattice spacing a at infinite temperature obtained from Eq. (4.19). Note that for $S = 1/2$ the normalization factor $\sqrt{4b'_0} = \sqrt{4S(S+1)/3}$ is unity. The quantum term proportional to $d/(3b'_0)$ in Eq. (4.18a) gives rise to some additional spin-dependence which vanishes for $S \rightarrow \infty$. For large S we obtain $\mathcal{D} = 0.193 S|J|a^2$ to leading order.

expansion of $\Delta(\mathbf{k}, 0)$ for small \mathbf{k} . From Eqs. (4.15) and (4.16) we obtain

$$\mathcal{D} = \frac{|J|\sqrt{b'_0}a^2}{2d} \left[\tilde{\Delta}_1(0) + 4\tilde{\Delta}_2^{\parallel}(0) + 2\tilde{\Delta}_2^{\perp}(0) \right]. \quad (4.19)$$

In the limit of high dimensions the solution of Eqs. (4.18) simplifies because to leading order in $1/d$ the first term on the right-hand side of Eq. (4.18a) without form factor dominates. In this limit we obtain $\tilde{\Delta}_1(0) = \sqrt{2d}$ and $\tilde{\Delta}_2^{\parallel}(0) = \tilde{\Delta}_2^{\perp}(0) = 0$, implying $\mathcal{D} = |J|a^2\sqrt{b'_0/2d}$. In the physically relevant case of three dimensions we have to solve Eqs. (4.18) numerically to obtain the value of \mathcal{D} . In Table I we present our numerical results for \mathcal{D} in three dimensions for different spin quantum numbers S . In the special case of $S = \frac{1}{2}$ our result $\mathcal{D} \approx 0.217|J|a^2$ is roughly 30% smaller than theoretical results obtained by extrapolating the short-time expansion of suitable correlation functions to long times [3–8, 10–13]. Surprisingly, controlled numerical results for the spin-diffusion coefficient of the three-dimensional Heisenberg model at infinite temperature are not available. Note, however, that there is experimental evidence [14] that extrapolations based on the short-time expansion tend to overestimate the numerical value of \mathcal{D} . In the following subsection we will use our method to calculate the high-temperature value of \mathcal{D} for a Heisenberg model on a body-centered cubic lattice relevant to the experiment of Ref. [14].

C. Spin diffusion on a body-centered cubic lattice including next-nearest-neighbor exchange

The measurement of the spin-diffusion coefficient \mathcal{D} in the ferromagnetic insulator $\text{Rb}_2\text{CuBr}_4 \cdot 2\text{H}_2\text{O}$ by Labrujere *et al.* [14] seems to be the only published experimental determination of \mathcal{D} in a three-dimensional Heisenberg magnet at high temperatures. The magnetic properties of the copper ions in this material can be described by a ferromagnetic spin $S = 1/2$ Heisenberg model on a body-centered cubic (bcc) lattice with nearest-neighbor exchange [14, 60] $|J_1|/2 \approx 0.49$ K and next-nearest-neighbor exchange $|J_2|/2 \approx 0.29$ K, as illustrated in Fig. 2. The spin-diffusion coefficient was measured at

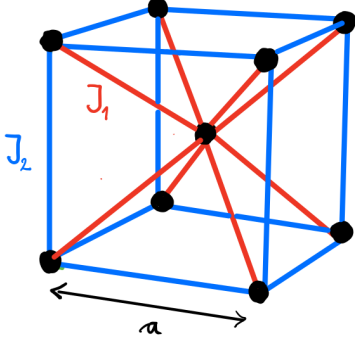


FIG. 2. Conventional unit cell of the body-centered cubic lattice with lattice spacing a . The black dots represent the magnetic copper ions in $\text{Rb}_2\text{CuBr}_4 \cdot 2\text{H}_2\text{O}$ which are coupled by nearest-neighbor exchange J_1 (red lines) and next-nearest-neighbor exchange J_2 (blue lines). The non-magnetic atoms of $\text{Rb}_2\text{CuBr}_4 \cdot 2\text{H}_2\text{O}$ are omitted.

two different temperatures $T = 20$ K and $T = 77$ K, which are two orders magnitude larger than the energy scales $|J_1|S^2$ and $|J_2|S^2$ associated with the exchange couplings. Since the bcc lattice is a Bravais lattice, we can use the formalism developed in this work to calculate the spin-diffusion coefficient. To explicitly solve the integral equation (3.51), we need the Fourier transform of the exchange couplings for the geometry shown in Fig. 2,

$$J(\mathbf{k}) = J_1(\mathbf{k}) + J_2(\mathbf{k}), \quad (4.20a)$$

$$J_1(\mathbf{k}) = 8J_1\gamma_{\mathbf{k}}^{\text{bcc}}, \quad (4.20b)$$

$$J_2(\mathbf{k}) = 6J_2\gamma_{\mathbf{k}}. \quad (4.20c)$$

Here the normalized bcc form factor is

$$\gamma_{\mathbf{k}}^{\text{bcc}} = \cos\left(\frac{k_x a}{2}\right) \cos\left(\frac{k_y a}{2}\right) \cos\left(\frac{k_z a}{2}\right), \quad (4.21)$$

and the normalized cubic form factor $\gamma_{\mathbf{k}}$ can be obtained by setting $d = 3$ in Eq. (4.11), i.e.,

$$\gamma_{\mathbf{k}} = \frac{1}{3} [\cos(k_x a) + \cos(k_y a) + \cos(k_z a)]. \quad (4.22)$$

As in the calculation of the dissipation energy $\Delta(\mathbf{k}, 0)$ for the cubic lattice described in Sec. IV B, we decompose $\Delta(\mathbf{k}, i\omega)$ into a finite number of form factors and solve the resulting non-linear equations for the amplitudes at $\omega = 0$ numerically. For a bcc lattice with nearest-neighbor and next-nearest-neighbor exchange six independent form factors are necessary to obtain a closed system of equations. Technical details of the calculation are given in Appendix A. In the simplified case of only nearest-neighbor exchange we obtain $\mathcal{D}_{\text{bcc}}^{J_2=0} \approx 0.18|J_1|a^2$ for $S = 1/2$, which is roughly a factor of $5/6$ smaller

than our result on a cubic lattice for the same value of J_1 . Our result for the ratio $\mathcal{D}_{\text{bcc}}/\mathcal{D}_{\text{cubic}}$ agrees with the corresponding ratio obtained by Morita [10, 11] using a different method. According to Ref. [14], in the experimentally studied material $\text{Rb}_2\text{CuBr}_4 \cdot 2\text{H}_2\text{O}$ the ratio of exchange couplings is $J_2/J_1 \approx 0.6$; with this value we obtain on a bcc lattice

$$\mathcal{D}_{\text{bcc}}^{J_2/J_1=0.6} \approx 0.23|J_1|a^2 = 0.46|J'_1|a^2, \quad (4.23)$$

where we have set $|J'_1| = |J_1|/2$ to facilitate the comparison [60] with Ref. [14], where the experimental result

$$\mathcal{D}_{\text{exp}} \approx (0.31 \pm 0.03)|J'_1|a^2 \quad (4.24)$$

is presented in terms of J'_1 . Our theoretical prediction (4.23) for the high-temperature spin-diffusion coefficient in $\text{Rb}_2\text{CuBr}_4 \cdot 2\text{H}_2\text{O}$ is about 30% larger than the corresponding experimental result in Eq. (4.24). With the exception of the method developed by Bennett and Martin [5] (which gives a prefactor 0.40 instead of our 0.46 in Eq. (4.23)) other theoretical approaches [4, 6, 8] predict even larger values for \mathcal{D}_{bcc} . We conclude that at high temperatures the measured value of the spin-diffusion coefficient in the ferromagnetic insulator $\text{Rb}_2\text{CuBr}_4 \cdot 2\text{H}_2\text{O}$ is significantly smaller than all available theoretical predictions.

A possible explanation for this discrepancy is that at high temperatures the relevant value of the next-nearest-neighbor coupling J_2 is not given by $J_2/J_1 = 0.6$ but has a value somewhere in the range $-0.4 \lesssim J_2/J_1 \lesssim 0$. As shown in Fig. 3, in this range \mathcal{D}_{bcc} exhibits a broad minimum as a function of J_2/J_1 which is reasonably close to the experimental value. Although this agreement might be accidental, a possible reason for the deviation of J_2/J_1 from the value 0.6 used in Ref. [14] could be a significant temperature-dependence of J_2 in the high-temperature regime probed in the experiment. This hypothesis is supported by the fact that in the related compound $\text{K}_2\text{CuCl}_4 \cdot 2\text{H}_2\text{O}$ a strong temperature-dependence of the nearest-neighbor exchange interaction has been observed [61], which decreases by a factor of five when raising T from 77 K to 300 K. As a possible reason the authors of [61] identified a low-lying optical phonon.

D. Anomalous spin diffusion in reduced dimensions

We now come back to the nearest-neighbor spin- S Heisenberg model on a hypercubic lattice and consider the case $d \leq 2$. Then it is not allowed to approximate $\tilde{\Delta}(\mathbf{q}, i\omega) \approx \tilde{\Delta}(\mathbf{q}, 0)$ in Eq. (4.18) because the frequency-dependence of $\tilde{\Delta}(\mathbf{q}, i\omega)$ is essential to cut the infrared divergence of the integrals. For small frequencies $|\omega| \ll |J|\sqrt{b'_0}$ the leading behavior of the relevant integrals can be obtained by expanding the integrands to leading order in \mathbf{q} ,

$$\tilde{\Delta}(\mathbf{q}, i\omega) = \tilde{\mathcal{D}}(i\omega)q^2 + \dots, \quad (4.25)$$

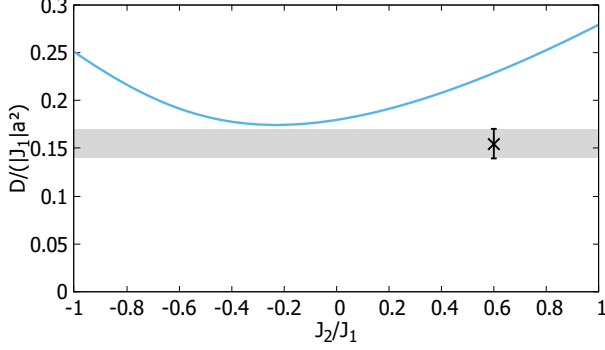


FIG. 3. Spin-diffusion coefficient \mathcal{D}_{bcc} for a spin 1/2 Heisenberg magnet with nearest-neighbor exchange J_1 and next-nearest-neighbor exchange J_2 on a bcc lattice at infinite temperature as a function of the ratio J_2/J_1 . The blue curve is our result obtained from the solution of the integral equation (3.51) for the dissipation energy $\Delta(\mathbf{k}, 0)$. The black cross at $J_2/J_1 = 0.6$ with error bar marks the experimental result of Labrujere *et al.* [14] obtained in the high-temperature regime of the magnetic insulator $\text{Rb}_2\text{CuBr}_4 \cdot 2\text{H}_2\text{O}$; the shaded area represents the experimental uncertainty assuming that the true value of J_2/J_1 is not known.

where

$$\tilde{\mathcal{D}}(i\omega) \equiv \frac{\mathcal{D}(i\omega)}{|J|\sqrt{b'_0}}. \quad (4.26)$$

The leading singular part of the integrals in Eq. (4.18) can then be obtained by approximating,

$$\int_{\mathbf{q}} \frac{f(\mathbf{q})}{|\tilde{\omega}| + \tilde{\Delta}(\mathbf{q}, i\omega)} \approx f(\mathbf{0}) \int_{\mathbf{q}} \frac{1}{|\tilde{\omega}| + \tilde{\mathcal{D}}(i\omega)q^2}, \quad (4.27)$$

where $f(\mathbf{q})$ is any of the enumerators in Eq. (4.18). Note that from Eq. (4.16) we find that the coefficient of order k^2 in the expansion of $\tilde{\Delta}(\mathbf{k}, i\omega)$ satisfies

$$\tilde{\mathcal{D}}(i\omega) = \frac{a^2}{6b'_0} \int_{\mathbf{q}} \frac{\gamma_{\mathbf{q}}}{|\tilde{\omega}| + \tilde{\Delta}(\mathbf{q}, i\omega)} + a^2 \int_{\mathbf{q}} \frac{1 - \gamma_{2\mathbf{q}}}{|\tilde{\omega}| + \tilde{\Delta}(\mathbf{q}, i\omega)}. \quad (4.28)$$

From this expression we conclude that the singular part of the spin-diffusion coefficient is completely determined by the self-energy contribution $2\Sigma_2(\mathbf{q}) - \Sigma_2(\mathbf{q} + \mathbf{k}) - \Sigma_2(\mathbf{q} - \mathbf{k}) \propto 1/b'_0$ to the high-temperature expansion (4.6) of the kernel $V(\mathbf{k}, \mathbf{q})$ of the integral equation (3.51). In dimensions $d \leq 2$ the leading singular part of the generalized diffusion coefficient can therefore be obtained from the solution of

$$\tilde{\mathcal{D}}(i\omega) = \frac{a^2}{6b'_0} \int_{\mathbf{q}} \frac{1}{|\tilde{\omega}| + \tilde{\mathcal{D}}(i\omega)q^2}. \quad (4.29)$$

In terms of dimensionful quantities this can also be written as

$$\mathcal{D}(i\omega) = \frac{J^2 a^2}{6} \int_{\mathbf{q}} \frac{1}{|\omega| + \mathcal{D}(i\omega)q^2}. \quad (4.30)$$

Consider first the case of one dimension, where the solution of Eq. (4.30) yields for the singular part of the generalized diffusion coefficient

$$\mathcal{D}(i\omega) = \left(\frac{|J|}{144|\omega|} \right)^{\frac{1}{3}} |J|a^2, \quad d = 1. \quad (4.31)$$

To obtain the retarded spin-spin correlation function and the dynamic structure factor, we should analytically continue $\mathcal{D}(i\omega)$ to real frequencies, $i\omega \rightarrow \omega + i0$, which amounts to replacing $|\omega| \rightarrow -i\omega$. The correct branch of the multi-valued function $(-i\omega)^{-1/3}$ is determined by the condition that the real part of $\mathcal{D}(\omega)$ must be positive to guarantee the positiveness of the dynamic structure factor in Eq. (4.3). This implies a complex anomalous diffusion coefficient,

$$\mathcal{D}(\omega) = \left(\frac{|J|}{144|\omega|} \right)^{\frac{1}{3}} |J|a^2 \left(\frac{\sqrt{3}}{2} + \frac{i}{2} \text{sgn}\omega \right), \quad (4.32)$$

where the real part $\text{Re}\mathcal{D}(\omega) = \sqrt{3}\text{Im}\mathcal{D}(\omega)\text{sgn}\omega$ has the same order of magnitude as the imaginary part. The corresponding dynamic structure factor $S(k_x, \omega)$ defined via Eq. (4.3) has, as a function of k_x , a broad maximum at $k_x = k_*$ determined by the condition

$$|\mathcal{D}(\omega)|k_*^2 = \omega, \quad (4.33)$$

implying

$$k_* \propto \omega^{2/3}. \quad (4.34)$$

In Fig. 4 we show the momentum dependence of the dynamic structure factor $S(k_x, \omega)$ for small momenta and three different frequencies. The dynamic exponent $z = 3/2$ implied by Eq. (4.34) and the superdiffusive singularity $\mathcal{D}(\omega) \propto |\omega|^{-1/3}$ are in agreement with recent calculations for integrable isotropic Heisenberg chains with nearest-neighbor coupling [16–24]. On the other hand, for non-integrable chains with larger spin $S > 1/2$ the situation is less clear [24]: some authors obtained normal diffusion [22], recognizing broken integrability as its cause, while others found that superdiffusion persists even for non-integrable chains [19]. The fact that for non-integrable chains our approach yields the same superdiffusive high-temperature spin dynamics as for integrable chains might be related to the fact our integral equation (3.51) takes only elastic scattering into account, as pointed out at the end of Sec. III B. While for integrable chains this approximation seems to be justified, in the case of non-integrable chains it might break down at very low energies.

Let us now consider the marginal case of $d = 2$ where the integral in Eq. (4.30) has a logarithmic singularity

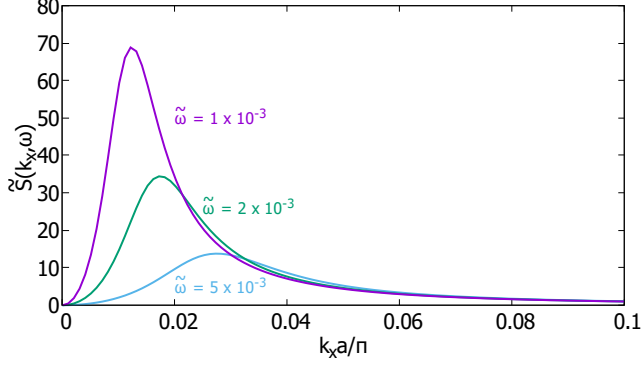


FIG. 4. Momentum dependence of the dimensionless dynamic structure factor $\tilde{S}(k_x, \omega) = S(k_x, \omega)|J|\sqrt{b'_0}$ for small momenta $|k_x| \ll \pi/a$ and frequencies $\tilde{\omega} = \omega/(|J|\sqrt{b'_0}) = 10^{-3}$ (violet curve), 2×10^{-3} (green curve) and 5×10^{-3} (blue curve) of a spin 1/2 Heisenberg chain with nearest-neighbor exchange J at infinite temperature.

which is cut by the frequency $|\omega|$. Retaining only the leading logarithm we obtain

$$\mathcal{D}(i\omega) = \sqrt{\ln \left(\frac{\mathcal{D}(i\omega)}{a^2|\omega|} \right) \frac{|J|a^2}{\sqrt{24\pi}}}, \quad d = 2. \quad (4.35)$$

The solution of this implicit equation can be expressed in terms of the so-called Lambert W -function (product logarithm) [62] which satisfies $W(x) = \ln[x/W(x)]$. Here we are interested only in the leading logarithm, which can be obtained by a simple iteration of the self-consistency equation (4.35). After analytic continuation to real frequencies we obtain for $|\omega| \ll J$,

$$\mathcal{D}(\omega) = \frac{|J|a^2}{\sqrt{24\pi}} \left[\sqrt{\ln \left(\frac{|J|}{\sqrt{24\pi}|\omega|} \right)} + i \frac{\pi}{4} \text{sgn} \omega \right]. \quad (4.36)$$

Note that for $\omega \rightarrow 0$ the real part of $\mathcal{D}(\omega)$ is logarithmically larger than the imaginary part, whereas in $d = 1$ the real- and imaginary part of $\mathcal{D}(\omega)$ in Eq. (4.32) have the same order of magnitude.

V. DISSIPATION ENERGY AND DYNAMIC STRUCTURE FACTOR FOR ALL WAVEVECTORS

So far we have focused on the leading term in the expansion $\Delta(\mathbf{k}, i\omega) = \mathcal{D}(i\omega)k^2 + \mathcal{O}(k^4)$ of the dissipation energy for small wavevectors which determines the frequency-dependent spin-diffusion coefficient $\mathcal{D}(i\omega)$. However, the solution of the integral equation (3.51) gives the dissipation energy $\Delta(\mathbf{k}, i\omega)$ and hence the dynamic structure factor for arbitrary wavevectors. The momentum dependence of $\Delta(\mathbf{k}, i\omega)$ is of particular interest for

Heisenberg magnets with exchange interactions beyond nearest neighbors because in this case $\Delta(\mathbf{k}, i\omega)$ and the corresponding dynamic structure factor $S(\mathbf{k}, \omega)$ defined via Eq. (4.2) can have characteristic features in the first Brillouin zone which can be used to derive constraints on competing exchange interactions. As far as we know, this effect has not been noticed before. In order to illustrate this effect, we have solved the integral equation (3.51) for $\Delta(\mathbf{k}, i\omega)$ in the low-frequency limit $|\omega| \ll |J_1|$ for a Heisenberg model with nearest-neighbor exchange J_1 and next-nearest neighbor exchange J_2 on cubic lattices in dimensions $d = 1, 2, 3$. Technical details of the calculation are given in Appendix B. For convenience we measure energies in units of $|J_1|\sqrt{b'_0}$, defining

$$\tilde{\Delta}(\mathbf{k}, \omega) \equiv \frac{\Delta(\mathbf{k}, \omega)}{|J_1|\sqrt{b'_0}}, \quad (5.1a)$$

$$\tilde{\omega} \equiv \frac{\omega}{|J_1|\sqrt{b'_0}}, \quad (5.1b)$$

$$\tilde{S}(\mathbf{k}, \omega) \equiv S(\mathbf{k}, \omega)|J_1|\sqrt{b'_0}. \quad (5.1c)$$

For a discussion of the dynamic structure factor $S(\mathbf{k}, \omega)$ as a function of the wavevector \mathbf{k} in the first Brillouin zone, we note that for small frequencies and for $ka = \mathcal{O}(1)$ we may approximate

$$\tilde{S}(\mathbf{k}, \omega) \approx \frac{b'_0}{\pi} \frac{\tilde{\Delta}_R(\mathbf{k}, \omega)}{|\tilde{\Delta}(\mathbf{k}, \omega)|^2}, \quad (5.2)$$

which allows us to deduce the qualitative behavior of $S(\mathbf{k}, \omega)$ from $\Delta(\mathbf{k}, \omega)$ and vice versa. In particular, we see that minima of $\Delta(\mathbf{k}, \omega)$ correspond to maxima of $S(\mathbf{k}, \omega)$, while maxima of $\Delta(\mathbf{k}, \omega)$ correspond to minima of $S(\mathbf{k}, \omega)$.

A. One dimension

Let us first consider the case $d = 1$, where according to Eq. (B3) the dimensionless dissipation energy can be written as

$$\tilde{\Delta}(k_x, i\omega) = \sum_{j=1}^4 [1 - \cos(jk_x a)] \tilde{\Delta}_j(i\omega). \quad (5.3)$$

The dimensionless amplitudes $\tilde{\Delta}_j(i\omega)$ at $T = \infty$ can be obtained analytically in the low-frequency limit by applying the approximation (4.27) to the integrals in the self-consistency equations (B4). In Fig. 5 we show the momentum-dependent part

$$\tilde{\Delta}(k_x) \equiv \frac{2}{\sqrt{3}} |\tilde{\omega}|^{\frac{1}{3}} \text{Re} \tilde{\Delta}(k_x, \omega + i0) \quad (5.4)$$

of the dimensionless dissipation energy of a J_1 - J_2 chain with spin 1/2 as a function of J_2/J_1 . In a range of negative coupling ratios starting at $J_2/J_1 = \mu_2 \approx -0.67$ and extending beyond $J_2/J_1 = -1$, the function $\tilde{\Delta}(k_x)$ exhibits a two-peak structure, with one maximum located

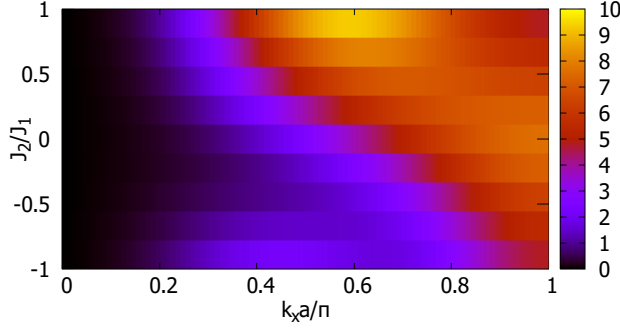


FIG. 5. Contour plot of the momentum-dependent part $\tilde{\Delta}(k_x)$ of the dimensionless dissipation energy defined in Eq. (5.4) for a J_1 - J_2 chain with spin 1/2 as a function of the coupling ratio $\mu = J_2/J_1$ in the interval $-1 \leq \mu \leq 1$.

at $k_x a = \pi$, a second maximum at $k_x a \lesssim \pi/2$, and a minimum somewhere in the interval $[\pi/2, \pi]$. If the coupling ratio $\mu = J_2/J_1$ is smaller than a certain value $\mu_- < -1$ (not shown in Fig. 5), the second maximum at $k_x a \lesssim \pi/2$ becomes the global maximum. On the other hand, for positive coupling ratio $J_2/J_1 > 0$ such a structure cannot be observed. For values of J_2/J_1 larger than the threshold $\mu_+ \approx 0.28$ the peak at $k_x a = \pi$ evolves into the global maximum in the interval $[\frac{\pi}{2}, \pi]$ and a local minimum at $k_x a = \pi$. This non-trivial momentum dependence gives rise to a two-peak structure in the dynamic structure factor, which according to Eqs. (5.1c), (5.2) and (5.4) can for small frequencies $|\omega| \ll |J_1|$ and large wavevectors $|k_x a| = \mathcal{O}(1)$ be written as

$$\tilde{S}(k_x, \omega) = \frac{\sqrt{3}b'_0|\tilde{\omega}|^{\frac{1}{3}}}{2\pi\tilde{\Delta}(k_x)}. \quad (5.5)$$

The momentum dependence of the dynamic structure factor in this regime is therefore given by the inverse of the function $\tilde{\Delta}(k_x)$ defined in Eq. (5.4), which we plot in Fig. 6 for three different values of J_2/J_1 , chosen as $-1, 0, 1$ in order to display all qualitative features. Note that in Fig. 6 we draw a different momentum range than in Fig. 4, so that the dominant peak for small wavevectors is not visible. The lineshape in Fig. 6 exhibits a second peak at short wavelengths, which moves from $k_x a = \pi$ for $J_2/J_1 = 1$ to a value in the interval $k_x a \in [\frac{\pi}{2}, \pi]$ for $J_2/J_1 = -1$. In the latter case the peak is surrounded by two local minima which is a direct consequence of the two maxima of $\tilde{\Delta}(k_x)$ which emerge for $J_2/J_1 < \mu_2 \approx -0.67$.

B. Two dimensions

Next, consider the case of two dimensions, where the dissipation energy $\Delta(\mathbf{k}, i\omega)$ exhibits a logarithmic depen-

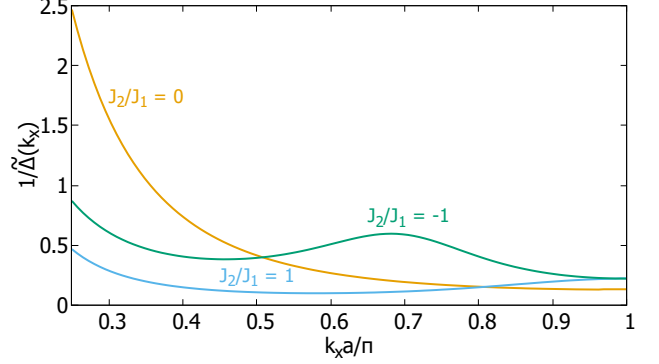


FIG. 6. Inverse of the momentum-dependent part $\tilde{\Delta}(k_x)$ of the dimensionless dissipation energy defined in Eq. (5.4) for a spin 1/2 chain for large momenta $k_x a > \pi/4$ and $J_2/J_1 = -1, 0, 1$ (green, orange, blue). According to Eq. (5.5), for $|\omega| \ll |J_1|$ this quantity is proportional to the dynamic structure factor.

dence on the frequency ω , which in the long-wavelength limit can be expressed in terms of the anomalous diffusion coefficient $\mathcal{D}(i\omega)$ defined in Eq. (4.35). The asymptotic limit $\omega \rightarrow 0$ of $\Delta(\mathbf{k}, i\omega)$ can be calculated analytically from the self-consistency equations (B14) for the amplitudes of its Fourier expansion (B11), using again the approximation (4.27). Since the logarithmic frequency-dependence survives also at short wavelengths, it is convenient to scale out the frequency-dependence by defining the momentum dependent dimensionless dissipation energy

$$\tilde{\Delta}(\mathbf{k}) \equiv \frac{\text{Re}\tilde{\Delta}(\mathbf{k}, \omega + i0)}{\sqrt{\ln\left(\frac{\sqrt{J_1^2 + 2J_2^2}}{\sqrt{24}\pi|\omega|}\right)}}. \quad (5.6)$$

Our results for $\tilde{\Delta}(\mathbf{k})$ in the first quadrant of the Brillouin zone for different values of J_2/J_1 are shown in Fig. 7. For sufficiently large negative values of J_2/J_1 starting at $J_2/J_1 = \mu_2 \approx -0.52$ and extending again beyond $J_2/J_1 = -1$, the function $\tilde{\Delta}(\mathbf{k})$ then exhibits two peaks at $\mathbf{k}a = (0, \pi)$ and $\mathbf{k}a = (\pi, \pi)$. Similar to the case of one dimension, for negative J_2/J_1 the global maximum is located at the corner $\mathbf{k}a = (\pi, \pi)$ of the Brillouin zone for much larger values of $|J_2|$ than for positive J_2/J_1 . On the other hand, for $J_2/J_1 > 0$ the function $\tilde{\Delta}(\mathbf{k})$ is more sensitive to the presence of J_2 ; at $J_2/J_1 = \mu_+ \approx 0.52$ the wavevector where $\tilde{\Delta}(\mathbf{k})$ exhibits a maximum shifts from $\mathbf{k}a = (\pi, \pi)$ to $\mathbf{k}a = (0, \pi)$. For $\omega \rightarrow 0$ and large wavevectors $|\mathbf{k}a| = \mathcal{O}(1)$ the dynamic structure factor can be obtained from

$$\tilde{S}(\mathbf{k}, \omega) = \sqrt{\ln\left(\frac{\sqrt{J_1^2 + 2J_2^2}}{\sqrt{24}\pi|\omega|}\right)} \frac{b'_0}{\pi\tilde{\Delta}(\mathbf{k})}. \quad (5.7)$$

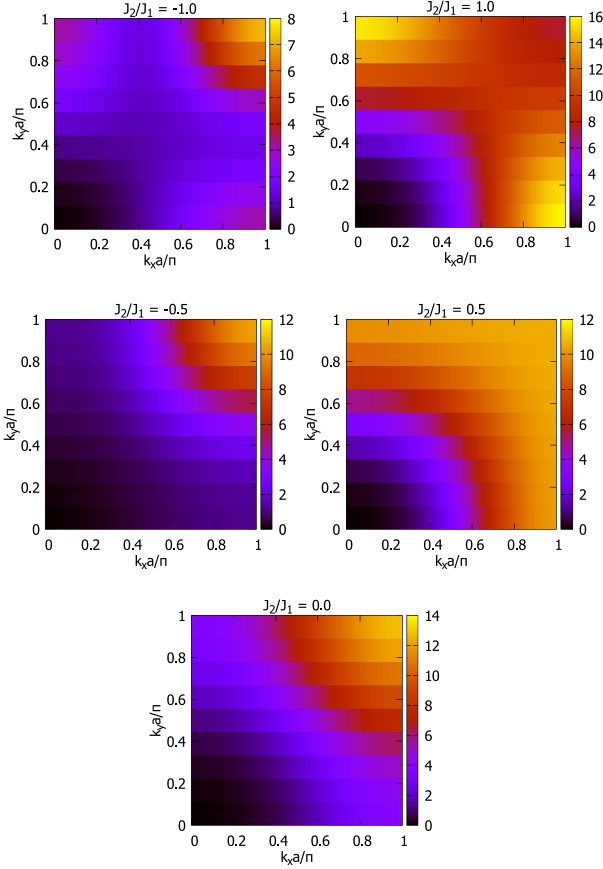


FIG. 7. Momentum dependent part of the rescaled dissipation energy $\tilde{\Delta}(\mathbf{k})$ at infinite temperature of a spin-1/2 J_1 - J_2 Heisenberg model on a square lattice, see Eq. (5.6). The contour plots are for $J_2/J_1 = -1, -0.5, 0, 0.5, 1$ (counterclockwise, starting from top left).

As in one dimension, the momentum dependence of $\tilde{S}(\mathbf{k}, \omega)$ is proportional to the inverse of $\tilde{\Delta}(\mathbf{k})$ which is plotted in Fig. 8 along the path $\mathbf{k}a = (0, \pi) \rightarrow (\pi, \pi)$ for $J_2/J_1 = -1, 0, 1$. One sees that for $J_2/J_1 = 1$ the short-wavelength peak is located at $\mathbf{k}a = (\pi, \pi)$, while for $J_2/J_1 = -1$ the dynamic structure factor exhibits a maximum on the path connecting the two local minima at $\mathbf{k}a = (0, \pi)$ and (π, π) .

C. Three dimensions

In $d = 3$ the dimensionless dissipation energy $\tilde{\Delta}(\mathbf{k}, \omega)$ has a finite limit $\tilde{\Delta}(\mathbf{k}, 0)$ for $\omega \rightarrow 0$, which can be obtained by numerically solving the system (B20) of equations for the amplitudes introduced in Eq. (B18). Our results for $\tilde{\Delta}(\mathbf{k}, 0)$ are shown in Fig. 9 as a function of $k_x, k_y \geq 0$ in the plane $k_z = \pi/a$ for different values of

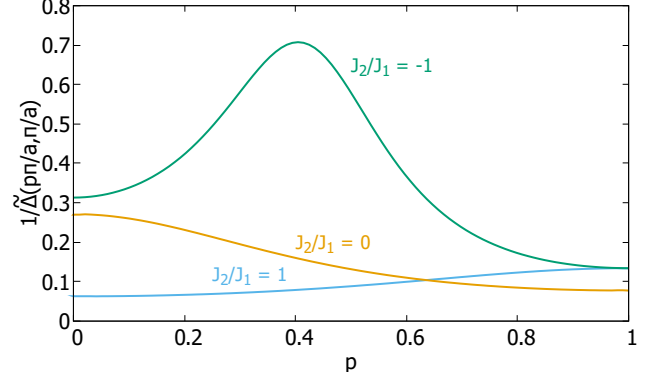


FIG. 8. Inverse of momentum dependent part $\tilde{\Delta}(\mathbf{k})$ of the dimensionless dissipation energy for a spin-1/2 square lattice J_1 - J_2 Heisenberg model at infinite temperature. The three curves represent the momentum dependence along the path $\mathbf{k}(p) = \frac{\pi}{a}(p, 1)$ for $J_2/J_1 = -1, 0, 1$ (green, orange, blue). According to Eq. (5.7) the curves are proportional to the low-frequency limit of the dynamic structure factor.

J_2/J_1 . The main qualitative features of the momentum dependence are similar to the behavior in reduced dimensions discussed above. For $J_2/J_1 < 0$ the maximum of $\tilde{\Delta}(\mathbf{k}, 0)$ at the corner $\mathbf{R} = \frac{\pi}{a}(1, 1, 1)$ of the Brillouin zone is more stable than for $J_2/J_1 > 0$. Furthermore, a two-peak structure emerges at \mathbf{R} and $\mathbf{X} = \frac{\pi}{a}(0, 0, 1)$ with $\mathbf{M} = \frac{\pi}{a}(0, 1, 1)$ remaining a saddle point. The degeneracy point where the peaks at \mathbf{X} and \mathbf{R} have equal height is $J_2/J_1 = \mu_- \approx -0.97$, in contrast to low dimensions where $\mu_- < -1$. For positive J_2/J_1 a simple crossover from \mathbf{R} to \mathbf{M} takes place at $J_2/J_1 = \mu_+ \approx 0.32$. Using Eq. (5.2) the low-frequency limit $\tilde{S}(\mathbf{k}, 0)$ of the dynamic structure factor becomes

$$\tilde{S}(\mathbf{k}, 0) = \frac{b'_0}{\pi \tilde{\Delta}(\mathbf{k}, 0)}, \quad (5.8)$$

which is shown in Fig. 10 for $J_2/J_1 = -1, 0, 1$ along the closed path $\mathbf{X} - \mathbf{M} - \mathbf{R} - \mathbf{X}$. For $J_2/J_1 = 1$ we obtain a second peak at \mathbf{R} . On the other hand, for $J_2/J_1 = -1$ the dynamic structure factor exhibits local minima at \mathbf{R} and \mathbf{X} while assuming intermediate maxima on the paths $\mathbf{X} - \mathbf{R}$ and $\mathbf{M} - \mathbf{R}$.

D. Common features in all dimensions

To conclude this section, let us summarize the robust features of the dissipation energy $\Delta(\mathbf{k}, i\omega)$ and the resulting dynamic structure factor $S(\mathbf{k}, \omega)$ at infinite temperature which are independent of the dimensionality of the system. For negative J_2/J_1 these quantities are less sensitive to the next-nearest neighbor coupling J_2 than for positive J_2/J_1 . In particular, for $J_2/J_1 < 0$ the cor-

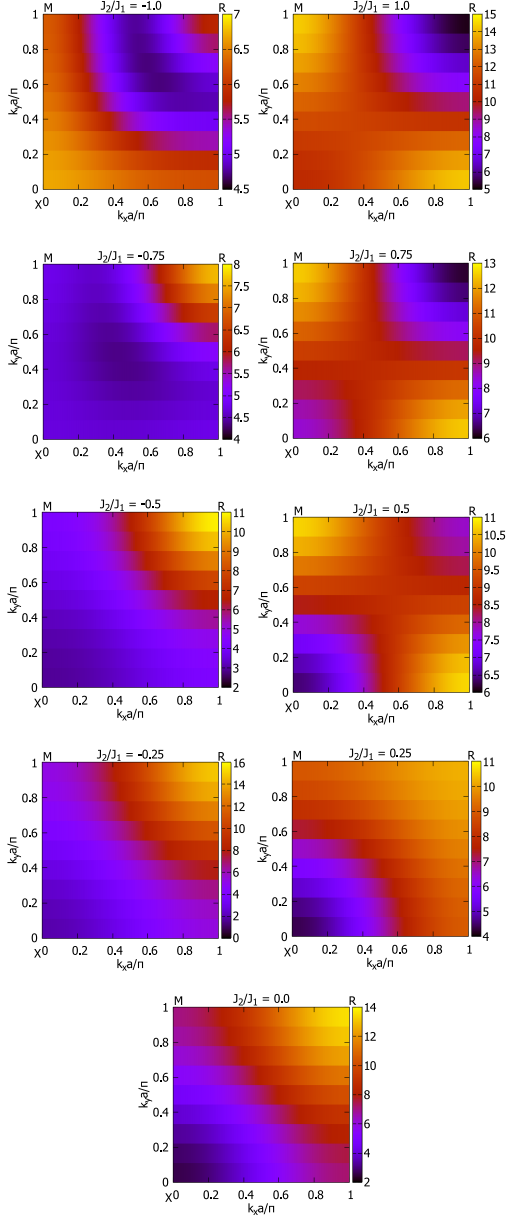


FIG. 9. Dimensionless dissipation energy $\tilde{\Delta}(\mathbf{k}, \omega = 0)$ in the plane $k_z = \pi/a$ of the spin-1/2 J_1 - J_2 Heisenberg model on a simple cubic lattice at infinite temperature. The contour plots are for $J_2/J_1 = -1, \dots, 1$ in steps of 0.25 (counterclockwise, starting from top left).

ner of the Brillouin zone $\mathbf{R} = (\pi/a, \dots, \pi/a)$ remains a maximum of $\Delta(\mathbf{k}, \omega)$ – and hence a minimum of $S(\mathbf{k}, \omega)$ – in a larger range of $|J_2/J_1|$ than for $J_2/J_1 > 0$. For sufficiently large negative $J_2/J_1 < \mu_2(d) < 0$ the function $\Delta(\mathbf{k}, i\omega)$ develops a second local maximum at a wavevector \mathbf{Q} distinct from \mathbf{R} . The corresponding dynamic structure factor $S(\mathbf{k}, \omega)$ then exhibits a local maximum some-

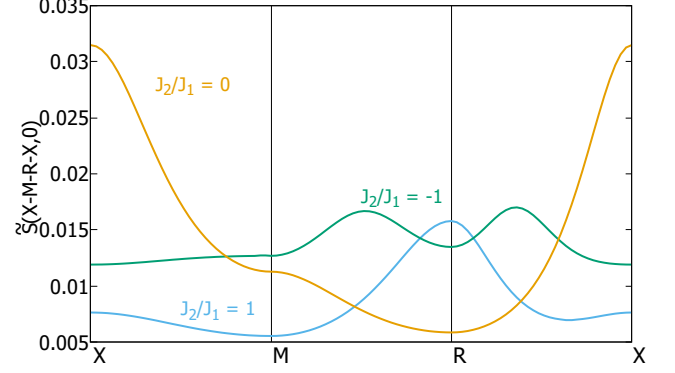


FIG. 10. Dimensionless dynamic structure factor $\tilde{S}(\mathbf{k}, 0) = S(\mathbf{k}, 0)|J_1|\sqrt{b_0'}$ given in Eq. (5.8) for a three-dimensional spin-1/2 Heisenberg magnet in a simple cubic lattice with nearest-neighbor exchange J_1 and next-nearest-neighbor exchange J_2 at infinite temperature. The plot is along the closed path in the first Brillouin zone $\mathbf{X} - \mathbf{M} - \mathbf{R} - \mathbf{X}$ described in the text for $J_2/J_1 = -1, 0, 1$ (green, orange, blue), see also Fig. 9.

where on a path connecting \mathbf{R} to \mathbf{Q} . This structure also persists for $J_2/J_1 < -1$. In the case of $J_2/J_1 > 0$ the position of the global maximum of $\Delta(\mathbf{k}, i\omega)$ changes at $J_2/J_1 = \mu_+(d)$, which leads for $J_2/J_1 > \mu_+$ to a short-wavelength peak of $S(\mathbf{k}, \omega)$ at $\mathbf{R} = (\pi/a, \dots, \pi/a)$. We conclude that for positive $J_2/J_1 > \mu_+(d)$ the dynamic structure factor exhibits in all dimensions a second peak at the corner \mathbf{R} of the first Brillouin zone. This peak is absent for negative J_2/J_1 , where in the regime $J_2/J_1 < \mu_2(d) < 0$ the dynamic structure factor exhibits local maxima along lines connecting local minima.

VI. SUMMARY AND CONCLUSIONS

In this work we have studied the spin dynamics of quantum Heisenberg models with arbitrary spin-rotationally invariant exchange couplings by means of a new variant of the functional renormalization group approach to quantum spin systems proposed in Ref. [25] and further developed in Refs. [26–28]. In our quest to establish the SFRG as a useful tool for calculating the spin dynamics of Heisenberg magnets without long-range magnetic order we have encountered a number of challenging technical problems which required non-trivial modifications of the established FRG formalism [35–39]:

1. First of all, we have avoided the problem of the non-existence of the Legendre transform of the generating functional of the connected correlation functions of an isolated spin by introducing a hybrid functional $\Gamma_\Lambda[\mathbf{m}^c, \boldsymbol{\eta}^q]$ [see Eq. (2.26)] where the static (classical) fluctuations associated with the magnetization field \mathbf{m}^c are treated differently

from the dynamic (quantum) fluctuations associated with the exchange field η^q . Our construction is motivated by the fact that in the classical sector the Legendre transform of the generating functional of static spin correlation functions is well-defined even for vanishing exchange couplings. Moreover, we know from previous calculations [25] that a Legendre transform to classical propagator-irreducible vertices yields better results for thermodynamic quantities than a formulation in terms of interaction-irreducible vertices [41–43].

2. Another technical subtlety of our approach is that at finite frequencies we define the notion of irreducibility with respect to the flowing inverse static propagator $\tilde{J}_\Lambda(\mathbf{q}) = G_\Lambda^{-1}(\mathbf{q})$ instead of the deformed bare exchange coupling. This results in a convenient parametrization of $G(\mathbf{k}, i\omega)$ which is crucial for implementing the restoration of ergodicity for any finite value of the exchange couplings.
3. To obtain a closed system of FRG flow equations for the static self-energy and the irreducible dynamic susceptibility which is compatible with the Ward identities due to spin-rotational invariance and the ergodicity for finite exchange couplings, we had to take the flow of the three-spin and four-spin vertices into account. We have done this with the help of the Ward identity $G_\Lambda(\mathbf{k} = 0, i\omega \neq 0) = 0$ and the continuity condition $G_\Lambda(\mathbf{k} \neq 0, i\omega \rightarrow 0) = G_\Lambda(\mathbf{k}, 0)$ due to ergodicity.
4. By assuming that the static spin correlations can be determined by some other method (such as a controlled high-temperature expansion) we have been able to transform the flow equation (3.42) for the irreducible dynamic susceptibility into a closed integral equation (3.51) for the dissipation energy $\Delta(\mathbf{k}, i\omega)$ which determines the dynamic spin-spin correlation function via Eq. (1.3).

Although we have preliminary evidence [44] that our integral equation (3.51) can be used to calculate the low-frequency spin dynamics in the entire paramagnetic regime, in this work we have focused on the high temperature regime $T \gg |J|$ where the static spin-spin correlation function $G(\mathbf{k})$ can be obtained via a controlled expansion in powers of J/T . We use the resulting $G(\mathbf{k})$ as an input for our integral equation (3.51) for the dissipation energy $\Delta(\mathbf{k}, i\omega)$. We emphasize that our approach does not make any a priori assumptions regarding the existence of normal spin diffusion, nor does it rely on an extrapolation of a high-frequency (short-time) expansion.

We have used our approach to calculate the spin-diffusion coefficient \mathcal{D} in three-dimensional Heisenberg magnets with nearest-neighbor and next-nearest-neighbor exchange on simple cubic and body centered cubic lattices. Our numerical results for \mathcal{D} are by a factor of up to two smaller than older predictions based on

the extrapolation of the short-time expansion [3–5, 7, 10–13], although the experimental result for \mathcal{D} reported in Ref. [14] is still somewhat smaller than our prediction. Furthermore, contrary to these older approaches [3–5, 7, 10–13], our method predicts anomalous diffusion in reduced dimensions $d \leq 2$. In particular, in $d = 1$ our result $\mathcal{D}(\omega) \propto |\omega|^{-1/3}$ for the frequency-dependence of the generalized diffusion coefficient agrees with recent investigations of spin chains [16–24], at least in cases where convergence of different numerical and analytic approaches has been achieved. Finally, we have also used our approach to calculate the full \mathbf{k} -dependence of the dynamic structure factor $S(\mathbf{k}, \omega)$ at high temperatures, which allows us to relate the short-distance behavior of $S(\mathbf{k}, \omega)$ to the nature of competing exchange interactions.

The methods developed in this work can be extended in many directions. Although here we have focused on the solution of the integral equation (3.51) for the dissipation energy $\Delta(\mathbf{k}, i\omega)$ at high temperatures, we have preliminary evidence [44] that Eq. (3.51) gives sensible results in the entire paramagnetic regime. In particular, by solving this integral equation for temperatures slightly above the critical temperature we can investigate the critical spin dynamics of Heisenberg magnets. Our method can also be used as an unbiased approach to frustrated quantum spin systems where even the calculation of thermodynamics like the phase diagram poses a serious challenge. In this context FRG approaches employing representations of the spin operators in terms of Abrikosov pseudo-fermions [63–68] have been successfully used to calculate static ground state properties of quantum spin systems. On the other hand, dynamic properties such as the dynamic structure factor have so far not been calculated within the pseudofermion FRG; in fact, at this point it is not clear whether the corresponding technical problems will be solved in the near future. Moreover, at finite temperatures the pseudofermion FRG becomes inaccurate because it introduces unphysical Hilbert space sectors. Although this problem can be elegantly avoided using an $SO(3)$ -symmetric representation of the spin operators in terms of Majorana fermions [69], this pseudo-Majorana FRG exhibits an unphysical divergence in the limit of vanishing temperature. In contrast, our SFRG approach allows us to calculate the spin-spin correlation function $G(\mathbf{k}, \omega)$ for vanishing and finite frequencies at all temperatures where the spin-rotational invariance is not spontaneously broken. In fact, by numerically solving the flow equations (3.42) and (3.44) we can in principle obtain both the static spin self-energy $\Sigma(\mathbf{k})$ and the dynamic dissipation energy $\Delta(\mathbf{k}, i\omega)$. Although the direct numerical solution of the flow equations (3.42) and (3.44) is beyond the scope of this work, we believe that the numerical solution of these equations will be very rewarding because it will allow us to obtain the dynamic structure factor $S(\mathbf{k}, \omega)$ of frustrated spin systems at low temperatures $T \ll |J|$, a quantity which is not accessible with pseudofermion FRG methods [63–69].

For completeness it should be mentioned that the idea

of working directly with physical spin correlation functions is also central to the equation of motion approach for quantum spin systems pioneered by Bogolyubov, Tyablikov, and others [70–72]. In this approach the infinite hierarchy of equations of motion for the spin correlation functions is closed by some decoupling procedure for correlation functions involving more than two spins, resulting in a closed self-consistency equation for the spin-spin correlation function. A notable example is given by the Tyablikov-decoupling [70–72] which for $S = 1/2$ Heisenberg ferromagnets amounts to approximating a mixed three-spin correlation function by a product of a transverse two-spin correlation function and the magnetization. While in the ordered phase this seems to be a reasonable approximation, it is only of limited use in the paramagnetic zero-field limit, especially when we are interested in the dynamics. An important difference between our SFRG approach and methods based on the decoupling of equations of motion for spin correlation functions is that SFRG is formulated in terms of irreducible vertices, which provide a more compact parametrization of higher order spin correlations and allow for sophisticated truncation strategies compatible with the constraints imposed by the Ward identities and the ergodicity of the system.

Experimentally, the dynamic structure factor can be measured via inelastic neutron scattering. Moreover, the nuclear spin-lattice relaxation rate in magnetic insulators measured in nuclear magnetic resonance (NMR) experiments is proportional to a weighted Brillouin zone average of $S(\mathbf{k}, \omega_N)$, where the NMR frequency ω_N is usually much smaller than the exchange couplings [73]. Our results for $S(\mathbf{k}, \omega)$ presented in Sec. V can therefore be used to calculate the high-temperature behavior of the NMR relaxation rate in Heisenberg magnets.

ACKNOWLEDGMENTS

This work was financially supported by the Deutsche Forschungsgemeinschaft (DFG) through project KO 1442/10-1.

APPENDIX A: HIGH-TEMPERATURE SPIN DIFFUSION ON A BCC LATTICE

In this appendix we give some technical details of the solution of the integral equation (3.51) for the dissipation energy $\Delta(\mathbf{k}, i\omega)$ on a body-centered cubic lattice at $T = \infty$ including next-nearest neighbor exchange. The geometry is shown in Fig. 2. The self-energy contribution to the relevant high-temperature limit of the kernel

$V(\mathbf{k}, \mathbf{q})$ in Eq. (4.6) can then be written as

$$\begin{aligned} & 2\Sigma_2(\mathbf{q}) - \Sigma_2(\mathbf{q} + \mathbf{k}) - \Sigma_2(\mathbf{q} - \mathbf{k}) \\ &= \frac{2J_1^2}{3} [2\gamma_{\mathbf{q}}^{\text{bcc}} - \gamma_{\mathbf{q}+\mathbf{k}}^{\text{bcc}} - \gamma_{\mathbf{q}-\mathbf{k}}^{\text{bcc}}] \\ &+ \frac{J_2^2}{2} [2\gamma_{\mathbf{q}} - \gamma_{\mathbf{q}+\mathbf{k}} - \gamma_{\mathbf{q}-\mathbf{k}}], \end{aligned} \quad (\text{A1})$$

where the form factors $\gamma_{\mathbf{k}}^{\text{bcc}}$ and $\gamma_{\mathbf{k}}$ are defined in Eqs. (4.21) and (4.22). Analogous to Eq. (4.15), it is convenient to introduce again the dimensionless quantities $\tilde{\Delta}(\mathbf{k}, i\omega) = \Delta(\mathbf{k}, i\omega)/(|J_1|\sqrt{b'_0})$ and $\tilde{\omega} = \omega/(|J_1|\sqrt{b'_0})$. The solution of our integral equation (3.51) can then be expressed in terms of six independent form factors,

$$\begin{aligned} \tilde{\Delta}(\mathbf{k}, i\omega) &= (1 - \gamma_{\mathbf{k}}^{\text{bcc}})\tilde{\Delta}_1^{\text{bcc}}(i\omega) + (1 - \gamma_{\mathbf{k}})\tilde{\Delta}_1^{\text{sc}}(i\omega) \\ &+ (1 - \gamma_{2\mathbf{k}}^{\text{bcc}})\tilde{\Delta}_2^{\text{bcc},\parallel}(i\omega) + (1 - \gamma_{\mathbf{k}}^{\perp})\tilde{\Delta}_2^{\text{sc},\perp}(i\omega) \\ &+ (1 - \gamma_{\mathbf{k}}^{\text{bcc},\text{sc}})\tilde{\Delta}_2^{\text{bcc},\text{sc}}(i\omega) + (1 - \gamma_{2\mathbf{k}})\tilde{\Delta}_2^{\text{sc},\parallel}(i\omega), \end{aligned} \quad (\text{A2})$$

where the off-diagonal form factor $\gamma_{\mathbf{k}}^{\perp}$ can be obtained by setting $d = 3$ in the general definition (4.17),

$$\begin{aligned} \gamma_{\mathbf{k}}^{\perp} &= \frac{1}{3} [\cos(k_x a) \cos(k_y a) + \cos(k_y a) \cos(k_z a) \\ &+ \cos(k_z a) \cos(k_x a)], \end{aligned} \quad (\text{A3})$$

and the mixed form factor $\gamma_{\mathbf{k}}^{\text{bcc},\text{sc}}$ is given by

$$\begin{aligned} \gamma_{\mathbf{k}}^{\text{bcc},\text{sc}} &= \frac{1}{3} \left[\cos\left(\frac{3k_x a}{2}\right) \cos\left(\frac{k_y a}{2}\right) \cos\left(\frac{k_z a}{2}\right) \right. \\ &\left. + (x \leftrightarrow z) + (x \leftrightarrow y) \right]. \end{aligned} \quad (\text{A4})$$

Introducing a short notation for the ratio of exchange couplings,

$$\mu = J_2/J_1, \quad (\text{A5})$$

the system (4.9) of self-consistency equations then reduces to the following six coupled equations,

$$\begin{aligned} \tilde{\Delta}_1^{\text{bcc}}(i\omega) &= \frac{4}{3b'_0} \int_{\mathbf{q}} \frac{\gamma_{\mathbf{q}}^{\text{bcc}}}{|\tilde{\omega}| + \tilde{\Delta}(\mathbf{q}, i\omega)} + 8 \int_{\mathbf{q}} \frac{1 + 3\gamma_{\mathbf{q}} + 3\gamma_{\mathbf{q}}^{\perp}}{|\tilde{\omega}| + \tilde{\Delta}(\mathbf{q}, i\omega)} \\ &- \tilde{\Delta}_2^{\text{bcc},\text{sc}}(i\omega) - 2\tilde{\Delta}_2^{\text{bcc},\parallel}(i\omega), \end{aligned} \quad (\text{A6a})$$

$$\tilde{\Delta}_2^{\text{bcc},\parallel}(i\omega) = -4 \int_{\mathbf{q}} \frac{\gamma_{2\mathbf{q}}^{\text{bcc}}}{|\tilde{\omega}| + \tilde{\Delta}(\mathbf{q}, i\omega)}, \quad (\text{A6b})$$

$$\tilde{\Delta}_2^{\text{bcc},\text{sc}}(i\omega) = -24\mu \int_{\mathbf{q}} \frac{\gamma_{\mathbf{q}}^{\text{bcc},\text{sc}}}{|\tilde{\omega}| + \tilde{\Delta}(\mathbf{q}, i\omega)}, \quad (\text{A6c})$$

$$\begin{aligned} \tilde{\Delta}_1^{\text{sc}}(i\omega) &= -12 \int_{\mathbf{q}} \frac{\gamma_{\mathbf{q}}}{|\tilde{\omega}| + \tilde{\Delta}(\mathbf{q}, i\omega)} \\ &+ 24\mu \int_{\mathbf{q}} \frac{\gamma_{\mathbf{q}}^{\text{bcc}}}{|\tilde{\omega}| + \tilde{\Delta}(\mathbf{q}, i\omega)} - \tilde{\Delta}_2^{\text{bcc},\text{sc}}(i\omega) \\ &+ \frac{\mu^2}{b'_0} \int_{\mathbf{q}} \frac{\gamma_{\mathbf{q}}}{|\tilde{\omega}| + \tilde{\Delta}(\mathbf{q}, i\omega)} \\ &+ 6\mu^2 \int_{\mathbf{q}} \frac{1 + \gamma_{2\mathbf{q}} + 4\gamma_{\mathbf{q}}^{\perp}}{|\tilde{\omega}| + \tilde{\Delta}(\mathbf{q}, i\omega)}, \end{aligned} \quad (\text{A6d})$$

$$\tilde{\Delta}_2^{\text{sc},\perp}(i\omega) = -12(1 + \mu^2) \int_{\mathbf{q}} \frac{\gamma_{\mathbf{q}}^\perp}{|\tilde{\omega}| + \tilde{\Delta}(\mathbf{q}, i\omega)}, \quad (\text{A6e})$$

$$\tilde{\Delta}_2^{\text{sc},\parallel}(i\omega) = -3\mu^2 \int_{\mathbf{q}} \frac{\gamma_{2\mathbf{q}}}{|\tilde{\omega}| + \tilde{\Delta}(\mathbf{q}, i\omega)}. \quad (\text{A6f})$$

According to Eq. (3.54) the spin-diffusion coefficient \mathcal{D} can then be obtained from the term of order k^2 in the expansion of $\Delta(\mathbf{k}, 0) = |J_1| \sqrt{b'_0} \tilde{\Delta}(\mathbf{k}, 0)$ in powers of the momentum, so that we finally arrive at the following expression for the spin-diffusion coefficient in the limit of infinite temperature,

$$\mathcal{D} = \frac{|J_1| \sqrt{b'_0} a^2}{6} \left[\frac{3}{4} \tilde{\Delta}_1^{\text{bcc}}(0) + 3 \tilde{\Delta}_2^{\text{bcc},\parallel}(0) + \frac{11}{4} \tilde{\Delta}_2^{\text{bcc},\text{sc}}(0) + \tilde{\Delta}_1^{\text{sc}}(0) + 4 \tilde{\Delta}_2^{\text{sc},\parallel}(0) + 2 \tilde{\Delta}_2^{\text{sc},\perp}(0) \right]. \quad (\text{A7})$$

APPENDIX B: HIGH-TEMPERATURE SPIN DIFFUSION ON HYPERCUBIC LATTICES

Here we give some technical details of the solution of the integral equation (3.51) on hypercubic lattice in dimensions $d = 1, 2, 3$ for a Heisenberg model with nearest-neighbor exchange J_1 and next-nearest-neighbor exchange J_2 .

1. One dimension

Setting again $\mu = J_2/J_1$, the Fourier transform of the exchange interaction in $d = 1$ is

$$J(\mathbf{k}) = 2J_1 [\cos(k_x a) + \mu \cos(2k_x a)]. \quad (\text{B1})$$

At high temperatures the self-energy contribution to the kernel $V(\mathbf{k}, \mathbf{q})$ in Eq. (4.6) can then be written as

$$\begin{aligned} & 2\Sigma_2(\mathbf{q}) - \Sigma_2(\mathbf{q} + \mathbf{k}) - \Sigma_2(\mathbf{q} - \mathbf{k}) \\ &= \frac{J_1^2}{6} \left[2 \cos(q_x a) - \cos((q_x + k_x) a) - \cos((q_x - k_x) a) \right. \\ & \quad \left. + \mu^2 [2 \cos(2q_x a) - \cos(2(q_x + k_x) a) - \cos(2(q_x - k_x) a)] \right]. \end{aligned} \quad (\text{B2})$$

The solution of the integral equation (3.51) in $d = 1$ can then be written as $\Delta(\mathbf{k}, i\omega) = |J_1| b'_0 \tilde{\Delta}(k_x, i\omega)$, where the dimensionless function $\tilde{\Delta}(k_x, i\omega)$ can be expressed in terms of four different form factors,

$$\tilde{\Delta}(k_x, i\omega) = \sum_{j=1}^4 [1 - \cos(j k_x a)] \tilde{\Delta}_j(i\omega). \quad (\text{B3})$$

With the abbreviations $\int_{q_x} = a \int_{-\pi/a}^{\pi/a} \frac{dq_x}{2\pi}$ and $\tilde{\omega} = \omega/(|J_1| b'_0)$ the self-consistency equations (4.9) for the am-

plitudes reduce to

$$\begin{aligned} \tilde{\Delta}_1(i\omega) &= \frac{1}{3b'_0} \int_{q_x} \frac{\cos(q_x a)}{|\tilde{\omega}| + \tilde{\Delta}(q_x, i\omega)} \\ &+ 2 \int_{q_x} \frac{1 + \cos(2q_x a)}{|\tilde{\omega}| + \tilde{\Delta}(q_x, i\omega)} - \tilde{\Delta}_3(i\omega), \end{aligned} \quad (\text{B4a})$$

$$\begin{aligned} \tilde{\Delta}_2(i\omega) &= \left(\frac{\mu^2}{3b'_0} - 1 \right) \int_{q_x} \frac{\cos(2q_x a)}{|\tilde{\omega}| + \tilde{\Delta}(q_x, i\omega)} \\ &+ 2\mu \int_{q_x} \frac{\cos(q_x a) + \mu}{|\tilde{\omega}| + \tilde{\Delta}(q_x, i\omega)} - \tilde{\Delta}_3(i\omega) - 2\tilde{\Delta}_4(i\omega), \end{aligned} \quad (\text{B4b})$$

$$\tilde{\Delta}_3(i\omega) = -2\mu \int_{q_x} \frac{\cos(3q_x a)}{|\tilde{\omega}| + \tilde{\Delta}(q_x, i\omega)}, \quad (\text{B4c})$$

$$\tilde{\Delta}_4(i\omega) = -\mu^2 \int_{q_x} \frac{\cos(4q_x a)}{|\tilde{\omega}| + \tilde{\Delta}(q_x, i\omega)}. \quad (\text{B4d})$$

For small frequencies $|\tilde{\omega}| \ll 1$ we obtain for the amplitudes to leading order

$$\tilde{\Delta}_1(i\omega) = \left(4 + \frac{1}{3b'_0} + 2\mu \right) \left[\frac{3b'_0}{2(1 + 4\mu^2)|\tilde{\omega}|} \right]^{1/3}, \quad (\text{B5a})$$

$$\tilde{\Delta}_2(i\omega) = \left(\frac{\mu^2}{3b'_0} - 1 + 4\mu^2 + 4\mu \right) \left[\frac{3b'_0}{2(1 + 4\mu^2)|\tilde{\omega}|} \right]^{1/3}, \quad (\text{B5b})$$

$$\tilde{\Delta}_3(i\omega) = -2\mu \left[\frac{3b'_0}{2(1 + 4\mu^2)|\tilde{\omega}|} \right]^{1/3}, \quad (\text{B5c})$$

$$\tilde{\Delta}_4(i\omega) = -\mu^2 \left[\frac{3b'_0}{2(1 + 4\mu^2)|\tilde{\omega}|} \right]^{1/3}. \quad (\text{B5d})$$

Substituting these expressions into Eq. (B3) and expanding to second order in k_x we obtain the anomalous spin-diffusion coefficient in $d = 1$,

$$\begin{aligned} \mathcal{D}(i\omega) &= \frac{|J_1| \sqrt{b'_0} a^2}{2} \left[\tilde{\Delta}_1(i\tilde{\omega}) + 4\tilde{\Delta}_2(i\tilde{\omega}) + 9\tilde{\Delta}_3(i\tilde{\omega}) + 16\tilde{\Delta}_4(i\tilde{\omega}) \right] \\ &= \left[\frac{|J_1|(1 + 4\mu^2)^2}{144|\omega|} \right]^{1/3} |J_1| a^2 \\ &= \left[\frac{\sqrt{J_1^2 + 4J_2^2}}{144|\omega|} \right]^{1/3} \sqrt{J_1^2 + 4J_2^2} a^2. \end{aligned} \quad (\text{B6})$$

2. Square lattice

On a square lattice the Fourier transform of the exchange couplings with nearest-neighbor exchange J_1 and next-nearest-neighbor exchange $J_2 = \mu J_1$ is

$$J(\mathbf{k}) = 4J_1 [\gamma_{\mathbf{k}} + \mu \gamma_{\mathbf{k}}^\perp], \quad (\text{B7})$$

where now

$$\gamma_{\mathbf{k}} = \frac{1}{2} [\cos(k_x a) + \cos(k_y a)], \quad (\text{B8})$$

$$\gamma_{\mathbf{k}}^\perp = \cos(k_x a) \cos(k_y a). \quad (\text{B9})$$

The self-energy contribution to the high temperature kernel $V(\mathbf{k}, \mathbf{q})$ defined in Eq. (4.6) can then be written as

$$\begin{aligned} & 2\Sigma_2(\mathbf{q}) - \Sigma_2(\mathbf{q} + \mathbf{k}) - \Sigma_2(\mathbf{q} - \mathbf{k}) \\ &= \frac{J_1^2}{3} \left[2\gamma_{\mathbf{q}} - \gamma_{\mathbf{q}+\mathbf{k}} - \gamma_{\mathbf{q}-\mathbf{k}} \right. \\ & \quad \left. + \mu^2 (2\gamma_{\mathbf{q}}^\perp - \gamma_{\mathbf{q}+\mathbf{k}}^\perp - \gamma_{\mathbf{q}-\mathbf{k}}^\perp) \right]. \end{aligned} \quad (\text{B10})$$

The solution of the integral equation (3.51) can be expressed in terms of five different form factors,

$$\begin{aligned} \tilde{\Delta}(\mathbf{k}, i\omega) &= (1 - \gamma_{\mathbf{k}}) \tilde{\Delta}_1(i\omega) + (1 - \gamma_{2\mathbf{k}}) \tilde{\Delta}_2^\parallel(i\omega) \\ & \quad + (1 - \gamma_{\mathbf{k}}^\perp) \tilde{\Delta}_2^\perp(i\omega) + (1 - \gamma_{2\mathbf{k}}^\perp) \tilde{\Delta}_{2,2}^\parallel(i\omega) \\ & \quad + (1 - \gamma_{\mathbf{k}}^{(2,1)}) \tilde{\Delta}_{2,1}(i\omega), \end{aligned} \quad (\text{B11})$$

where we have introduced the mixed form factor

$$\gamma_{\mathbf{k}}^{(2,1)} = \frac{1}{2} [\cos(2k_x a) \cos(k_y a) + \cos(k_x a) \cos(2k_y a)]. \quad (\text{B12})$$

The self-consistency equations (4.9) for the amplitudes can then be written in the following form

$$\begin{aligned} \tilde{\Delta}_1(i\omega) &= \frac{2}{3b'_0} \int_{\mathbf{q}} \frac{\gamma_{\mathbf{q}}}{|\tilde{\omega}| + \tilde{\Delta}(\mathbf{q}, i\omega)} \\ & \quad + 4 \int_{\mathbf{q}} \frac{1 + \gamma_{2\mathbf{q}} + 2\gamma_{\mathbf{q}}^\perp}{|\tilde{\omega}| + \tilde{\Delta}(\mathbf{q}, i\omega)} - \tilde{\Delta}_{2,1}(i\omega), \end{aligned} \quad (\text{B13a})$$

$$\tilde{\Delta}_2^\parallel(i\omega) = -2(1 + 2\mu^2) \int_{\mathbf{q}} \frac{\gamma_{2\mathbf{q}}}{|\tilde{\omega}| + \tilde{\Delta}(\mathbf{q}, i\omega)}, \quad (\text{B13b})$$

$$\begin{aligned} \tilde{\Delta}_2^\perp(i\omega) &= \left(\frac{2\mu^2}{3b'_0} - 4 \right) \int_{\mathbf{q}} \frac{\gamma_{\mathbf{q}}^\perp}{|\tilde{\omega}| + \tilde{\Delta}(\mathbf{q}, i\omega)} \\ & \quad + 8\mu \int_{\mathbf{q}} \frac{\gamma_{\mathbf{q}}}{|\tilde{\omega}| + \tilde{\Delta}(\mathbf{q}, i\omega)} + 4\mu^2 \int_{\mathbf{q}} \frac{1}{|\tilde{\omega}| + \tilde{\Delta}(\mathbf{q}, i\omega)} \\ & \quad + 8\mu^2 \int_{\mathbf{q}} \frac{\gamma_{2\mathbf{q}}}{|\tilde{\omega}| + \tilde{\Delta}(\mathbf{q}, i\omega)} - \tilde{\Delta}_{2,1}(i\omega) - 2\tilde{\Delta}_{2,2}^\parallel(i\omega), \end{aligned} \quad (\text{B13c})$$

$$\tilde{\Delta}_{2,2}^\parallel(i\omega) = -2\mu^2 \int_{\mathbf{q}} \frac{\gamma_{2\mathbf{q}}^\perp}{|\tilde{\omega}| + \tilde{\Delta}(\mathbf{q}, i\omega)}, \quad (\text{B13d})$$

$$\tilde{\Delta}_{2,1}(i\omega) = -8\mu \int_{\mathbf{q}} \frac{\gamma_{\mathbf{q}}^{(2,1)}}{|\tilde{\omega}| + \tilde{\Delta}(\mathbf{q}, i\omega)}. \quad (\text{B13e})$$

For small frequencies $|\omega| \ll |J_1|$ the solution of the above equations is to leading logarithmic order given by

$$\tilde{\Delta}_1(i\omega) = 2 \left(\frac{1}{3b'_0} + 8 + 4\mu \right) \sqrt{\frac{3b'_0 \ln \left(\frac{|J_1| \sqrt{1+2\mu^2}}{\sqrt{24\pi} |\omega|} \right)}{2\pi(1+2\mu^2)}}, \quad (\text{B14a})$$

$$\tilde{\Delta}_2^\parallel(i\omega) = -2(1+2\mu^2) \sqrt{\frac{3b'_0 \ln \left(\frac{|J_1| \sqrt{1+2\mu^2}}{\sqrt{24\pi} |\omega|} \right)}{2\pi(1+2\mu^2)}}, \quad (\text{B14b})$$

$$\begin{aligned} \tilde{\Delta}_2^\perp(i\omega) &= 2 \left(8\mu^2 + 8\mu + \frac{\mu^2}{3b'_0} - 2 \right) \\ & \quad \times \sqrt{\frac{3b'_0 \ln \left(\frac{|J_1| \sqrt{1+2\mu^2}}{\sqrt{24\pi} |\omega|} \right)}{2\pi(1+2\mu^2)}}, \end{aligned} \quad (\text{B14c})$$

$$\tilde{\Delta}_{2,2}^\parallel(i\omega) = -2\mu^2 \sqrt{\frac{3b'_0 \ln \left(\frac{|J_1| \sqrt{1+2\mu^2}}{\sqrt{24\pi} |\omega|} \right)}{2\pi(1+2\mu^2)}}, \quad (\text{B14d})$$

$$\tilde{\Delta}_{2,1}(i\omega) = -8\mu \sqrt{\frac{3b'_0 \ln \left(\frac{|J_1| \sqrt{1+2\mu^2}}{\sqrt{24\pi} |\omega|} \right)}{2\pi(1+2\mu^2)}}. \quad (\text{B14e})$$

The resulting anomalous diffusion coefficient on a square lattice is

$$\begin{aligned} \mathcal{D}(i\omega) &= \frac{|J_1| \sqrt{b'_0} a^2}{4} \left[\tilde{\Delta}_1(i\omega) + 4\tilde{\Delta}_2^\parallel(i\omega) + 2\tilde{\Delta}_2^\perp(i\omega) \right. \\ & \quad \left. + 8\tilde{\Delta}_{2,2}^\parallel(i\omega) + 5\tilde{\Delta}_{2,1}(i\omega) \right] \\ &= \sqrt{\frac{\ln \left(\frac{|J_1| \sqrt{1+2\mu^2}}{\sqrt{24\pi} |\omega|} \right)}{24\pi}} |J_1| \sqrt{1+2\mu^2} a^2. \end{aligned} \quad (\text{B15})$$

Keeping in mind that $|J_1| \sqrt{1+2\mu^2} = \sqrt{J_1^2 + 2J_2^2}$, we see that in the expansion of $\Delta(\mathbf{k}, i\omega)$ to order k^2 the next-nearest-neighbor interaction J_2 can be taken into account via the following replacement of the nearest-neighbor interaction, $|J_1| \rightarrow \sqrt{J_1^2 + (a'/a)^2 J_2^2}$, where a' is the distance between next-nearest neighbors. From Eq. (B6) it is clear that this is also true in one dimension. Effects depending on the sign of J_2/J_1 can be only seen by expanding $\Delta(\mathbf{k}, i\omega)$ beyond the leading order, implying that these effects are only visible for momenta $ka = \mathcal{O}(1)$.

3. Simple cubic lattice

For a simple cubic lattice with nearest-neighbor exchange J_1 and next-nearest-neighbor exchange $J_2 = \mu J_1$ the Fourier transform of the exchange interaction is

$$J(\mathbf{k}) = 6J_1 [\gamma_{\mathbf{k}} + 2\mu \gamma_{\mathbf{k}}^\perp], \quad (\text{B16})$$

where the form factors $\gamma_{\mathbf{k}}$ and $\gamma_{\mathbf{k}}^\perp$ are defined in Eqs. (4.22) and (A3), respectively. The self-energy contribution to the high temperature kernel $V(\mathbf{k}, \mathbf{q})$ defined

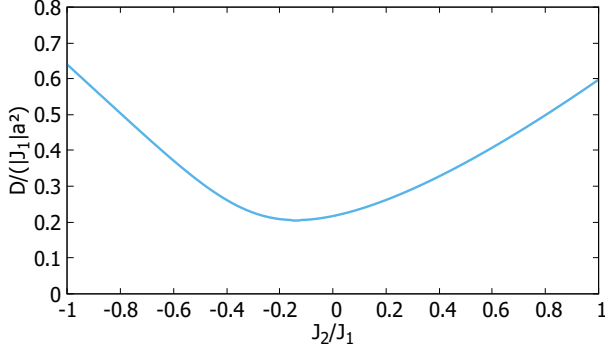


FIG. 11. Spin-diffusion coefficient \mathcal{D} for a spin-1/2 Heisenberg model on a simple cubic lattice with nearest-neighbor interaction J_1 and next-nearest-neighbor interaction J_2 as a function of J_2/J_1 for $T = \infty$.

in Eq. (4.6) is then

$$\begin{aligned} & 2\Sigma_2(\mathbf{q}) - \Sigma_2(\mathbf{q} + \mathbf{k}) - \Sigma_2(\mathbf{q} - \mathbf{k}) \\ &= \frac{J_1^2}{2} \left[2\gamma_{\mathbf{q}} - \gamma_{\mathbf{q}+\mathbf{k}} - \gamma_{\mathbf{q}-\mathbf{k}} \right. \\ & \quad \left. + 2\mu^2 (2\gamma_{\mathbf{q}}^\perp - \gamma_{\mathbf{q}+\mathbf{k}}^\perp - \gamma_{\mathbf{q}-\mathbf{k}}^\perp) \right]. \end{aligned} \quad (\text{B17})$$

At high temperatures, the solution $\Delta(\mathbf{k}, i\omega)$ of the integral equation (3.51) can be expressed in terms of seven different form factors. Hence, the dimensionless dissipation energy $\tilde{\Delta}(\mathbf{k}, i\omega) = \Delta(\mathbf{k}, i\omega)/(|J_1|\sqrt{b'_0})$ can be written in the following form,

$$\begin{aligned} \tilde{\Delta}(\mathbf{k}, i\omega) &= (1 - \gamma_{\mathbf{k}})\tilde{\Delta}_1(i\omega) + (1 - \gamma_{2\mathbf{k}})\tilde{\Delta}_2^\parallel(i\omega) \\ &+ (1 - \gamma_{\mathbf{k}}^\perp)\tilde{\Delta}_2^\perp(i\omega) + (1 - \gamma_{2\mathbf{k}}^\perp)\tilde{\Delta}_{2,2}^\parallel(i\omega) \\ &+ (1 - \gamma_{\mathbf{k}}^{(2,1,0)})\tilde{\Delta}_{2,1,0}(i\omega) + (1 - \gamma_{\mathbf{k}}^{(2,1,1)})\tilde{\Delta}_{2,1,1}(i\omega) \\ &+ (1 - \gamma_{\mathbf{k}}^{(1,1,1)})\tilde{\Delta}_{1,1,1}(i\omega), \end{aligned} \quad (\text{B18})$$

where we have introduced three additional form factors

$$\begin{aligned} \gamma_{\mathbf{k}}^{(2,1,0)} &= \frac{1}{6} \left[\cos(2k_x a) \cos(k_y a) + \cos(k_x a) \cos(2k_y a) \right. \\ & \quad \left. + (x \leftrightarrow z) + (y \leftrightarrow z) \right], \end{aligned} \quad (\text{B19a})$$

$$\begin{aligned} \gamma_{\mathbf{k}}^{(2,1,1)} &= \frac{1}{3} \left[\cos(2k_x a) \cos(k_y a) \cos(k_z a) \right. \\ & \quad \left. + (x \leftrightarrow z) + (y \leftrightarrow z) \right], \end{aligned} \quad (\text{B19b})$$

$$\gamma_{\mathbf{k}}^{(1,1,1)} = \cos(k_x a) \cos(k_y a) \cos(k_z a). \quad (\text{B19c})$$

The self-consistency equations (4.9) for the amplitudes are

$$\begin{aligned} \tilde{\Delta}_1(i\omega) &= \frac{1}{b'_0} \int_{\mathbf{q}} \frac{\gamma_{\mathbf{q}}}{|\tilde{\omega}| + \tilde{\Delta}(\mathbf{q}, i\omega)} + 6 \int_{\mathbf{q}} \frac{1 + \gamma_{2\mathbf{q}} + 4\gamma_{\mathbf{q}}^\perp}{|\tilde{\omega}| + \tilde{\Delta}(\mathbf{q}, i\omega)} \\ & \quad - \tilde{\Delta}_{2,1,0}(i\omega) - \tilde{\Delta}_{1,1,1}(i\omega), \end{aligned} \quad (\text{B20a})$$

$$\tilde{\Delta}_2^\parallel(i\omega) = -3(1 + 4\mu^2) \int_{\mathbf{q}} \frac{\gamma_{2\mathbf{q}}}{|\tilde{\omega}| + \tilde{\Delta}(\mathbf{q}, i\omega)}, \quad (\text{B20b})$$

$$\begin{aligned} \tilde{\Delta}_2^\perp(i\omega) &= \left(\frac{2\mu^2}{b'_0} + 24\mu^2 - 12 \right) \int_{\mathbf{q}} \frac{\gamma_{\mathbf{q}}^\perp}{|\tilde{\omega}| + \tilde{\Delta}(\mathbf{q}, i\omega)} \\ &+ 24\mu \int_{\mathbf{q}} \frac{\gamma_{\mathbf{q}}}{|\tilde{\omega}| + \tilde{\Delta}(\mathbf{q}, i\omega)} + 12\mu^2 \int_{\mathbf{q}} \frac{1 + 2\gamma_{2\mathbf{q}}}{|\tilde{\omega}| + \tilde{\Delta}(\mathbf{q}, i\omega)} \\ & - \tilde{\Delta}_{2,1,0}(i\omega) - \tilde{\Delta}_{1,1,1}(i\omega) - 2\tilde{\Delta}_{2,2}^\parallel(i\omega) - 2\tilde{\Delta}_{2,1,1}(i\omega), \end{aligned} \quad (\text{B20c})$$

$$\tilde{\Delta}_{2,2}^\parallel(i\omega) = -6\mu^2 \int_{\mathbf{q}} \frac{\gamma_{2\mathbf{q}}^\perp}{|\tilde{\omega}| + \tilde{\Delta}(\mathbf{q}, i\omega)}, \quad (\text{B20d})$$

$$\tilde{\Delta}_{2,1,0}(i\omega) = -24\mu \int_{\mathbf{q}} \frac{\gamma_{\mathbf{q}}^{(2,1,0)}}{|\tilde{\omega}| + \tilde{\Delta}(\mathbf{q}, i\omega)}, \quad (\text{B20e})$$

$$\tilde{\Delta}_{2,1,1}(i\omega) = -24\mu^2 \int_{\mathbf{q}} \frac{\gamma_{\mathbf{q}}^{(2,1,1)}}{|\tilde{\omega}| + \tilde{\Delta}(\mathbf{q}, i\omega)}, \quad (\text{B20f})$$

$$\tilde{\Delta}_{1,1,1}(i\omega) = -24\mu \int_{\mathbf{q}} \frac{\gamma_{\mathbf{q}}^{(1,1,1)}}{|\tilde{\omega}| + \tilde{\Delta}(\mathbf{q}, i\omega)}. \quad (\text{B20g})$$

The spin-diffusion coefficient at infinite temperature is then given by

$$\begin{aligned} \mathcal{D} &= \frac{|J_1|\sqrt{b'_0}a^2}{6} \left[\tilde{\Delta}_1(0) + 4\tilde{\Delta}_2^\parallel(0) + 2\tilde{\Delta}_2^\perp(0) + 8\tilde{\Delta}_{2,2}^\parallel(0) \right. \\ & \quad \left. + 5\tilde{\Delta}_{2,1,0}(0) + 6\tilde{\Delta}_{2,1,1}(0) + 3\tilde{\Delta}_{1,1,1}(0) \right]. \end{aligned} \quad (\text{B21})$$

In Fig. 11 we show a graph of \mathcal{D} for spin $S = 1/2$ as a function of $\mu = J_2/J_1$. The asymmetry with respect to $\mu \rightarrow -\mu$ has also been found on a bcc lattice in Fig. 3. In contrast, in reduced dimensions the anomalous spin-diffusion coefficient $\mathcal{D}(i\omega)$ in Eqs. (B6) and (B15) is symmetric with respect to $\mu \rightarrow -\mu$.

-
- [1] B. I. Halperin and P. C. Hohenberg, *Hydrodynamic Theory of Spin Waves*, Phys. Rev. **188**, 898 (1969).
 [2] D. Forster, *Hydrodynamic Fluctuations, Broken Symmetry, and Correlation Functions*, (Benjamin, Reading, 1975).

- [3] P. G. De Gennes, *Inelastic magnetic scattering of neutrons at high temperatures*, J. Phys. Chem. Solids **4**, 223 (1958).
 [4] H. Mori and K. Kawasaki, *Theory of Dynamical Behaviors of Ferromagnetic Spins*, Prog. Theor. Phys. **27**, 529

- (1962).
- [5] H. S. Bennett and P. C. Martin, *Spin diffusion in the Heisenberg paramagnet*, Phys. Rev. **A138**, 608 (1965).
 - [6] P. Résibois and M. De Leener, *Irreversibility in Heisenberg Spin Systems. I. General Formalism and Kinetic Equations in the High-Temperature Limit*, Phys. Rev. **152**, 305 (1966).
 - [7] A. G. Redfield and W. N. Yu, *Moment-method calculation of magnetization and interspin-energy diffusion*, Phys. Rev. **169**, 443 (1968).
 - [8] R. A. Tahir-Kheli and D. G. McFadden, *Space-Time Correlations in Exchange-Coupled Paramagnets at Elevated Temperatures*, Phys. Rev. **182**, 604 (1969).
 - [9] M. Blume and J. Hubbard, *Spin Correlation Functions at High Temperatures*, Phys. Rev. B **1**, 3815 (1970).
 - [10] T. Morita, *Spin Diffusion in the Heisenberg Magnets at Infinite Temperature*, Phys. Rev. B **6**, 3385 (1972).
 - [11] T. Morita, *Spin Diffusion Constant for the Heisenberg Magnet at High Temperatures*, J. Phys. Soc. Jpn. **39**, 1217 (1975).
 - [12] P. Kopietz, *Thouless number and spin diffusion in quantum Heisenberg ferromagnets*, Mod. Phys. Lett. B **7**, 1747 (1993).
 - [13] M. Böhm, H. Leschke, M. Henneke, V. S. Viswanath, J. Stolze, and G. Müller, *Spectral signature of quantum spin diffusion in dimensions $d = 1, 2$ and 3*, Phys. Rev. B **49**, 417 (1994).
 - [14] J. Labrujere, T. O. Klaassen, and N. J. Poulis, *Spin dynamics in a 3D Heisenberg ferromagnet in the paramagnetic state II*, J. Phys. C: Solid State Phys. **15**, 999 (1982).
 - [15] G. Müller, *Anomalous Spin Diffusion in Classical Heisenberg Magnets*, Phys. Rev. Lett. **60**, 2785 (1988).
 - [16] M. Ljubotina, M. Znidaric, and T. Prosen, *Spin diffusion from an inhomogeneous quench in an integrable system*, Nat. Commun. **8**, 16117 (2017).
 - [17] S. Gopalakrishnan, R. Vasseur, and B. Ware, *Anomalous relaxation and the high-temperature structure factor of XXZ spin chains*, PNAS **116**, 16250 (2019).
 - [18] S. Gopalakrishnan and R. Vasseur, *Kinetic Theory and Spin Diffusion and Superdiffusion in XXZ Spin Chains*, Phys. Rev. Lett. **122**, 127202 (2019).
 - [19] J. De Nardis, M. Medenjak, C. Karrasch, and E. Ilievski, *Anomalous Spin Diffusion in One-Dimensional Antiferromagnets*, Phys. Rev. Lett. **123**, 186601 (2019).
 - [20] J. De Nardis, M. Medenjak, C. Karrasch, and E. Ilievski, *Universality Classes of Spin transport in One-Dimensional Isotropic Magnets: The Onset of Logarithmic Anomalies*, Phys. Rev. Lett. **124**, 210605 (2020).
 - [21] V. B. Bulchandani, *Kardar-Parisi-Zhang universality from soft gauge modes*, Phys. Rev. B **101**, 041411(R) (2020).
 - [22] M. Dupont and J. E. Moore, *Universal spin dynamics in infinite-temperature one-dimensional quantum magnets*, Phys. Rev. B **101**, 121106(R) (2020).
 - [23] J. De Nardis, S. Gopalakrishnan, R. Vasseur, and B. Ware, *Stability of superdiffusion in nearly integrable spin chains*, arXiv:2102.02219v2 [cond-mat.stat-mech] 1 Mar 2021.
 - [24] V. B. Bulchandani, S. Gopalakrishnan, and E. Ilievski, *Superdiffusion in spin chains*, arXiv:2103.01976v1 [cond-mat.stat-mech] 2 Mar 2021.
 - [25] J. Krieg and P. Kopietz, *Exact renormalization group for quantum spin systems*, Phys. Rev. B **99**, 060403(R) (2019).
 - [26] D. Tarasevych, J. Krieg, and P. Kopietz, *A rich man's derivation of scalings laws for the Kondo model*, Phys. Rev. B **98**, 235133 (2018).
 - [27] R. Goll, D. Tarasevych, J. Krieg, and P. Kopietz, *Spin functional renormalization group for quantum Heisenberg ferromagnets: Magnetization and magnon damping in two dimensions*, Phys. Rev. B **100**, 174424 (2019).
 - [28] R. Goll, A. Rückriegel, and P. Kopietz, *Zero-magnon sound in quantum Heisenberg ferromagnets*, Phys. Rev. B **102**, 224437 (2020).
 - [29] T. Machado and N. Dupuis, *From local to critical fluctuations in lattice models: A nonperturbative renormalization-group approach*, Phys. Rev. E **82**, 041128 (2010).
 - [30] A. Rançon and N. Dupuis, *Nonperturbative renormalization group approach to the Bose-Hubbard model*, Phys. Rev. B **83**, 172501 (2011).
 - [31] A. Rançon and N. Dupuis, *Nonperturbative renormalization group approach to strongly correlated lattice bosons*, Phys. Rev. B **84**, 174513 (2011).
 - [32] A. Rançon and N. Dupuis, *Universal thermodynamics of a two-dimensional Bose gas*, Phys. Rev. A **85**, 063607 (2012).
 - [33] A. Rançon and N. Dupuis, *Thermodynamics of a Bose gas near the superfluid-Mott-insulator transition*, Phys. Rev. A **86**, 043624 (2012).
 - [34] A. Rançon, *Nonperturbative renormalization group approach to quantum XY spin models*, Phys. Rev. B **89**, 214418 (2014).
 - [35] J. Berges, N. Tetradis, and C. Wetterich, *Nonperturbative renormalization flow in quantum field theory and statistical physics*, Phys. Rep. **363**, 223 (2002).
 - [36] J. M. Pawłowski, *Aspects of the functional renormalization group*, Ann. Phys. **322**, 2831 (2007).
 - [37] P. Kopietz, L. Bartosch, and F. Schütz, *Introduction to the Functional Renormalization Group*, (Springer, Berlin, 2010).
 - [38] W. Metzner, M. Salmhofer, C. Honerkamp, V. Meden, and K. Schönhammer, *Functional renormalization group approach to correlated fermion systems*, Rev. Mod. Phys. **84**, 299 (2012).
 - [39] N. Dupuis, L. Canet, A. Eichhorn, W. Metzner, J. M. Pawłowski, M. Tissier, and N. Wschebor, *The nonperturbative functional renormalization group and its applications*, Phys. Rep. **910**, 1 (2021).
 - [40] C. Wetterich, *Exact evolution equation for the effective potential*, Phys. Lett. B **301**, 90 (1993).
 - [41] V. G. Vaks, A. I. Larkin, and S. A. Pikin, *Thermodynamics of an ideal ferromagnetic substance*, Zh. Eksp. Teor. Fiz. **53**, 281 (1967) [Sov. Phys. JETP **26**, 188 (1968)].
 - [42] V. G. Vaks, A. I. Larkin, and S. A. Pikin, *Spin waves and correlation functions in a ferromagnetic*, Zh. Eksp. Teor. Fiz. **53**, 1089 (1967) [Sov. Phys. JETP **26**, 647 (1968)].
 - [43] Yu. A. Izyumov and Yu. N. Skryabin, *Statistical Mechanics of Magnetically Ordered Systems*, (Springer, Berlin, 1988).
 - [44] D. Tarasevych and P. Kopietz, unpublished.
 - [45] R. Kubo, *Statistical-Mechanical Theory of Irreversible Processes. I. General Theory and Simple Applications to Magnetic and Conduction Problems*, J. Phys. Soc. Japan **12**, 570 (1957).
 - [46] R. M. Wilcox, *Bounds for the Isothermal, Adiabatic, and Isolated Static Susceptibility Tensors*, Phys. Rev. **174**,

- 624 (1968).
- [47] P. C. Kwok and T. D. Schultz, *Correlation functions and Green functions: zero-frequency anomalies*, J. Phys. C **2**, 1196 (1969).
 - [48] R. Pirc and B. G. Dick, *Exact isolated and isothermal susceptibilities for an interacting dipole-lattice system*, Phys. Rev. B **9**, 2701 (1974).
 - [49] Y. Chiba, K. Asano, and A. Shimizu, *Anomalous behavior of Magnetic Susceptibility by Quench Experiments in Isolated Quantum Systems*, Phys. Rev. Lett. **124**, 110609 (2020).
 - [50] L. D'Alessio, Y. Kafri, A. Polkovnikov, and M. Rigol, *From quantum chaos and eigenstate thermalization to statistical mechanics and thermodynamics*, Adv. Phys. **65**, 239 (2016).
 - [51] F. Schütz, L. Bartosch, and P. Kopietz, *Collective fields in the functional renormalization group for fermions, Ward identities, and the exact solution of the Tomonaga-Luttinger model*, Phys. Rev. B **72**, 035107 (2005).
 - [52] L. Bartosch, A. Ferraz, and P. Kopietz, *Renormalization of the BCS-BEC crossover by order parameter fluctuations*, Phys. Rev. B **80**, 104514 (2009).
 - [53] A. A. Katanin, *Fulfillment of Ward identities in the functional renormalization group approach*, Phys. Rev. B **70**, 115109 (2004).
 - [54] K. Kawasaki, *Correlation Function Approach to the Transport Coefficients near the Critical Point. I*, Phys. Rev. **150**, 291 (1966).
 - [55] W. Götze, *Recent tests of the mode-coupling theory for glassy dynamics*, J. Phys.: Condens. Matter **11**, A1 (1999).
 - [56] S. P. Das, *Mode-coupling theory and the glass transition in supercooled liquids*, Rev. Mod. Phys. **76**, 785 (2004).
 - [57] H. Mori, *Transport, Collective Motion, and Brownian Motion*, Prog. Theor. Phys. **33**, 423 (1965).
 - [58] J. Hubbard, *Spin-correlation functions in the paramagnetic phase of a Heisenberg ferromagnet*, J. Phys. C: Solid State Phys. **4**, 53 (1971).
 - [59] The full solution of the integral equation implies non-analytic corrections to diffusion which appear if we expand the dissipation function beyond leading order in momentum and frequency.
 - [60] Note that Labrujere *et al.* [14] define the Heisenberg Hamiltonian via $\mathcal{H} = -\sum_{i \neq j} J'_{ij} \mathbf{S}_i \cdot \mathbf{S}_j$. Comparing this with our Hamiltonian (2.1) we conclude that with our normalization of the exchange couplings J_{ij} we should identify $J_{ij} = -2J'_{ij}$.
 - [61] T. A. Kennedy, S. H. Choh, and G. Seidel, *Temperature Dependence of the Exchange Interaction in $K_2\text{CuCl}_4 \cdot 2\text{H}_2\text{O}$* , Phys. Rev. B **2**, 3645 (1970).
 - [62] R. M. Corless, G. H. Gonnet, D. E. G. Hare, D. J. Jeffrey, and D. E. Knuth, *On the Lambert W function*, Adv. Comput. Math. **5**, 329 (1996).
 - [63] J. Reuther and P. Wölfle, *J_1 - J_2 frustrated two-dimensional Heisenberg model: Random phase approximation and functional renormalization group*, Phys. Rev. B **81**, 144410 (2010).
 - [64] J. Reuther and R. Thomale, *Functional renormalization group for the anisotropic triangular antiferromagnet*, Phys. Rev. B **83**, 024402 (2011).
 - [65] J. Reuther, R. Thomale, and S. Trebst, *Finite-temperature phase diagram of the Heisenberg-Kitaev model*, Phys. Rev. B **84**, 100406(R) (2011).
 - [66] F. L. Buessen and S. Trebst, *Competing magnetic orders and spin liquids in two- and three-dimensional kagome systems: Pseudofermion functional renormalization group perspective*, Phys. Rev. B **94**, 235138 (2016).
 - [67] J. Thoenniss, M. K. Ritter, F. B. Kugler, J. von Delft, and M. Punk, *Multiloop pseudofermion functional renormalization for quantum spin systems: Application to the spin-1/2 kagome Heisenberg model*, arXiv:2011.01268v1 [cond-mat.str-el] 2 Nov 2020.
 - [68] D. Kiese, T. Müller, Y. Iqbal, R. Thomale, and S. Trebst, *Multiloop functional renormalization group approach to quantum spin systems*, arXiv:2011.01269v2 [cond-mat.str-el] 11 Jun 2021.
 - [69] N. Niggemann, B. Sbierski, and J. Reuther, *Frustrated Quantum Spins at finite Temperature: Pseudo-Majorana functional RG approach*, Phys. Rev. B **103**, 104431 (2021).
 - [70] N. N. Bogolyubov and S. V. Tyablikov, Dokl. Akad. Nauk SSSR **126**, 53 (1959) [Sov. Phys.-Dokl. **4**, 604 (1959)].
 - [71] R. A. Tahir-Kheli and D. Ter Haar, *Use of Green Functions in the Theory of Ferromagnetism. I. General Discussion of the Spin-S Case*, Phys. Rev. **127**, 88 (1962).
 - [72] A. I. Akhiezer, V. G. Bar'yakhtar, and S. V. Peletminskii, *Spin Waves*, (North Holland, Amsterdam, 1968).
 - [73] D. Beeman and P. Pincus, *Nuclear Spin-Lattice Relaxation in Magnetic Insulators*, Phys. Rev. **166**, 359 (1968).